SAND79-8015

Unlimited Release

UC-62

A Description and Assessment of Large Solar Power Systems Technology

Compiled by L. N. Tallerico

Sandia Laboratories
energy report

A DESCRIPTION AND ASSESSMENT OF
LARGE SOLAR POWER SYSTEMS TECHNOLOGY

Compiled By
L. N. Tallerico
Large Power Systems Division 8452
Sandia Laboratories, Livermore

ABSTRACT

This document summarizes the systems being developed by the Department of Energy's Large Solar Thermal Central Power System Program. Included are the technical concepts upon which the systems are based and, to the extent possible, estimated cost, performance, and assessment of typical systems. The intent is to provide potential users with an overview of present technologies and those technologies that will be available within the next few years.

Sandia Laboratories' assessments of the strengths and weaknesses of each technology have been included in the hope that developers of the technology will be able to improve component and system designs to the point where they become fully competitive with alternate energy sources. This document will be revised periodically (possibly at one-two year intervals) to incorporate new developments. Questions and comments are encouraged; they should be addressed to Large Power Systems Division 8452, Solar Energy Department, Sandia Laboratories, Livermore, CA 94550.

FOREWORD

This document summarizes the systems being developed by the Department of Energy's Large Solar Thermal Central Power System Program. Included are the technical concepts upon which the systems are based and, to the extent possible, estimated cost, performance, and assessment of typical systems. The intent is to provide potential users with an overview of present technologies and those technologies that will be available within the next few years.

Sandia Laboratories' assessments of the strengths and weaknesses of each technology have been included in the hope that developers of the technology will be able to improve component and system designs to the point where they become fully competitive with alternate energy sources. This document will be revised periodically (possibly at 1-2 year intervals) to incorporate new developments.

Further information on the particular designs may be obtained from the the reports presented is in the bibliography.

The cost of these systems is important to prospective users. This report contains cost estimates by commercial contractors and Sandia Laboratories. In many cases these cost projections may differ because of differences in assumptions, degree of optimism, or approach. In all cases we have tried to specify who made the estimates. No claim is made that contractor estimates are more or less accurate than the Sandia estimates. However, Sandia has attempted to normalize out the differences which are not attributable to fundamental technological differences.

The opinions expressed in this document are based on the best available information and on independent analysis. However, since new technology is being developed rapidly, conclusions presented in this document may not hold in the future. Therefore, potential users of Large Power Systems technology are urged to make their own assessment of alternatives and draw their own conclusions.

TABLE OF CONTENTS

TABLES

GLOSSARY

CAPACITY FACTOR - The ratio of the average load on a power plant for the period of time considered to the nameplate rating of the machine.

DESIGN POINT - The time of year for which a system is sized.

HELIOSTAT - A mirror and tracking mechanism. The mirror is moved so that the sun's rays are reflected continuously in a fixed direction toward a fixed target. (The term collector is frequently used interchangeably with heliostat.)

HOURS OF STORAGE - The number of hours a plant can produce electricity at its "storage-rated" capacity when operating, exclusively from a fully charged storage subsystem.

HYBRID SYSTEM - A power generating system composed of a solar energy collection subsystem and a non-solar energy subsystem.

LINE FOCUS SYSTEM - A solar power generating system utilizing linear concentrators located parallel to the receiver.

LEVELIZED BUSBAR ENERGY COST - The constant annual revenue per unit of energy required over the lifetime of a plant to compensate for its fixed and variable costs, interest costs and shareholder return (mills per kWh).

NAMEPLATE RATING - The full-load continuous rating of a power plant under specified conditions as designated by the manufacturer.

RECEIVER - A tower-mounted device which intercepts solar energy reflected from a heliostat field and transfers it to a suitable heat transport fluid.

REPOWERING - Repowering consists of retrofitting existing fossil power plants with solar energy collection systems in order to displace a portion or all of the fossil fuel normally used.

RESERVE MARGIN - The amount of installed capacity which is in excess of the predicted system annual peak.

SOLAR MULTIPLE - Solar multiple is defined as:

$$SM = P_t/P_n$$

P_t = Thermal power from receiver at the design point after accounting for downcomer and piping losses.

P_n = Thermal power required to operate the turbine generator at peak electrical output when operating from the receiver only.

SOLAR PLANT CAPACITY CREDIT - The amount of network generating capacity which is displaced by a solar-power plant.

STORAGE CAPACITY - The amount of net electrical energy which can be delivered from a fully charged storage subsystem (MW_e-h).

HEAT TRANSPORT - The medium which absorbs the energy in the receiver and delivers it to other portions of the system.

WORKING FLUID - The medium which powers the turbine.

INTRODUCTION

The Department of Energy (DOE) is developing three categories of large scale solar thermal power systems: (1) storage coupled central receiver, (2) line focus, and (3) hybrid. The storage coupled central receiver concept, presented in Figure 1, consists of a field of individually guided mirrors called heliostats that redirect the sun's energy to a receiver mounted on top of a tower. In the receiver, the radiant solar energy is absorbed in a circulating (heat transport) fluid, and then is either used to power a turbine or an industrial process or is transferred to a storage system for use during a later period. Development has been conducted on designs which use one of five different heat transport fluids - air, helium, salt, sodium, or water/steam. In an electrical generating system, the air and helium systems are coupled to a Brayton cycle turbine; the salt, sodium and water/steam systems are coupled to a Rankine cycle turbine. The line focus solar central power system (Figure 2) is a storage-coupled power system that collects and concentrates solar thermal energy along a linear receiver and transports this energy to a central location for conversion into electricity or opertion of an industrial process. The two types of storage coupled systems, line focus and central receiver, are discussed separately in this document because of their technology differences. In the hybrid concept (Figure 3), the storage-coupled system is combined with a conventional fossil fuel energy source so that the plant can operate using either solar energy or fossil fuel, or the two simultaneously.

HELIOSTAT FIELD   RECEIVER

THERMAL STORAGE

TURBINE/ GENERATOR

1 STORAGE CHARGING CYCLE
2 DIRECT GENERATION CYCLE
3 GENERATION FROM STORAGE
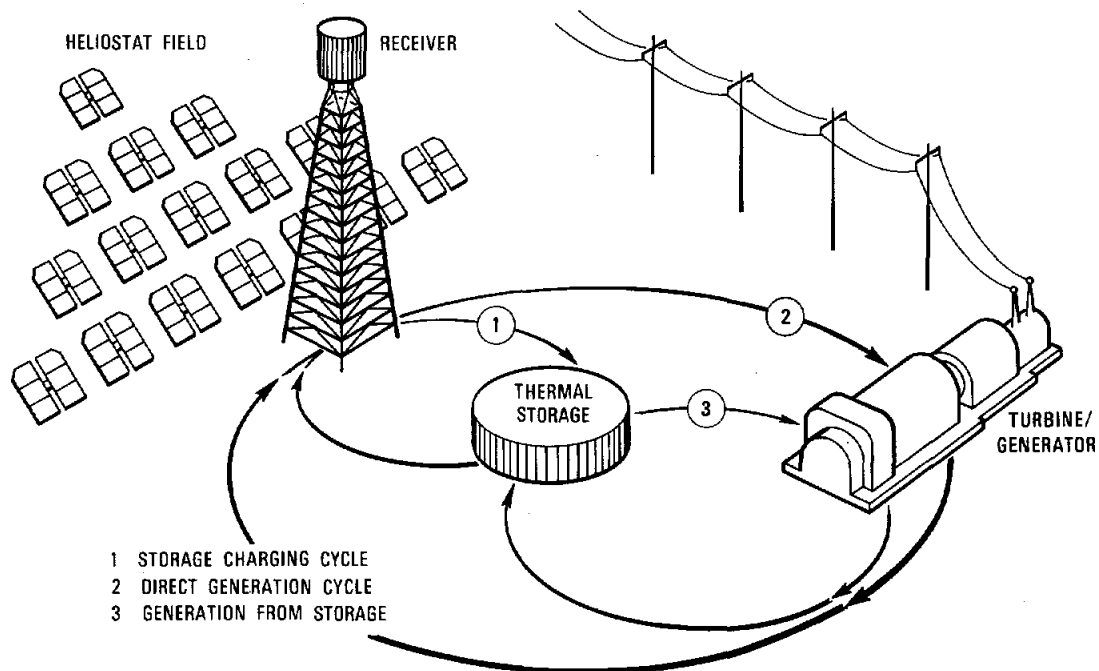
Figure 1. Storage Coupled

CONCENTRATOR/RECEIVER

THERMAL
STORAGE

TURBINE/GENERATOR
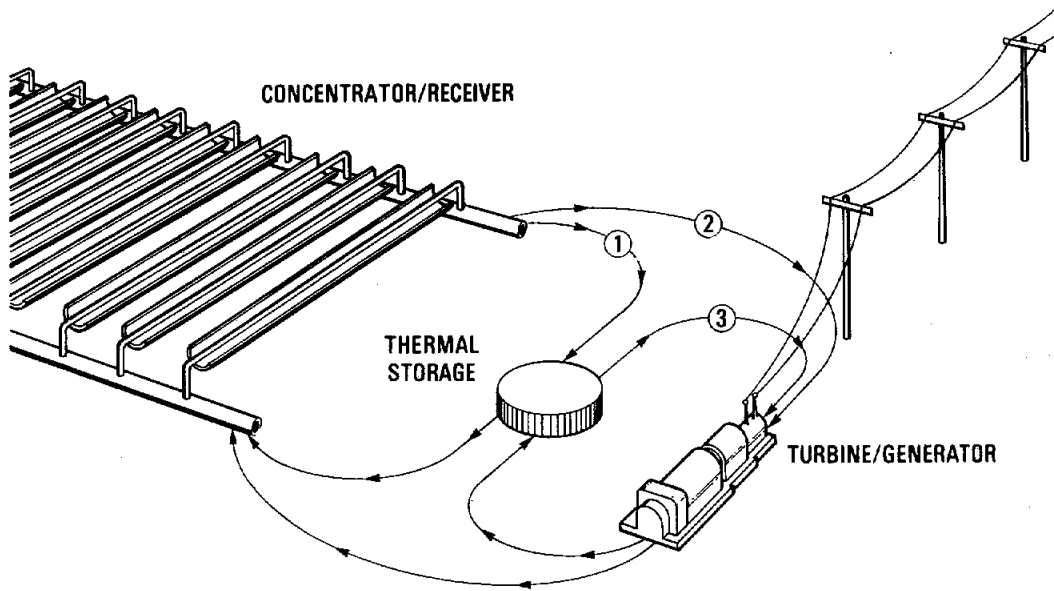
1 STORAGE CHARGING CYCLE
2 DIRECT GENERATION CYCLE
3 STORAGE GENERATION CYCLE

Figure 2. Line Focus

HELIOSTAT FIELD

RECEIVER

THERMAL
STORAGE

BOILER

FUEL

TURBINE/
GENERATOR
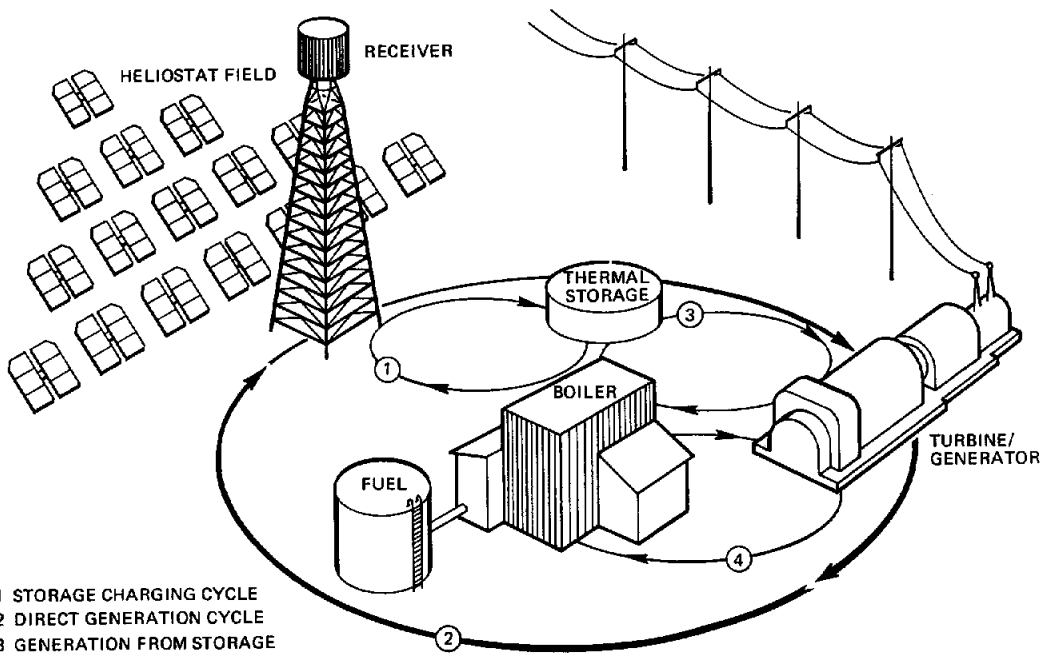
1 STORAGE CHARGING CYCLE
2 DIRECT GENERATION CYCLE
3 GENERATION FROM STORAGE
4 GENERATION FROM OIL, GAS OR COAL

Figure 3. Hybrid

16

A schedule for the Large Power System Program is shown in Figure 4. The development of first-generation receivers, heliostats, and energy storage subsystems has been completed, and the technology is being used in the detailed design and construction of a 10-MW$_e$ pilot plant at Barstow. Improved systems and component technology are being developed so that additional technology options will be available early in FY81 for the detailed design and construction of one or more repowering projects. Further improvements in heliostat, receiver, and energy storage subsystems will continue to be made through FY83 with the goal of incorporating them in commercial applications.

	CY79	CY80	CY81	CY82	CY83	
	FY79	FY80	FY81	FY82	FY83	
10MW$_e$ BARSTOW PILOT PLANT	PREPRODUCTION HELIOSTAT DESIGN & TEST	DESIGN AND CONSTRUCTION			OPERATION	
RECEIVER TESTING (CRTF)	EPRI MDAC EPRI BOEING B&V	MARTIN G.E.				
REPOWERING	ISSUE RFP CONCEPTUAL DESIGNS		PROJECT DESIGN CONSTRUCTION			
COGENERATION		ISSUE RFP CONCEPTUAL DESIGNS		PROJECT DESIGN CONSTRUCTION		
SYSTEMS	ADVANCED RECEIVER SYSTEM DEVELOPMENT HYBRID, LINE FOCUS CONCEPT DESIGN					
HELIOSTAT	2nd GENERATION NEW IDEAS		3rd GENERATION			
RECEIVER	ADVANCED RECEIVER DESIGN ADVANCED WATER/STEAM DESIGN					
ENERGY STORAGE (DIVISION OF ENERGY STORAGE SYSTEMS)	INTERNAL INSULATION DEVELOPMENT	DESIGN AND TEST BUFFER STORAGE DESIGN AND TEST DIURNAL STORAGE				

Figure 4. Large Power Systems Program Schedule

The technology described in this document can be used for many applications such as repowering existing electrical generating plants, retrofit of industrial processes to replace fossil energy with solar energy, and the construction of new electrical generation, industrial, or agricultural process plants. The initial emphasis of the Large Power Systems Program was on the design of new electrical power generation and thus much of the information in this document relates to this application. More recent studies have shown promising markets for the other applications and the next revision of this document will incorporate these results.

GENERAL DISCUSSION

The storage-coupled, hybrid, and line focus systems incorporate many common subsystems. The storage-coupled and hybrid designs are very similar except for the hybrid non-solar components (i.e., boilers and heaters). The line focus systems are similar to the storage-coupled systems except for the design of the collector/receiver. Therefore, the storage-coupled subsystems are presented first, followed by a discussion of the subsystems which are unique to hybrid and line focus systems, respectively.

Storage-Coupled Systems

The goal of the studies on the storage-coupled systems is to develop technologies for improving the cost effectiveness and increasing the potential breadth of application of the central receiver concept. Five receiver heat transport fluids - water, salt, sodium, air, and helium - have been proposed for storage-coupled applications. A summary of the programs related to storage-coupled systems is presented in Table I. A simplified schematic of a first-generation water/steam system is presented in Figure 5. This design limits the system performance because it contains two separate steam loops: steam from the receiver, and steam from storage. The steam generated from the receiver is at a higher temperature and pressure than the steam generated from storage [520°C/10MPa vs 280°C/3MPa]. The steam generated from storage is at the lower temperature because 1) the maximum operating temperature of the storage fluid is ~300°C, and 2) there is a temperature drop associated with the transfer of energy in the two heat exchangers. A dual-admission turbine is required to efficiently accept the steam at the two different inlet temperatures and pressures.

The efficiency and relative subsystem cost for the proposed first-generation water/steam commercial plant is presented in Table II. Fifty-five percent of the annual energy directed to the heliostats reaches the receiver. The balance of the energy is lost because of atmospheric attenuation, cosine losses, and optical losses. Only a small fraction of these losses is directly attributable to the heliostat. The receiver and storage subsystems are relatively efficient, and their percentage of the total cost is relatively low. The turbine efficiency is lower than might be expected because of the constraints imposed by the storage system.

TABLE I

SUMMARY OF STORAGE-COUPLED SYSTEMS PROJECTS

Project	Responsible Company	Status
Preliminary Design of 100-MW Central Receiver and 10-MW Pilot Plant	Honeywell Martin Marietta McDonnell-Douglas	Complete
Design/Construction of 10-MW$_e$ Pilot Plant - Barstow	McDonnell Douglas	Construction In Progress
Advanced Central Receiver Program Phase I Conceptual Design		
Air Brayton	Boeing	Complete
Sodium	Energy Systems Group	Complete
Sodium	General Electric	Complete
Salt	Martin Marietta	Complete
Advanced Central Receiver Program Phase II: Research Experiments		
Salt	Martin Marietta	In Progress
Sodium	General Electric	In Progress
Advanced Water/Steam Program	Babcock & Wilcox Combustion Engineering Martin Marietta	In Progress In Progress In Progress
Heat Pipe Receiver	Dynatherm	Feasibility Study Complete
Ceramic Receiver	Sanders	Small Prototype Tested Complete
Direct Absorption Receiver	Sandia	In Progress
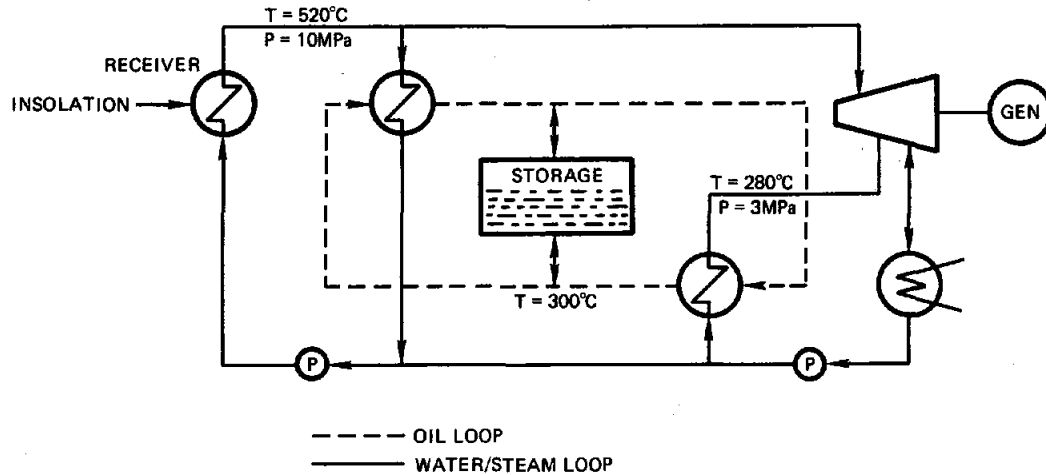
Figure 5. First-Generation Water/Steam System

TABLE II

EFFICIENCY/COST OF FIRST-GENERATION WATER/STEAM SYSTEMS

	Subsystem Efficiency* (%)	Cost** (%)
Heliostats***	55	51
Receiver/Tower	88	16
Storage	87	11
Turbine	31	7

   * Annual average; solar multiple = 2; 7 hours of storage; 12% attenuation
  ** % of total plant cost, n^{th} plant
*** Includes atmospheric attenuation, cosine losses, shadowing, and blocking

Even though the cost of the turbine in an electrical generating system is a small percentage of the total system cost, it is cost-effective to increase the turbine efficiency primarily because it reduces the number of heliostats required for a given output. Thus, emphasis has been placed on minimizing heliostat costs and developing techniques for improving the efficiency of solar central systems. Three promising technologies for improving the plant efficiency were defined in preliminary studies conducted by Aerospace, Sandia, and others. These studies indicate that it may be possible to improve the efficiency of solar central receivers by using alternate "working fluids" in the receiver. Specifically, four candidate materials were selected: air, helium, molten salt, and sodium. The air and helium are coupled to a Brayton cycle turbine; the draw salt and sodium are coupled to a Rankine cycle turbine.

In the Brayton system, Figure 6, the heat transport fluid is also used to charge and discharge the storage medium. Brayton turbines are desirable because they are compatible with cyclic loading and have high efficiencies. In the sodium and salt systems, Figure 7, the working fluid may be used as the storage medium; however, a heat exchanger is required to transfer the energy to a Rankine cycle turbine loop. This configuration is highly desirable because it is possible to have high-temperature storage and the turbine need only operate from steam at one temperature and pressure. Thus, high efficiency reheat turbines can be used. In addition, the turbine is isolated from the short-term insolation transients imposed on the receiver.
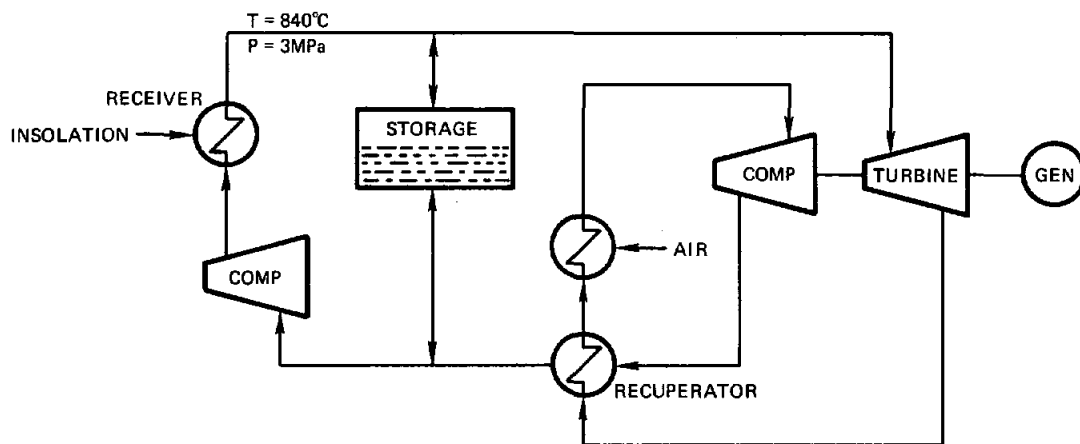
Figure 6. Brayton System

22
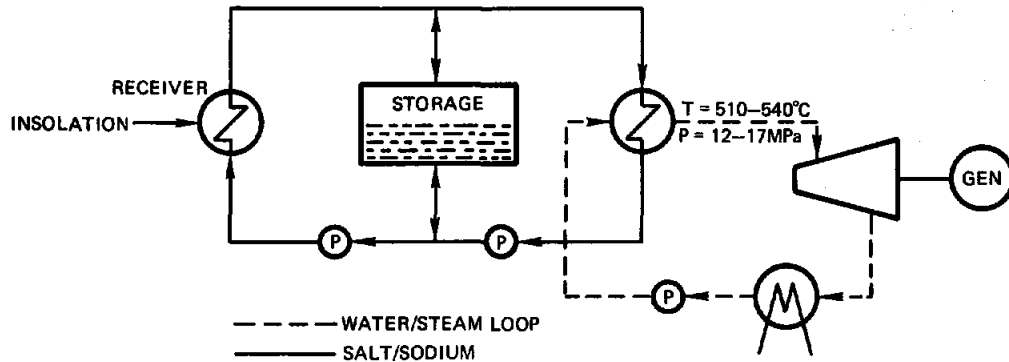
Figure 7. Salt/Sodium System

Collectors

The collector subsystem has as its basic function the interception, redirection, and concentration of direct solar radiation to the receiver subsystem. The collector subsystem for a solar central receiver consists of a field of tracking mirrors, called heliostats, and a tracking control system to maintain continuous focus of the direct solar radiation on the receiver. In a 100-MW$_e$ solar central receiver power plant, there can be 15,000 to 25,000 heliostats, depending on the size and the reflectivity of the mirrors and the desired charging ratio of the energy storage subsystem.

The collector subsystem components are:

a. Heliostats

    1. Mirror modules
    2. Structural support
    3. Drive units, sensors, cabling, etc
    4. Foundations

b. Heliostat Controllers (HC)

    1. Drive motor controller
    2. Position sensor
    3. Interface with HAC

c. Heliostat Array Controller (HAC)

    1. Master control interface including electronics
    2. Time base, software computers

d. <u>Heliostat Field Controllers (HFC)</u>

    1. Controller and power supplies
    2. Heliostat Controller, array interfaces, and software

e. <u>Support Equipment and Procedures</u>

    1. Installation, alignment, operation, and maintenance

Figure 8 illustrates a representative heliostat configuration.
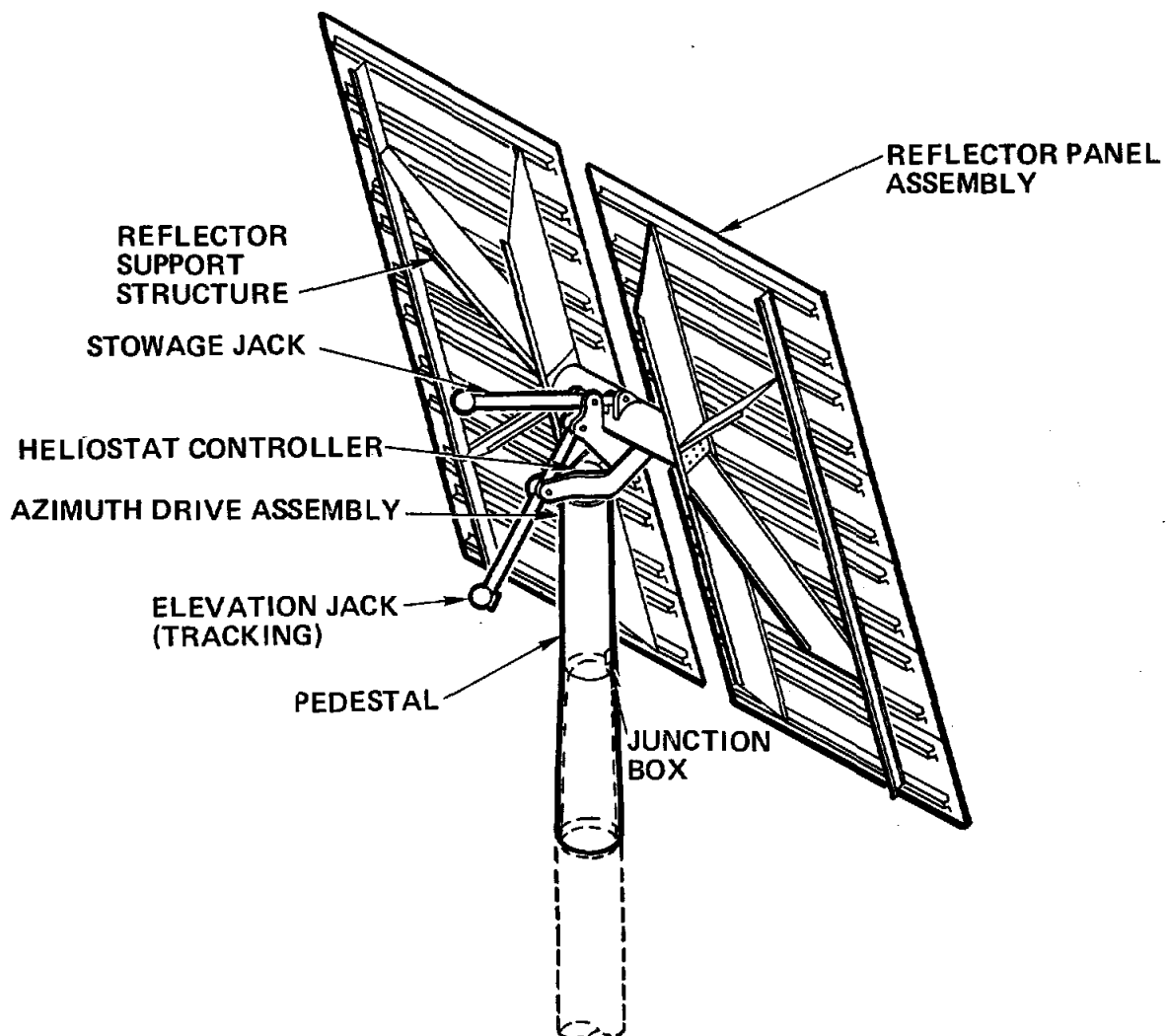
Figure 8. Prototype Heliostat Baseline

Receivers

The receiver is a relatively unique heat exchanger in that the heat exchange surface is subjected to an intermittent, non uniform - typically one sided - heat flux and concomitant thermal stress. Therefore, it is imperative to design the receiver to withstand the fatigue associated with this stress. The size of the receiver is determined by calculating the maximum flux that the absorbers can withstand for the specified life.

There are two basic types of receivers: exposed and cavity. In an exposed receiver the insolation impinges directly on the tubes or surface which contains the working fluid. Exposed receivers are typically cylindrical and have a length-to-diameter ratio of approximately 1. In contrast, in cavity receivers the insolation enters one or more relatively small apertures and then impinges on a heat exchanger surface directly or after it has been reflected internally.

The specific receiver type selected will depend upon the application. The main parameters affecting receiver design are:

(1) Required working fluid temperature
(2) Flux capability of absorber
(3) Efficiency

Operating temperature is extremely important because of its impact on receiver efficiency. With each receiver design, it is necessary to estimate the radiation, convection, and conductive losses. Of these, the radiation and convection are predominant. Since the radiative loss varies with the fourth power of the temperature, this loss mechanism becomes extremely large at high temperatures (>800°C); therefore, cavity designs tend to be selected for high-temperature applications.

A low flux capability results in a large receiver surface area. As the surface area is increased, external losses increase in external configurations; therefore, a cavity design would tend to be more efficient and perhaps more cost effective.

Cavity receivers have better thermal control characteristics and tend to protect the panels from the elements (wind, rain, snow, hail, and low temperatures). However, to take full advantage of its enclosed configuration, a cavity receiver may require some form of closure for the large aperture(s). For the same thermal power, external receivers tend to be smaller than cavity receivers, require less structure, and cost less to fabricate.

Towers

The tower supports the solar receiver at the desired location above the heliostat field and anchors the vertical piping. Both steel frame and tapered concrete towers have been proposed. A study is in progress to evaluate the relative costs for towers ranging in height, excluding the receiver, from 100 to 330 meters and capable of supporting receivers and associated equipment from 90,000 to 360,000 kg. Other variables to be considered are seismic zone, maximum wind velocity, soil shear modulus, and allowable soil bearing pressure. The study will show under which conditions steel or concrete towers are the most economical and will provide an estimated cost.

Thermal Storage

Energy storage plays an important role in the operation of a solar thermal power plant. Storage can act as a buffer between the solar portion of the plant and the electrical generating portion to protect the turbine from rapid variations in inlet conditions caused by clouds passing over the collector field. In addition, storage can extend the plant's operation into periods of little or no insolation and provide efficient turbine seal heating during periods of turbine inactivity. Energy storage concepts that first require electric generation, e.g. pumped water, compressed air, flywheel, or battery storage, do not fulfill the basic requirement of buffering the turbine from solar insolation variations; therefore, thermal energy storage is preferable for this solar energy application.

Thermal storage concepts can be classified into three categories: sensible-heat, latent-heat (phase change), and thermochemical (reversible chemical reactions). Of these, sensible-heat systems are clearly within the current state-of-the-art and present a low technical risk and thus a low development risk. Both latent-heat and thermochemical storage systems require considerable additional development before they can be evaluated in detail and considered for implementation on a large scale.

Two basic sensible heat concepts have been proposed: separate hot and cold tanks and a single tank thermocline. In the hot/cold concept, the storage medium flows from the hot tank through a heat exchanger, where the energy is transferred to the turbine working fluid, and then into a cold tank. The thermocline concept is based on the fact that it is possible to obtain a sharp temperature gradient within a tank if the storage media has a low thermal diffusivity. When the tank is fully charged, it is at a uniform temperature. During discharge three distinct regions - one hot, one cold, and a transition zone - are developed within the tank. In the case of both these concepts, if the working fluid which flows through the receiver does not have good storage properties, a separate media may be used in storage. In this case, a heat exchanger is used to isolate the two media.

The primary focus in latent-heat systems has been on liquid-solid phase changes, making use of the heat of fusion. Three of the major problems areas in such systems are: (1) designing to accommodate the volume change upon phase transition, (2) ensuring that the system will maintain a clean transi-

26

tion between solid and liquid without long-term changes in the structure and composition, and (3) preventing solid buildup on heat-transfer surfaces, which rapidly drops the heat-transfer rates during discharge. The last of these problems has been particularly difficult to solve in a fashion practical for large-scale, inexpensive, and reliable 30-year operation.

Although considerable research effort has been expended on thermochemical storage concepts, major technical problems remain for all of the reaction systems under consideration. More importantly, even if the technical problems could be solved, thermochemical systems would not be competitive with the advanced sensible systems currently being developed for short-duration (diurnal) energy storage. The inherent disadvantages of the thermochemical systems are high power related costs due to system complexity and efficiencies significantly lower than those anticipated for the sensible systems.

As a result of many studies and for the reasons summarized very briefly above, sensible-heat thermal storage has received the major emphasis in research and development.

Electrical Power Generation System (EPGS)

Since EPGS subsystems have been developed for conventional power plants and represent a mature technology no research and development has been sponsored by the solar program. Both Rankine and Brayton cycle turbine generators can be used in solar power systems, but the Rankine turbines tend to be more easily adapted to solar applications. Steam conditions can readily be achieved in solar steam generators which match the throttle conditions for a wide range of steam turbines.

In the first-generation water steam systems, the receiver outlet steam temperature and pressure were typical of turbine conditions used in comparatively small or older power plants (10 MPa, 510°C). However, a portion of the steam was used to heat a thermal storage medium that subsequently produced steam at a considerably lower temperature and pressure than the original turbine throttle conditions (e.g. 2.8 MPa, 280°C). These lower conditions require a turbine with dual admission capability and limit plant operating conditions to pressures lower than many conventional power plants. Turbines are available for these systems and all other portions of the EPGS are conventional.

In other solar concepts, the solar energy is absorbed by fluids other than water/steam, and therefore may be used in Brayton or Rankine turbine cycles or stored directly at higher temperatures than earlier systems. Thus, any steam produced from the working fluid, either directly or from storage, can be at the desired throttle conditions, which permits a wider range of turbine selection.

Steam turbines are available in a wide variety of sizes, configurations, and operating conditions. As noted previously, the dual admission option restricts selection somewhat because dual admission machines have not been made for pressures exceeding about 10 MPa due to the difficulty in penetrating the double shell required for those higher pressures. Availability of dual admission in sizes above 200 MW_e may also be limited.

If the working fluid is air or some other suitable gas, a Brayton cycle machine may be used to generate power. However, typical Brayton cycle plant operating temperatures are higher than those being proposed for solar Brayton systems. Thus, gas turbine selection becomes somewhat more involved than a similar selection of a steam turbine. There is no question that gas turbines can be obtained now for application to solar plants, but their efficiency may not be comparable to conventional Brayton cycle machines.

Brayton cycle turbines are not as readily available for solar applications, since they have historically used combustion products as the working fluid. Typical gas turbine operating conditions are different than those proposed for solar Brayton systems; consequently, a machine designed for the desired temperature and pressure ratio may not exist. In addition, gas turbines are not available in sizes above about 100 MW$_e$; however, they are available in a variety of intercooling, regenerating, and reheating combinations.

Master Control

The master control system (MCS) (Figure 9) consists of three primary subsystems, each with its own computer and associated software:

- Operational control system (OCS)
- Data acquisition system (DAS)
- Peripheral control system (PCS)
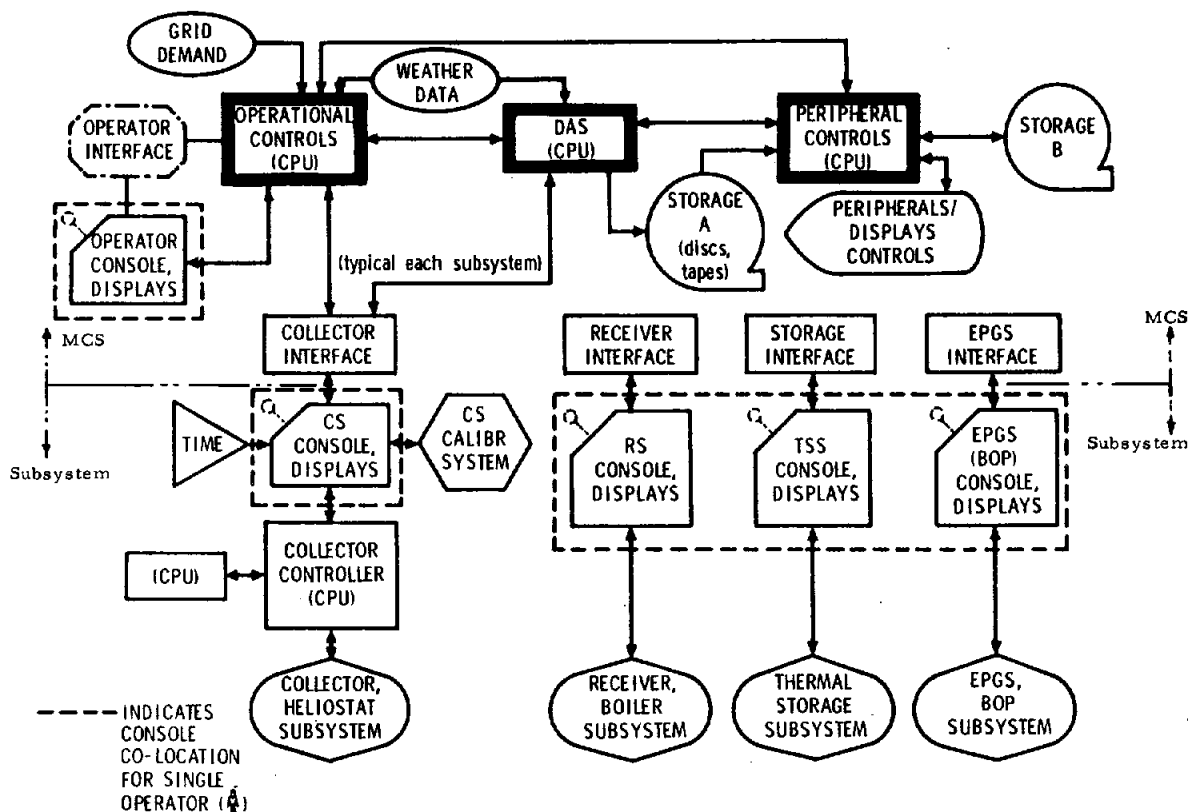
Figure 9. MCS Configuration

MCS integrates the independent controls of the four subsystems (collector, receiver, storage and electric power generation). The master control system operational modes are:

- Automatic - no operator interaction required
- MCS Manual - operator interaction
- Subsystem Manual - operator control of each subsystem

The basic MCS features are:

- Independent control within each Pilot Plant Subsystem (PPS)
- Coordination of control of each PPS by MCS
- Flexible computer set-point control
- Independent peripheral controller for multipurpose utilization

Supervisory control is provided by the OCS, which has a single operator console and interfaces to each plant and MCS subsystem. The OCS stands alone (i.e., is able to function without the DAS and/or PCS) in this role of supervisory control. As such, the OCS contains the data acquisition and displays required for operational control. Additional interfaces are required to obtain grid demand and weather data.

Evaluation data control is provided by the DAS, which interfaces with each plant and the MCS subsystem. The DAS stands alone (i.e., is able to function without the OCS) in the role of data requests and displays. A subset of this evaluation data set is issued and received by the OCS. An additional interface will be required to obtain weather data.

The PCS is primarily a controller for the evaluation displays, a software development computer, and an on-site simulation computer. In the event of an OCS failure, the PCS provides a back-up for the OCS.

The MCS functions include:

a. Coordinated and cascade plant control modes

b. "Set-point" interactive control of functionally indpendent subsystem controls

c. Comprehensive operational displays consistent with manual monitoring and intervention into plant control

d. Operational alerts or alarms of plant or significant subsystem upset conditions

e. Automatic safety or protective actions prudently isolated from system control

f. Data acquisition capabilities: operational and evaluation, on demand and continuous

g. "Bumpless" control transfer between MCS and subsystem control; automatic or manual control

h. Operator involvement only when operationally desired

i. Separation between control and evaluation DAS capabilities

j. Use generally similar, interchangeable units for all MCS and CS computer functions

k. Maximum information transfer via graphic displays shall be used to achieve operational comprehension

l. Should MCS fail, control of each PPS shall allow safe operation

The Design of Central Receiver Systems

This section discusses the issues which must be addressed in designing a storage-coupled solar central receiver system. In practice, many factors go into the final design selection; for the sake of simplicity, only minimizing the cost of energy is considered in this section. To illustrate the concepts involved, the results of several example calculations are presented. The results are intended to indicate the major qualitative features of central receiver systems; the actual quantitative values are meant to be representative but not the "best" or "official" values. All of the examples consider only an external cylindrical receiver.

Central receiver systems can only concentrate the direct insolation (i.e., only that part of sunlight that can cast a sharp shadow) and not the diffuse insolation. The time dependence of energy collected by the receiver follows that of the insolation. In calculating the annual efficiency, the time dependent performance is weighted by the time dependent insolation, which gives greatest influence to the performance around noon.

The performance of the heliostat field is defined in terms of optical efficiency, which is equal to

$$\frac{\text{net power intercepted by receiver}}{(\text{solar power/area}) \times \text{mirror area}}$$

The optical efficiency includes the cosine, shadowing, blocking, mirror reflectivity, atmospheric transmittance, and spillage. The net efficiency for producing electricity includes the receiver efficiency (e.g. radiation losses) and the thermal-to-electric efficiency.

The amount of insolation reflected by the heliostat is proportional to the amount of sunlight intercepted. The reflected power is, therefore, proportional to the cosine between the heliostat normal and the incident sun rays. The ratio of the area perpendicular to the sun rays to the total area of the heliostat is called the cosine effect. The heliostat is oriented so that the incident sunlight is reflected onto the receiver. If the sun is due south, then the heliostats due north of the tower will be almost perpendicular to the sun rays and therefore have almost the maximum cosine efficiency of 1.0. At the same time, heliostats due south of the tower will have a low

cosine efficiency. Since the insolation is greatest on an annual basis when the sun is in the southern sky, the annual cosine will be greatest in the northern part of the heliostat field. Thus, in the northern hemisphere, heliostat fields are usually biased toward the north of the tower.

Shadowing occurs when a part of a heliostat is in the shadow of another heliostat. Similarly, blocking occurs when part of the sunlight reflected by a heliostat hits the back of another heliostat. While both effects increase if the heliostats are closer together, blocking has a more pronounced effect on the layout of heliostat fields. As heliostats are placed at greater radial distances from the tower, the receiver appears to be closer to the horizon. Heliostats must, therefore, be placed at greater radial separations to be able to see the receiver.

Not all the sunlight that clears the heliostats reaches the vicinity of the receiver. Some of the energy is scattered and absorbed by the atmosphere. A typical value for a good visibility day is a 10% loss per kilometer. The losses increase with greater amounts of water vapor or particulate count in the atmosphere.

The size of the image formed by a heliostat depends on the size of the heliostat, the size of the sun (because rays from the center and edge of the sun striking one point on a heliostat are not exactly parallel), and errors in the heliostat surface and pointing. Focusing a heliostat cannot produce a point image because of the finite size of the sun. Focusing can, however, produce an overall smaller image than an unfocused heliostat because the effect of the heliostat size on the image size is reduced. With a fixed-focus heliostat, off-axis aberation effects cause some incremental spread in image size; the relative amount depends on the heliostat size, the slant range, and the off-axis angle, which varies throughout the day. Even with perfect focusing and perfect optics, the size of the image increases as the distance from the heliostat to the receiver increases because of the finite angle subtended by the sun. The minimum image size is 9.3 m/km of range.

If the receiver is not big enough to intercept the entire image of the heliostat, some of the energy will be "spilled" around the receiver. While spillage can be eliminated by increasing the size of the receiver, at some point this becomes counterproductive because of increased receiver losses (e.g., radiation and convection) and receiver costs.

The dependence of the annual performance on the position of the heliostat relative to the tower is shown by the contour plot in Figure 10 for one representative case using a cylindrical external receiver. The efficiency includes all the effects described above plus the heliostat (0.90) and receiver reflectivity (0.03). Two general features are apparent in Figure 10. First, at a given radial distance the performance becomes better as the heliostat moves from south around to north of the tower, because the cosine effect is much better in the north part of the field. Second, except for the maximum due north, the performance decreases in any direction as the radial distance of the heliostat increases. This decrease is caused by an increase in the atmospheric attenuation and spillage losses.
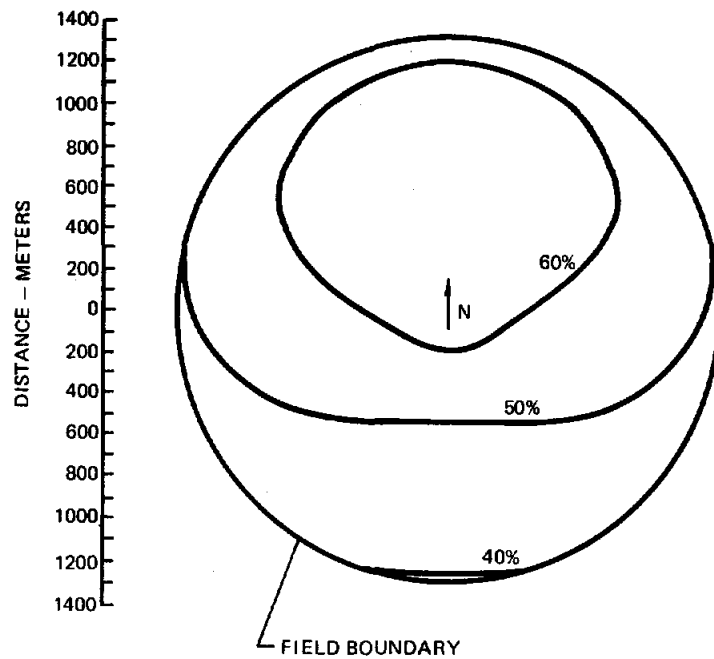
Figure 10. Annual Heliostat Efficiency

A typical heliostat field for an external receiver would have a circular inner boundary and an outer boundary that has the shape of the 0.55 contour line. The annual average efficiency for a whole heliostat field is found by integrating the efficiency at a given location times the density of heliostats. The average field efficiences are given in Table III for one representative system.

In addition to performance, the costs of central receiver systems are required in design optimization. The cost of components depends on the technology used and the size. Many central receiver components (e.g., electric power system, receiver, storage, heat exchangers) exhibit an economy of scale; that is, larger components are relatively cheaper per unit size. A breakdown of the relative capital costs are also given in Table III. The dominant subsystem is the helisotat field, which typically accounts for about one-half the capital cost. The electric power generation system is generally the next largest expense, followed by storage. Storage costs are, of course, dependent on the size of the system.

If the performance and cost of central receiver components are known as a function of technology and size, the system can be optimized as follows:

(1) Select the technology to be considered (e.g., sodium, salt, or water cooled receivers, glass or plastic helisotats).

(2) Determine the system variables (e.g., tower height, receiver size) and constraints, if any, (e.g., fixed turbine size, peak flux limit on receiver).

(3) Optimize the system variables for each technology. For each combination of design variables, lay out the heliostat field and then use the performance and costs to determine the cost of energy. The set of variables with the lowest energy cost is the best design for that technology. Finally, the technology with the overall lowest energy cost is the optimum design.

In addition to the cost of energy, the final decision will be made considering factors such as ecology, reliability, and system impact.

TABLE III

PERFORMANCE AND COST OF A REPRESENTATIVE SYSTEM

Performance Breakdown

Cosine effect	0.79
Mirror reflectivity	0.90
Shadowing + Blocking	0.96
Atmospheric Attenuation	0.91
Spillage	0.98
Receiver reflectivity	0.97
Net optical efficiency	0.59

Cost Breakdown

Heliostat Field	52%
Electric Power System	18%
Storage	10%
Receiver	5%
Tower	3%
Pipes + Heat Exchanger	8%
Other	4%

Representative optimized heliostat fields for a single module 50 and 300-MW$_e$ plant using an external receiver are shown in Figure 11. The similarity between the fields is obvious. The fields have outer boundaries that follow the performance contours in Figure 1 as discussed above. The density of heliostats, chosen to minimize blocking, is greatest at the inner boundary and decreases with increasing radial distance from the tower. The field average ratio of mirror/land area is typically 0.20 to 0.25. The shape of the helisotat field remains relatively constant over a wide range of power levels.

DISTANCE – METERS

POWER = 100

DISTANCE – METERS

POWER = 300
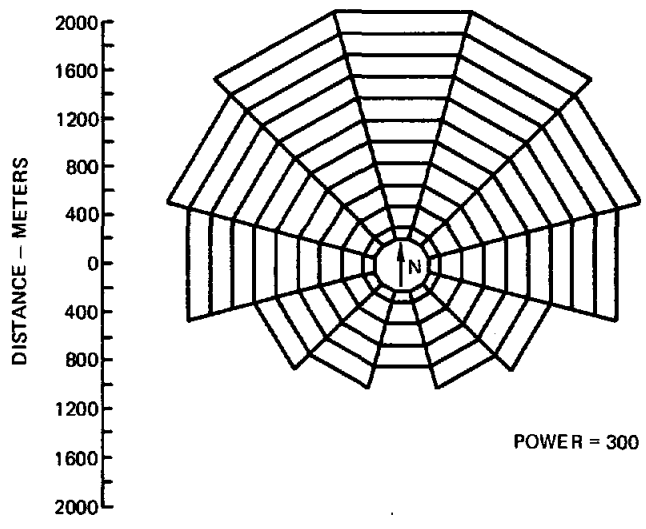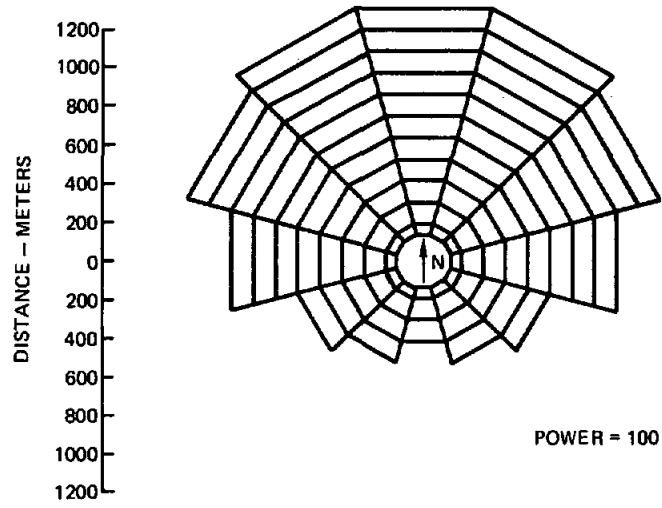
Figure 11. Field Layout

An example of the variation of the optimal tower height and receiver size with design power level is shown in Figure 12. Both the tower height and receiver size increase with the power level, obeying approximately a (power level)$^{1/2}$ dependence.
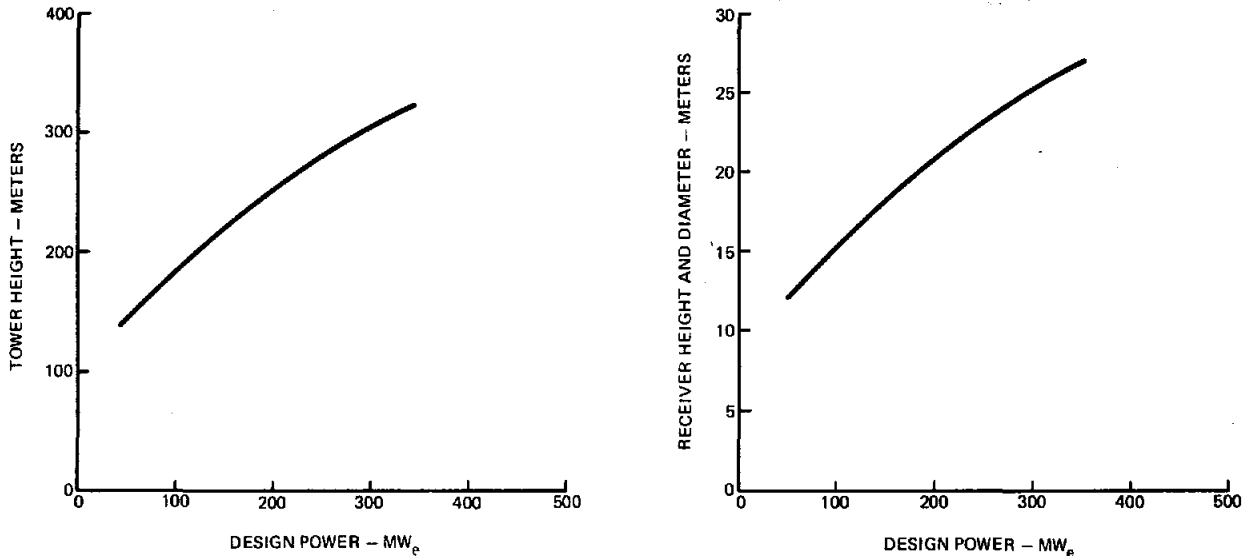
Figure 12. Optimum Tower Height and Receiver Size

An example of the variation of the optical efficiency and capital costs is shown in Figure 13. All efficiency terms are relatively constant over the range of power levels except for atmospheric attenuation. As shown in Figure 13, as the tower height increases, the distance from heliostat to receiver increases, and therefore the atmospheric transmission decreases. This results in a small decrease in optical efficiency with increasing power level. The electric power generating efficiency, however, increases with power level and partially offsets the optical inefficiency.

The capital cost per unit of power decreases with power, especially at the low power levels. The decrease is due to the economy of scale in some of the components, particularly the electric power generating system. At larger power levels the heliostat field accounts for a larger fraction of the total capital cost.

The levelized busbar energy cost is shown in Figure 14 as a function of power level for an example system. The busbar cost is dependent on the performances, capital costs, and economics of the utility. The values reflect an 18% fixed change rate and include operation and maintenance, spare parts, and contingency funds. The energy cost exhibits a very broad minimum, indicating a great deal of flexibility in applying central receiver systems. The relatively flat energy cost versus power level curve represents the balance between the slowly decreasing performance and costs.
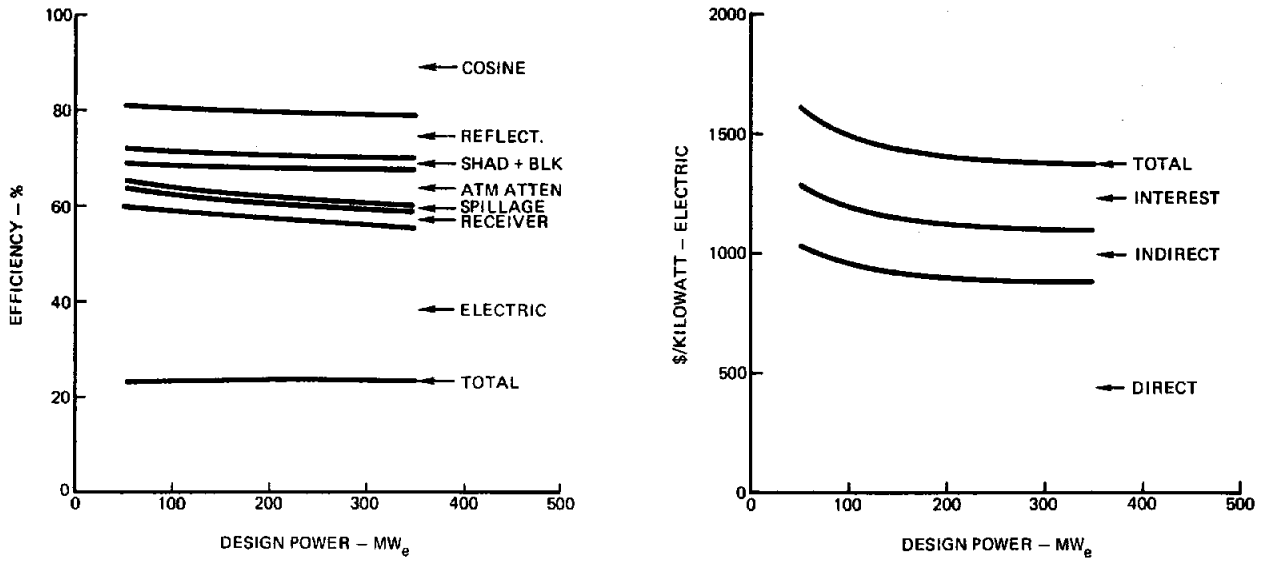
Figure 13. Optical Efficiency and Capital Costs
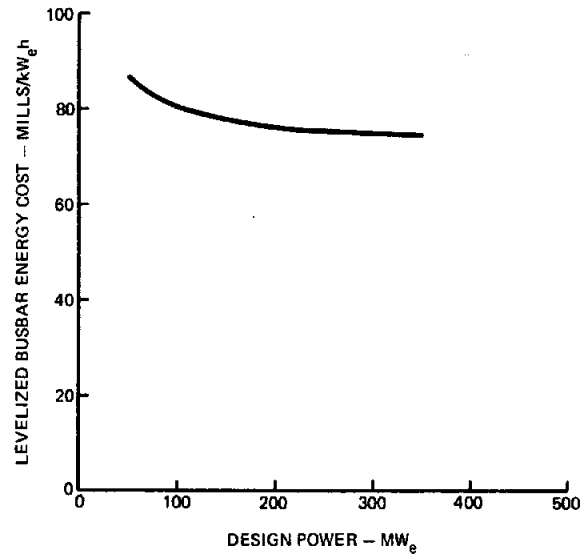
Figure 14. Cost of Energy

Capacity Factor

This section relates the capacity factor of a plant to the size of the heliostat field and storage unit. The capacity factor of a plant is the ratio of the average annual load to the nameplate rating. Given a nameplate rating for the plant EPGS, it is useful to think of the size of the related mirror field in terms of its "solar multiple" and the size of the storage in terms of its "number of hours." Of the two, "hours of storage" is the easiest to conceptualize. If a plant has one hour of storage, then with a fully charged storage unit, the plant could produce full output for one hour. However, there is some ambiguity in the definition. For example, if a 100-MW_e salt or sodium plant has six hours, it could produce 100 MW_e for six hours; but if a 100-MW_e first-generation water steam plant has six hours of storage, it can produce only 70 MW_e electric for six hours. In other words, the number of storage hours is in reference to the plant's rating when it is operating from storage, which may not be the nameplate rating.

The "solar multiple" of a mirror field is the ratio of the thermal power output of the field when the sun is at its most favorable geometric position to the maximum thermal power which can be input to the turbine. The intensity of direct normal insolation is frequently assumed to be 950 w/m^2 since, this value is not exceeded more than one or two percent of the daylight hours of the year. Thus with a solar multiple of one, it is possible, but not likely, that the field would produce more power than can be supplied directly to the turbine. For most daylight hours of the year, such a field would produce less power than would be necessary to run the turbine at full output.

The relationship between the size of the mirror field and the size of the storage unit may be varied. Figure 15 shows how the plant capacity factor is influenced by the field and storage sizes. These curves were derived using a turbine priority dispatch policy; i.e., energy is sent to storage only if there is more than can be used in the turbine. As is indicated in Figure 15, for each solar multiple there is a size of storage unit beyond which the plant capacity factor will not be increased. At first glance, building a plant with an "oversized" storage unit would not appear to be cost effective. However, in an actual utility operating situation, turbine priority dispatch would probably not be used; rather, the solar plant would be dispatched to minimize the utility variable costs. Thus, the flexibility obtained by having an "oversized" storage unit could make it cost effective.

It is clear then that the buyer of a solar plant must size each of the components to optimize his particular system. In order to give some feeling for the relationship between field and storage sizes, the combination which minimizes the plant busbar energy cost for each capacity factor is shown by the dashed lines in Figure 15.
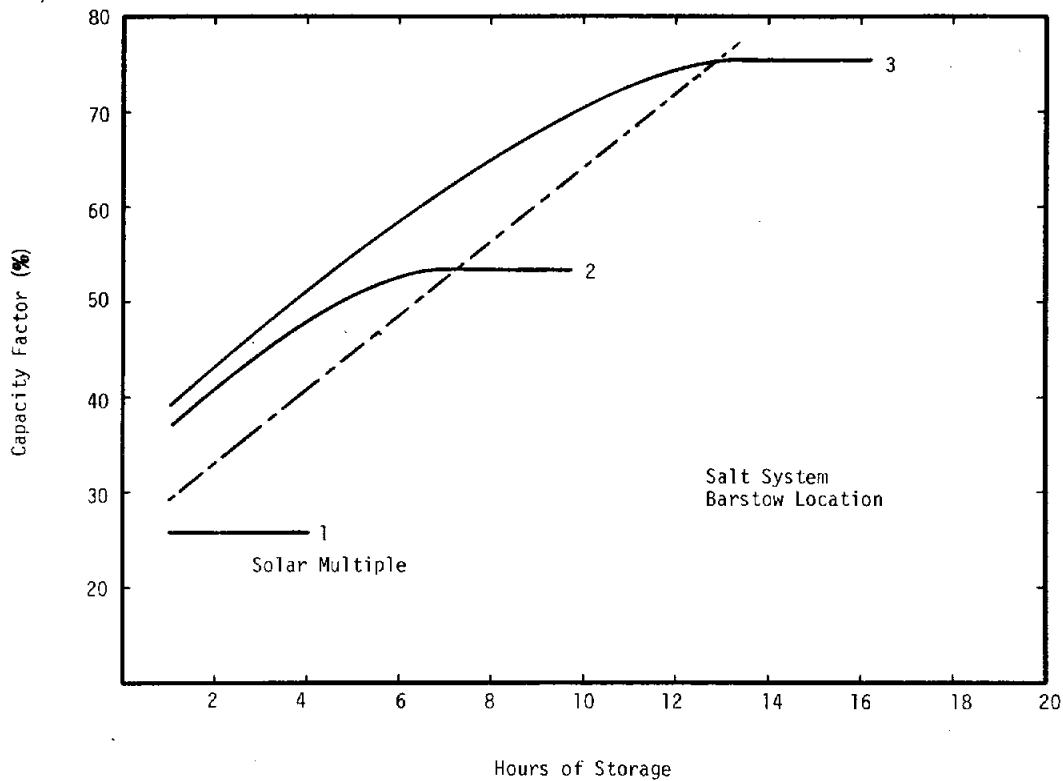
Figure 15.   Relationship of Collector Field and Storage Size
to Plant Capacity Factor

Capacity Credit of Solar Plants

The capacity credit of a solar plant measures its impact on the required system installed reserve margin. For example, if solar plants receive no capacity credit, then for every solar plant installed, a conventional plant of the same name plate capacity must also be installed. There have been numerous studies (e.g., References 18, 36, 37) which considered this issue. These analyses are consistent in their conclusion that stand-alone solar plants can achieve significant capacity credit. Figure 16, a reproduction from Reference 39, shows that with sufficient storage capacity roughly 1 MW_e of conventional capacity must be added in reserve for every 2 MW_e of stand-alone solar capacity for solar penetrations between 6 and 20 percent. (Note in Figure 16 that the reserve margin increases by roughly eleven percent when twenty percent of the system is solar.) That conclusion was based on a specific system, load shape and insolation data. Properly designed and operated hybrid plants will achieve capacity credit equivalent to that of conventional plants.

38
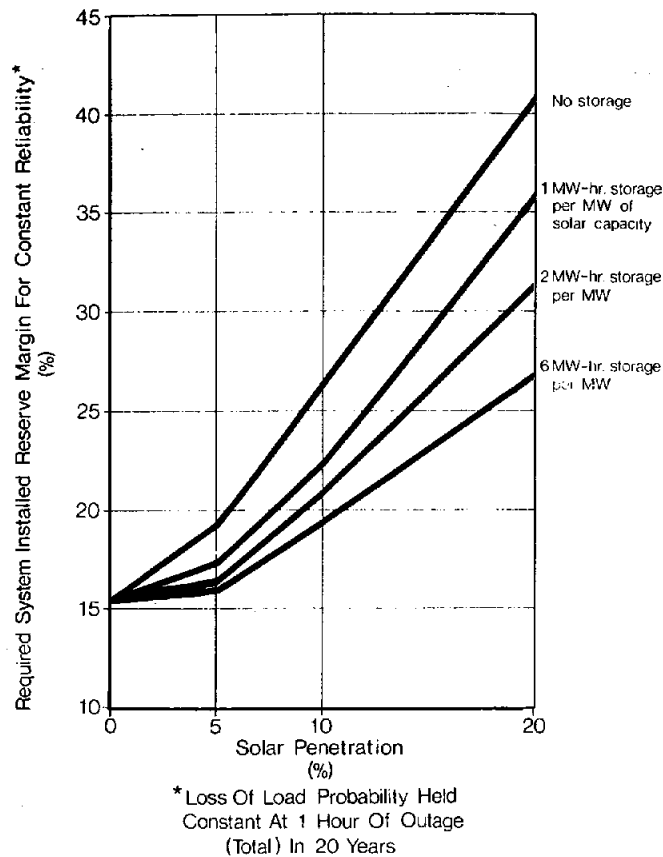
Figure 16. Required Installed Reserve Margin vs Solar Penetration

System and Energy Costs

With many uncommercialized technologies, there is far greater uncertainty relative to the cost of the system than there is with the technical performance parameters. This is certainly the case for specific solar thermal plant subsystems, heliostats being the prime example. However, some subsystems are either familiar components being used in a new way, such as concrete towers, or components with which there is some industrial experience in non-solar applications, such as liquid sodium/salt steam generators. The intent of this section is twofold--first, to show the breakdown of the estimated capital and busbar energy costs of these plants, and second to present cost breakdowns for each of the subsystems in enough detail to allow the reader to make his own assessment of the uncertainties.

The cost estimates are based on conceptual rather than preliminary or detailed designs. Nonetheless, all subsystems (with the exception of the collector) will be familiar to anyone who estimates the cost of large thermal power systems. As mentioned in the technical section on heliostats, there have been many studies of the processes involved in their manufacture. These studies have all indicated that the near-term DOE heliostat cost goal ($70/m^2) can be met. Not only has there been reasonable agreement on the total heliostat cost, but there is also a general consistency between items of the estimated heliostat cost breakdowns.

Knowledge of power rating and capacity factor is not enough to specify the cost of a solar plant since many different size storage units may be coupled with the same heliostat field and turbine. In fact, the buyer of a solar plant will size the storage subsystem based on considerations related to the load profile and the balance of the system. Figure 17a shows plant busbar energy cost for a salt system over a range of capacity factors optimized (minimum busbar energy cost) when a turbine priority dispatch strategy is used. The operational and maintenance costs and economic assumptions on which these charts are based are as follows:

* System Financial and Operating Lifetime   30 years

* Federal and State Effective Income Tax Rate   50%

* Annual Rate of Return on Bonds   10%

* Effective Cost of Money   10%

* Interest and Escalation During Construction for
    Solar Plants Based on Details of 5.5 Year
    Construction Schedule

* Double Declining Balance Depreciation Over 30 Years

* Capital Escalation Rate   8%

* Operations and Maintenance Costs Escalate at 8%

* Year of Commercial Operation   1990

* General Inflation   8%

* No Investment Tax Credit

The estimated total installed capital costs on which these figures were based are shown in Figure 17b. These curves were scaled from a salt system with a capacity factor of approximately 40%. Note in this figure that the cost would not change by more than 10% even if the amount of storage were doubled, indicating that dispatch strategies other than turbine priority will not significantly change the plant capital or busbar energy costs. A summary of the detail cost estimates for salt, sodium, and air technologies is presented in Table IV. The estimates are for a 100-MW$_e$ plant with a solar multiple of 1.5 and three hours of storage. These are normalized numbers which were based on contractor inputs for conceptual designs. To date, the validity of these numbers has not been verified by independent detailed cost estimates.

The first reaction to these energy costs is that they were considerably higher than the cost of electrical energy produced by conventional means. It should be remembered that these are 30 year levelized costs and 30 year levelized costs of fossil produced electricity is expected to be more than twice present costs.

40
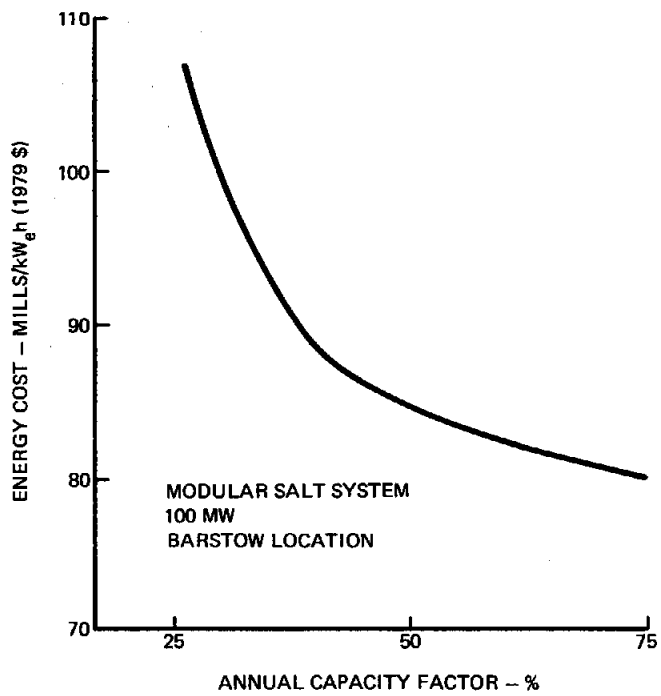
Figure 17a. Levelized Busbar Energy Cost
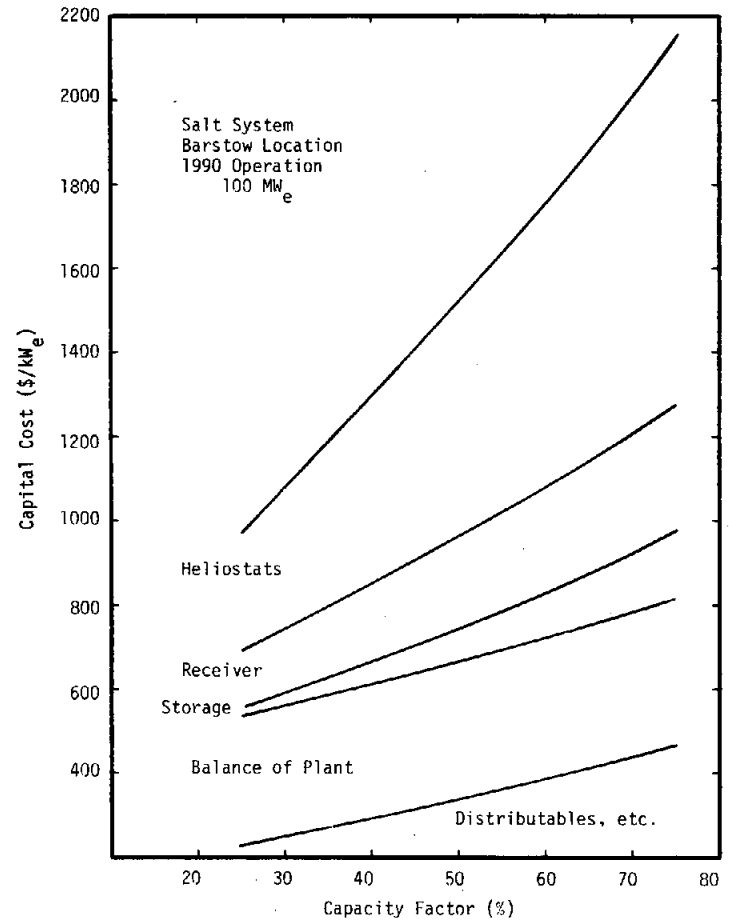
Figure 17b. System Capital Cost

41

TABLE IV

ESTIMATED CAPITAL COST, $X10^3$; 100 MW$_E$
1.5 SOLAR MULTIPLE; 3 HOURS STORAGE
(SANDIA NORMALIZED ESTIMATE)

SUMMARY	SODIUM	AIR/BRAYTON	SALT
4100 Site, Structures, and Miscellaneous Equipment	7,700	8,400	7,700
4200 Turbine Plant Equipment	19,000	31,700	19,000
4300 Electric Plant Equipment	4,000	4,000	4,000
4400 Collector Equipment	45,000	48,000	45,000
4500 Receiver Equipment	13,700	32,000	17,900
4600 Thermal Storage Equipment	10,400	18,300	4,300
4800 Distributables and Indirects	29,000	44,100	29,500
4900 Master Control			
Total Invested Cost	128,800	186,500	127,400

Hybrid Systems

A solar central receiver hybrid power system consists of a solar energy collection subsystem and a non-solar energy subsystem at a single, common site. They would typically be operated in the intermediate or base capacity mode so that the output is essentially independent of variations in insolation. The solar energy may be combined, before or after conversion to mechanical or electrical form, with energy from a non-solar source. The non-solar sources may be fossil-fueled, hydro-electric, geothermal or other possible energy sources; nuclear energy sources, however, were not studied.

Two hybrid configurations are possible -- parallel and series. In the "parallel" configuration, the solar central receiver is capable of fully satisfying the system load under conditions of adequate insolation; at other times, the solar input is supplemented, or completely replaced, by thermal energy from the non-solar source. The system also incorporates a thermal storage unit, which is charged with excess energy from the receiver, and discharged to the inlet port on the turbine prime mover. In the "series" arrangement, the non-solar source may provide supplemental energy as before,

maintaining full turbine inlet temperature or pressure under reduced insolation conditions; it may also be employed on a continuous basis to enhance the overall performance of the plant (as, for example, by the use of fossil fuel combustion to increase the temperature or pressure of the working fluid above a limit imposed by solar receiver material constraints). Many other combinations and interface arrangements are possible; for example, the solar and non-solar inputs may be combined at a later stage in the energy conversion sequence by mechanical or hydraulic coupling of separate prime movers or even at the primary terminals of the plant output transformer.

Line Focus Systems

Line focus solar central power systems fall into two categories: central linear receivers and distributed linear receivers (Figures 18 and 19). The central linear receiver system consists of a long elevated receiver used in conjunction with multiple rows of focused, linear concentrators located parallel to the receiver. The distributed linear receiver system incorporates an individual linear receiver along the focal zone of each concentrator. In both of these systems the receivers generally have lengths much greater than their cross sectional dimensions. Each concentrator is a focusing type, in which focusing can be achieved by curved, segmented, or slatted construction. These concentrators may have a single axis drive mechanism which controls their orientation and/or focal length to maintain an image of the sun on a linear receiver. An alternative to tracking or focusing concentrators is to have the concentrator stationary and the receiver move so that it is always in the focal zone. Major subsystems include concentrators, receiver(s), heat transport, energy storage, electrical power generation, and master control.

Normally, line focus concentrators have one-axis tracking rather than the two-axis tracking required for point focus systems. This may mean fewer drives, bearings, and mounts. It may also mean that the concentrator can be closer to the ground and therefore will require less supporting structure and foundation due to reduced wind loading. The line focus systems may have a higher reflector surface density in the concentrating field because the collector may be essentially continuous in one dimension. This may mean lower optical losses and lower operation and maintenance costs. Line focus systems, for the same collector area, typically yield both lower fluid outlet temperatures and lower receiver efficiencies than point focus systems because of a lower concentration ratio.

COLLECTOR

RECEIVER

THERMAL
STORAGE

TURBINE/GENERATOR

1 STORAGE CHARGING CYCLE
2 DIRECT GENERATION CYCLE
3 STORAGE GENERATION CYCLE
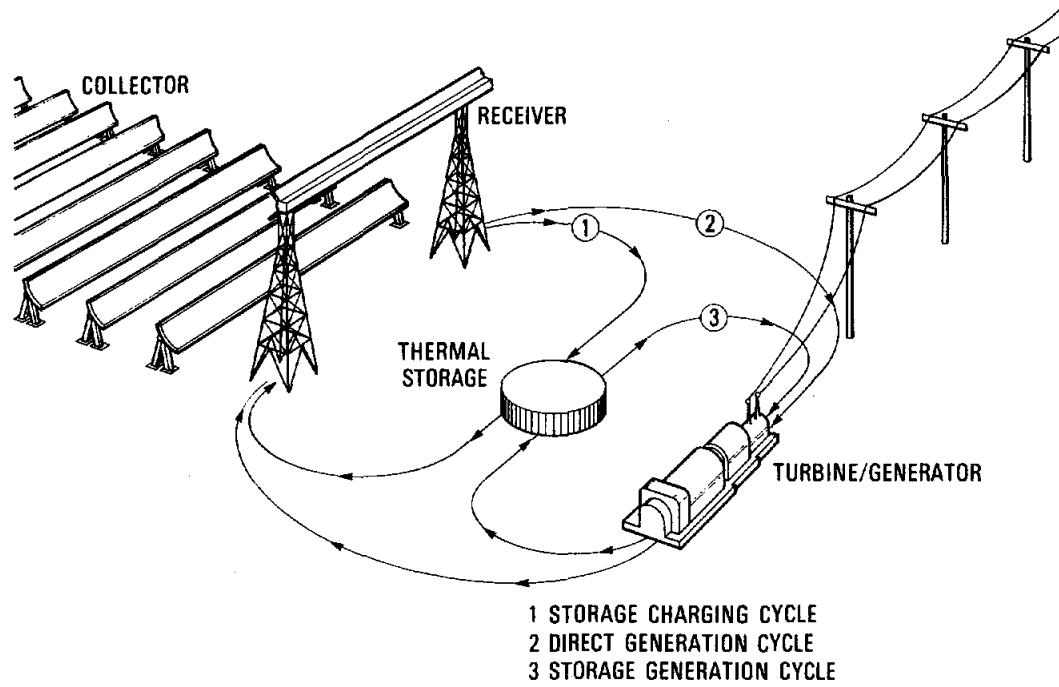
Figure 18. Line Focus (Central Receiver)

CONCENTRATOR/RECEIVER

THERMAL
STORAGE

TURBINE/GENERATOR

1 STORAGE CHARGING CYCLE
2 DIRECT GENERATION CYCLE
3 STORAGE GENERATION CYCLE
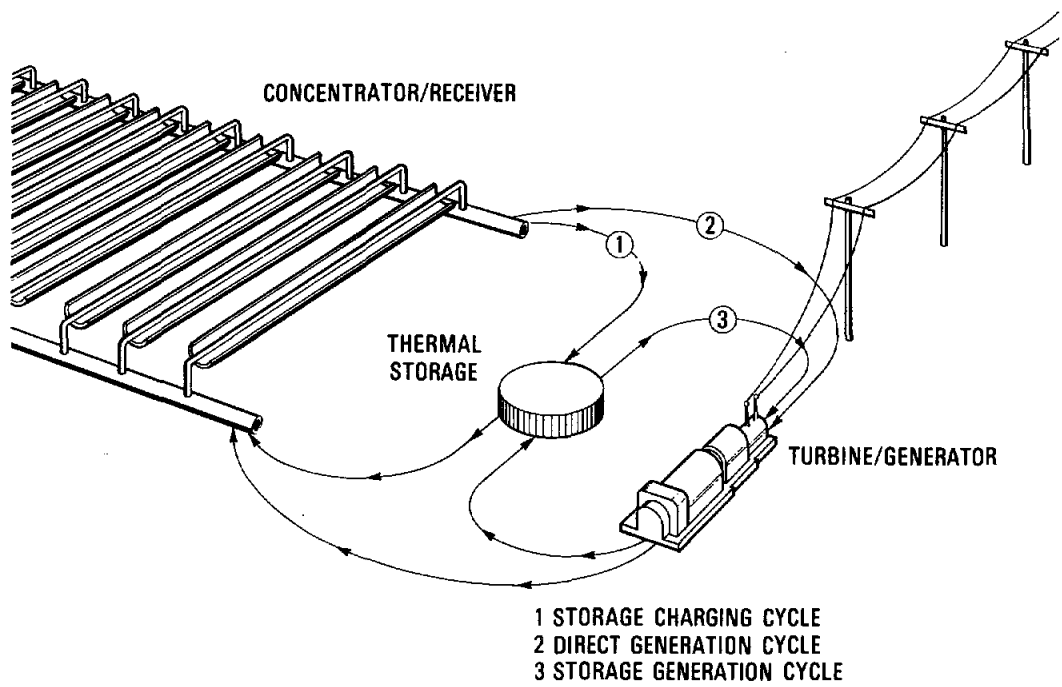
Figure 19. Line Focus (Distributed Receiver)

RESEARCH AND DEVELOPMENT ACTIVITES

A detailed discussion of the heliostat, storage-coupled, hybrid, and line focus activities is presented in this section. The heliostat activities are covered in a separate section because the heliostat development is being conducted as a separate, independent activity. The storage-coupled concepts are covered in greatest detail because of the available information and state-of-development of the concepts.

Collector Subsystem

The heliostat field constitutes the largest fraction of the costs for solar central power generation. For this reason, particular emphasis is being given to the cost reduction of these components. Heliostat cost goals have been established as a result of allocating overall power plant cost targets to the various subsystems. The present goal of the heliostat development program is to achieve an installed cost of $65/m^2 at 90% reflectivity. The attainment of this goal, in conjunction with cost targets for other subsystems, will provide a competitive alternative to the use of oil and natural gas for electric power generating utilities in the late 1980's and 1990's.

First-Generation Designs

A concentrated heliostat development effort was initiated in 1975 when four contractor teams led by Boeing Engineering and Construction Company, Honeywell Incorporated, Martin Marietta Aerospace, and McDonnell Douglas Astronautics were funded to complete design studies for first-generation heliostat concepts. These two-year efforts culminated in the fabrication and testing of prototype heliostats based on the concepts developed. As shown in Figure 20, the Honeywell, Martin Marietta, and McDonnell Douglas designs are examples of heliostats that use a mirror that is exposed to the environment; the Boeing design illustrates a second type in which the reflective surface is an aluminized or silvered plastic membrane that is protected from the environment by a plastic enclosure (dome). An extensive design critique and costing evaluation for each of the designs were undertaken to select the best heliostat design for the 10-MW$_e$ pilot plant planned for Barstow, California. The design developed by McDonnell Douglas was chosen in mid 1977 as the best conceptual solution to the pilot plant needs. One of each of the prototypes developed by the contractors was subsequently installed in Livermore, California, where continued testing and evaluation are being conducted.
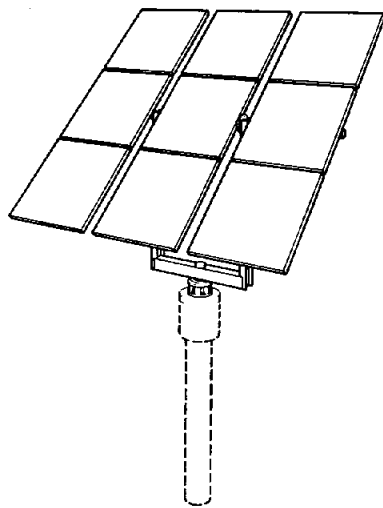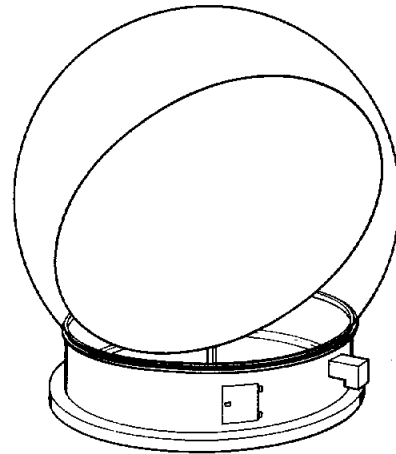
MARTIN-MARIETTA
BOEING
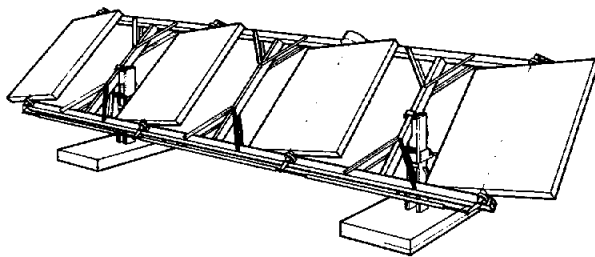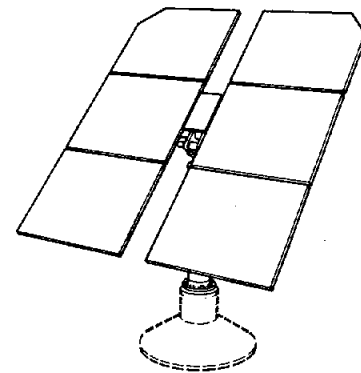
HONEYWELL
McDONNELL DOUGLAS

Figure 20.   First Generation Heliostats

Prototype Heliostats

Conceptual designs for components applicable to the second generation of heliostats were initiated in October of 1977.   Contracts were awarded to Boeing Engineering and Construction, General Electric, McDonnell Douglas Astronautics, and Solaramics Incorporated.   The purpose of the program was to significantly reduce the cost of the first-generation designs.   Each contracor developed a heliostat design with associated manufacturing, assembly, instal- lation, and maintenance approaches.   Capital and operations and maintenance costs were estimated for a one-time production of 2,500 units and for contin- uous production rates of 25,000, 250,000, and 1,000,000 units per year. Drawings of the four heliostat designs are shown in Figure 21.

46

OBJECTIVES

- Low Cost Mass Production Design
- Detail Cost Estimates
- Broad Industry Participation
- Identify Required R&D

BOEING

GENERAL ELECTRIC

McDONNELL DOUGLAS

WESTINGHOUSE

SOLARAMICS
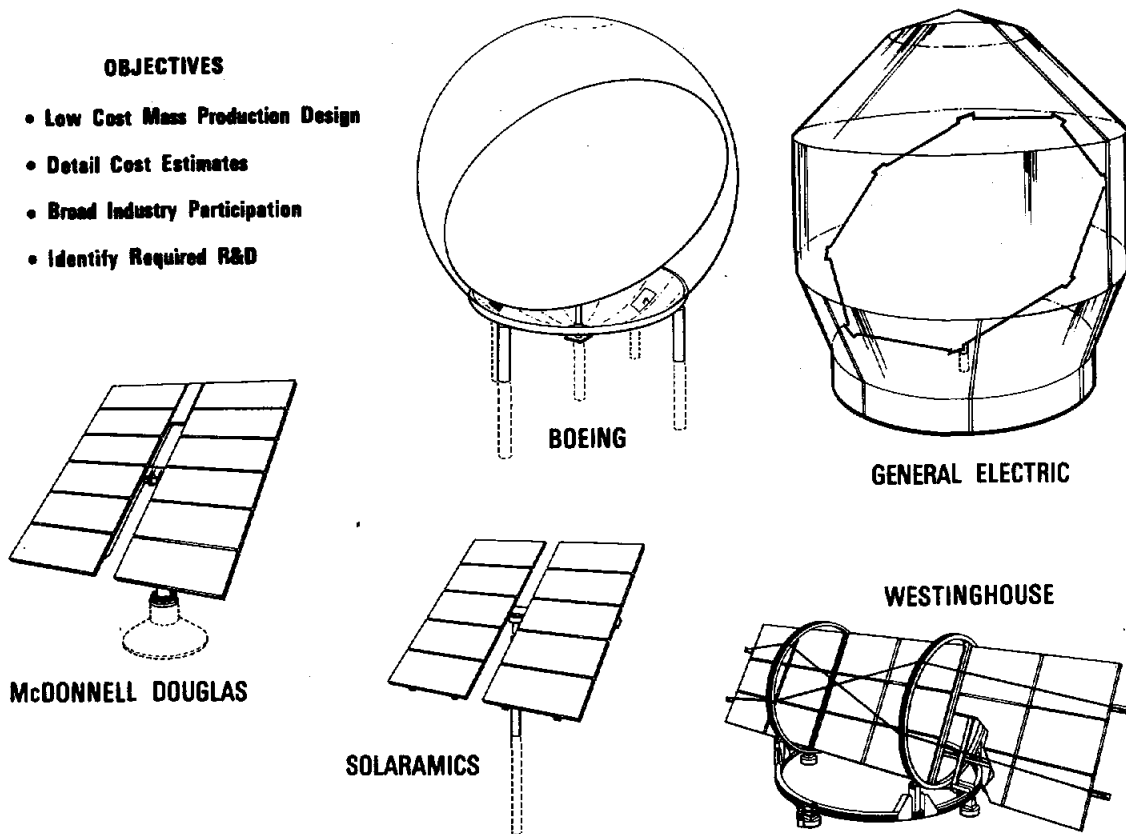
Figure 21. Prototype Heliostats

In addition to the four designs entirely funded with federal dollars, an encouraging precedent in heliostat development is that Westinghouse is developing a heliostat entirely funded with their internal funds. Under a no-cost agreement with Westinghouse, Sandia has been periodically reviewing their design progress and will test a resulting prototype at a DOE facility. In exchange, Westinghouse has agreed to publicly disclose design features and costing numbers generated. As a result, five prototype heliostats were under development rather than just the four that are fully federally funded.

The major changes that McDonnell Douglas has made to its first-generation design are (1) increasing the reflective area from 37.5 to 49 m^2, (2) refining the drive mechanism, (3) replacing the styrofoam core mirror modules with laminated glass, and (4) designing a tapered fit pedestal/foundation and two-part mirror assembly for easy field installation. The projected operations and maintenance (O&M) costs appear to be low, and the annual capital costs for a 100-MW_e field are lower than for all of the other designs, with the exception of the General Electric heliostat. The main issue to be resolved for the McDonnell Douglas design is the life of the mirror edge seal. The cost estimates at high production rates may be high because more vertical integration and improved mass production techniques are believed possible.

Boeing has lowered the cost of their heliostat by replacing the cylindrical enclosure base with a steel dish mounted on stanchions. The enclosure is now a 9.75 m diameter, single-piece, plastic dome, blown to a thickness of 0.007 cm by a yet-to-be-developed process. The heliostat design has remained essentially the same, although it has increased in size from 48 to 66 m². There are several major concerns with this design. First, both the annual capital and total costs for this heliostat are the highest of the four concepts. Second, data on the mechanical and optical properties of the enclosure and reflector plastics are very limited, and the useful life of the plastics cannot be predicted accurately at this time. Third, considerable process development is needed to manufacture one-piece domes. Finally, more vertical integration and mass production methods are needed to lower the cost.

The General Electric heliostat was designed for high volume, low cost production. The three-piece zippered enclosure of 0.007 cm thick weatherized plastic is attached to an earth-filled bag foundation. The heliostat has an octagonal stretch-frame reflector of aluminized mylar and molded plastic drive components. The major concerns with this heliostat are high O&M costs and high technical risk. As with the Boeing design, the optical and mechanical life of the plastics is unknown. Also, the foundation design appears to be especially high-risk, with little cost advantage over other foundation concepts. The total annual cost of the General Electric heliostat concept is potentially competitive with the McDonnell Douglas concept at high producton rates (250,000 units/year).

Unique features of the Solaramics heliostat include 0.025-cm thick microglass mirrors mounted on panels of foamed glass, a one-piece ceramic pedestal set in place with high density urethane foam, and an azimuthal axis which is tilted 23° from vertical away from the receiver. Linear actuators with bell crank mechanisms are used for both azimuth and elevation drives. The design appears to be cost effective but requires further testing and analysis to verify the cost and reduce uncertainties about the design. Process development is needed for both the foamed glass mirror panels and the ceramic pedestal. The microglass has handling problems, and the mirror module is untested. The drive system with the tilted axis is only a conceptual design at this time and has potentially high backlash and low stiffness. However, the drive system is worth further investigation because of its potential low cost. Finally, production costs of the heliostat can probably be reduced by further use of mass production techniques.

A summary of the design characteristics and costs of the four prototype heliostat is given in Table V. This table also lists the Barstow pilot plant heliostat design characteristics and costs for comparison. Further development of the conceptual heliostat designs that are designated prototype heliostats were limited to component studies in 1979. In late 1978 a new solicitation for detailed heliostat design, test unit fabrication, and side-by-side comparative testing was initiated. This effort, which will lead to four or five different contractor projects, will utilize all previous heliostat data and has been designated the Second-Generation Heliostats.

48

TABLE V

PROTOTYPE HELIOSTAT SUMMARY

	Pilot Plant MDAC Nth Plant	MDAC	BEC	GE	Solaramics
Significant Design Features	Styrofoam - Core Mirror Modules, Inverted Stow, Pedestal-Mounted Drives & Reflective Unit	Laminated Glass Mirror Modules, Inverted Stow, Pedestal-Mounted Drives & Reflective Unit	One-Piece Enclosure, Dish Base with 3-Pedestal Foundation, Ring Stretched Reflector	Zippered 3-Piece Enclosure, Earth-Filled Bag Foundation, Octagonal Stretch-Frame Reflector	Foamed Glass - Micro-Glass Modules, One Piece Ceramic Pedestal Foundation, Pedestal-Mounted Drives and Reflective Unit
Reflective Area (m^2)	37.5	49	66	55	38.6
Heliostats/ 100 MW_e	23300	16900	20300	26100	21100
Gimbaled Weight (lb)	3005	3668	366	164	3658
Total Weight (lb) (w/o concrete)	3520	4041	2390	468	5995
Net Reflectivity	.91	.92-.95	.70	.64	.95
Capital Cost* $(\$/m^2)$	95	62	54	27	76
Annual Cost** ($/100MW$_e$/yr) Capital* O&M Total	8.6×10^6 1.5×10^6 10.1×10^6	5.3×10^6 $.7 \times 10^6$ 6.0×10^6	7.6×10^6 2.0×10^6 9.6×10^6	4.4×10^6 3.0×10^6 7.4×10^6	6.3×10^6 $.7 \times 10^6$ 7.0×10^6

*250,000 heliostats per year, 8% fee and 10% contingency included
**Includes land and field wiring

The different design concepts and materials for the major components which might be used on a heliostat with glass mirrors and on enclosed heliostats are listed in Tables VI and VII respectively. Some of the rationale for the different design choices are also given. Contracts will be let to several successful bidders for heliostat design, fabrication of prototypes, testing and cost estimates.

Cost/Performance Analysis

The current basis for heliostat cost and performance comparison is the life-cycle cost of a field of heliostats capable of producing 500 MW_t. It is necessary to use life-cycle costs for a fair comparison because the plastic designs have low capital and high O&M costs, while for the glass designs the opposite is true. It is necessary to use total field cost and performance because the cost (per heliostat) of land and wiring and the energy loss due to spillage and attenuation increase with field size, and the enclosed designs require larger fields. The life-cycle costs are expressed as the uniform (levelized) annual cost of the 500-MW_t field, assuming a 30-year life, 11 percent after-tax cost of money, 50 percent income tax rate, 6 percent inflation, and Sum-of-the-Year's-Digits accelerated depreciation. This is intended to simulate a typical utility company's economic analysis.

The results of the cost and performance evaluation are shown in Figure 22. The cost of the two glass heliostats is approximately 60 percent of the cost of the plastic designs at the 25,000/year production rate, while at higher production rates the McDonnell Douglas heliostat is about 20 percent cheaper than the nearest competitor. There is considerable uncertainty in these life-cycle cost estimates because they depend on costs derived by four different costing methods, projections from different production scenarios, varying degrees of design maturity, and preliminary performance estimates. Despite the uncertainties, the estimated cost advantage of glass heliostats at the low production rate (25,000/year) is large enough to be considered significant.

For both plastic and glass designs, 60-90 percent of the O&M cost is the cost of washing at the optimum frequency. This cost is greater for the plastic domes because approximately five times as much dome surface area must be washed for a given reflector area. Possible differences in dirt accumulation rates between glass and plastic may alter the differences in O&M costs; however, data are not available at this time.

The Sandia computer code DELSOL was used to generate a cost-optimal field layout and calculate the annual performance of the field. Different pointing accuracies, receiver sizes, and tower heights were investigated to ensure that the comparison was not biased in favor of any one heliostat design. The results of this effort were the required number of heliostats and the required land area, which were combined with the costs per heliostat and $1.66/$m^2$ for land to yield a total field cost.

50

TABLE VI

DESIGN CONCEPTS FOR HELIOSTAT COMPONENTS: GLASS MIRRORS

COMPONENT DESIGN CONCEPT	MATERIALS	RATIONALE
Foundation		
Poured In-place Pile	Reinforced Concrete	Stability Low Cost
Poleset Supported Pile	Pre-stressed Concrete	Low Cost Fast Installation
Support Structure		
Central Pedestal	Galvanized Steel Thinwall Pipe	Strength Weatherability
	Pre-stressed Concrete	Weatherability Fast Installation
Large Drive Wheels	Painted Steel	Large Dimensional Tolerances Reduced Loads
Drive Mechanisms		
Harmonic Drive Linear Screw Drives Conventional Gear Box	Steel	Low Backlash Stiffness
Mirror Support Structure		
Truss Assemblies Roll Formed Steel	Painted Steel Galvanized Steel	Commercially Available Producibility

TABLE VI (cont'd)

COMPONENT DESIGN CONCEPT	MATERIALS	RATIONALE
Wiring and Electronics		
Direct Burial Cable, Electronics in Field	Conventional Cables & Electronics	Low Cost
Mirrors		
Thin Glass, 2nd Surface, Silvered Mirror	Corning Fusion Glass Aluminsolicate Lime Borosilicate	High Specular Reflectivity
	Float Glass Soda Lime	
Microglas, 2nd Surface, Silvered Mirror	Soda Lime	High Specular Reflectivity
Silver w/Protective Covercoat	Silicone	Reflectivity Producibility
Mirror Substrate		
Steel, Polystyrene Sandwich	Galvanized Steel Styrofoam 1B	Low Stress in Glass
Steel, Honeycomb Sandwich	Painted Steel AL Honeycomb	Thermal Stability
Foamed Glass	Solaramics Pittsburgh Corning	Thermal Staility Matched Expansion coefficient Low Stress in Glass

TABLE VI (cont'd)

COMPONENT DESIGN CONCEPT	MATERIALS	RATIONALE
Float Glass Steel Support	Soda Lime Glass	Producibility Thermal Stability Low Stress in Glass
Float Glass Edge Support	Soda Lime Glass	Producibility Thermal Stability Low Stress in Glass
Transfer Molded Epoxy Fiberglas	Epoxy Glass	Producibility

TABLE VII

DESIGN CONCEPTS FOR HELIOSTAT COMPONENTS: ENCLOSED HELIOSTATS

COMPONENT DESIGN CONCEPT	MATERIALS	RATIONALE
Foundation/Dome Support		
Buried Soil Filled Plastic Bag	30 mil Reinforced Polyester	Producibility
Molded Plastic Bowl w/Concrete Piles	Plastic	Producibility
Support Structure		
Steel Pipe	Steel	Rigidity
Al Tubing/Steel Pipe	Aluminum/HSLA Steel, Galvanized	Producibility
Drive Mechansims		
Linear Motors	Molded Lexan Drive Wheel	Producibility Few Parts Low Backlash
Wiring, Electronics, Blower Motors		
Direct Burial Cable Field Electronics Permanently Lubricated ac Motors	Conventional	Low Costs
Mirror Support Structure		
Stretch Frame	AL Tubing Steel Wire	Producibility
Folding Frame	AL Tubing	Producibility
Enclosure		
One Piece Thermoformed Dome, Zippered Sections, or Bonded Gores	Weatherized Polyester Polyvinylidene Fluoride	Low Costs Weatherability Low Flammability
Mirror		
Stretched Film	Aluminized Mylar (.002" Thick) Silvered Mylar w/Overcoat	Light Weight High Reflectivity Light Weight
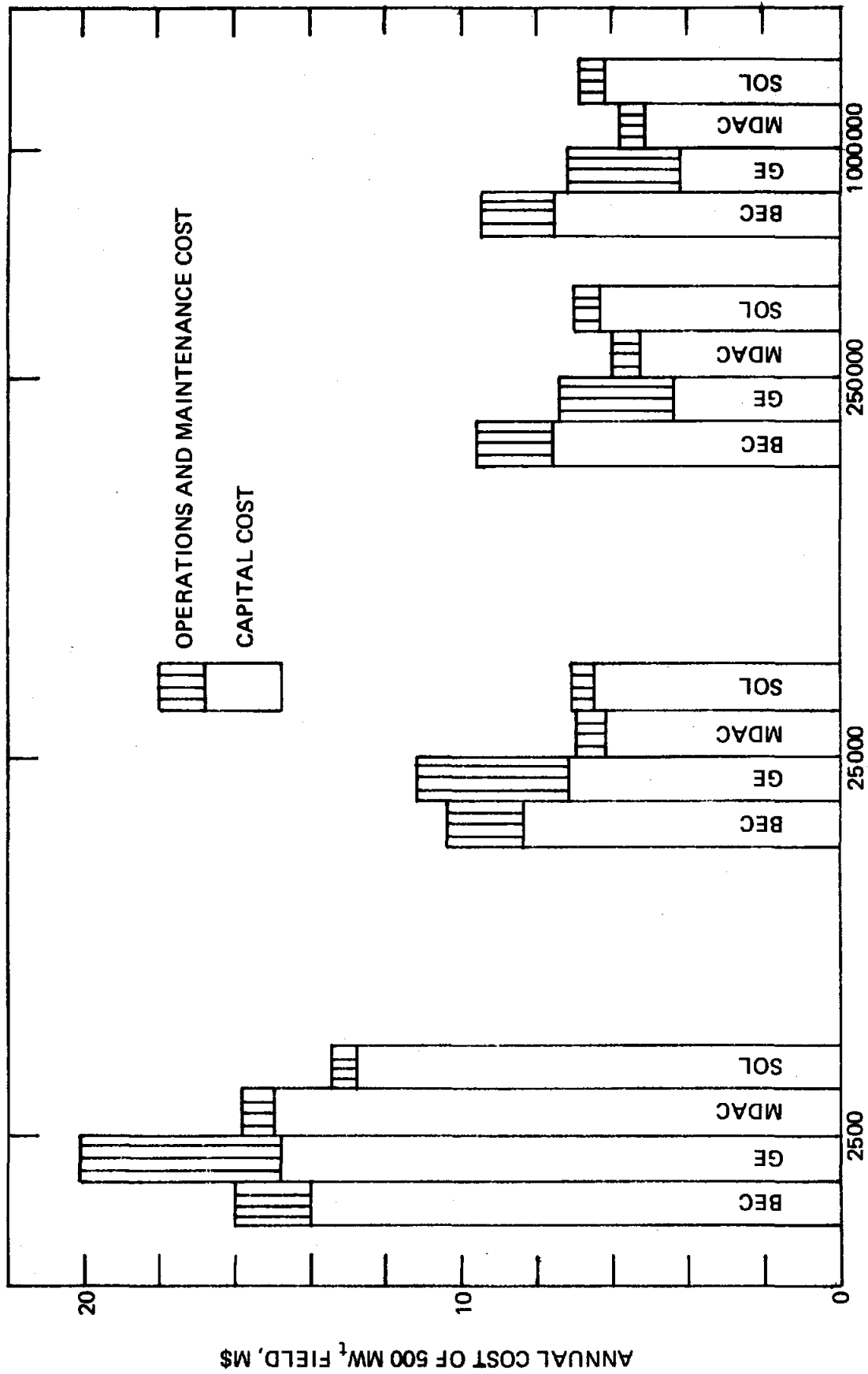
Figure 22. Adjusted Annual Cost of Collector Field

Figure 23 shows the cost estimates for three different glass and
steel heliostats. CRTF is the Martin Marietta heliostat installed at the
Central Receiver Test Facility, MDAC PDR is the McDonnell Douglas heliostat
proposed for the 10 MW pilot plant, and MDAC prototype is the new McDonnell
Douglas design described above. The prices paid and estimated costs (in 1978
dollars) are divided by mirror area and clean reflectivity to obtain the
$/m^2-R figures shown. The horizontal lines are drawn at the average lot
price or cost; actual unit cost should decrease during each production run.

Figure 23 also presents the expected heliostat cost as a function of
production experience. Costs decrease for a combination of reasons, including
improved design, automated production, assembly, installation, labor learning,
and increased production volume. The cost estimates come from detailed
costing of point designs (including production and installation scenarios),
but they all happen to fall within a band of 85% learning curves. This much
cost reduction is commonly achieved in mass production, so the cost estimates
appear to be credible.

Storage-Coupled Systems

Five working fluids are being investigated in storage-coupled designs:
water/steam, air, helium, molten salt, and sodium. The water/steam system is
the most developed and, as a result, it will be used for the 10-MW$_e$ pilot plant
currently under construction. These systems were developed during the first-
and second-generation water/steam programs and the Advanced Central Receiver
Program. The details of each of the programs are presented in the following
sections.

First Generation Water/Steam

DOE funded two water/steam solar programs: first generation and second
generation. The "first-generation" program began in June, 1975 and was a
two-year research and development program to develop the necessary technology
for a solar central receiver pilot plant. Three contract teams--headed by
Honeywell, Martin Marietta, and McDonnell Douglas--conducted parallel and
competing programs to develop conceptual designs for the pilot plant.
Concurrent with these efforts, a fourth contractor, Boeing Engineering and
Construction, designed a heliostat that could be incorporated into the pilot
plant designs.

To reduce development time, the Rankine water/steam cycle with the steam
generated in the receiver was chosen by DOE for the first-generation central
receiver system. Although water/steam systems do not offer optimal performance,
large scale demonstration of the system within ten years is feasible without
major technological advancements. In addition, commercial technology in the
electrical power generation field directly applicable to the receiver-steam
generator and turbine can be integrated into this relatively simple solar
power concept.
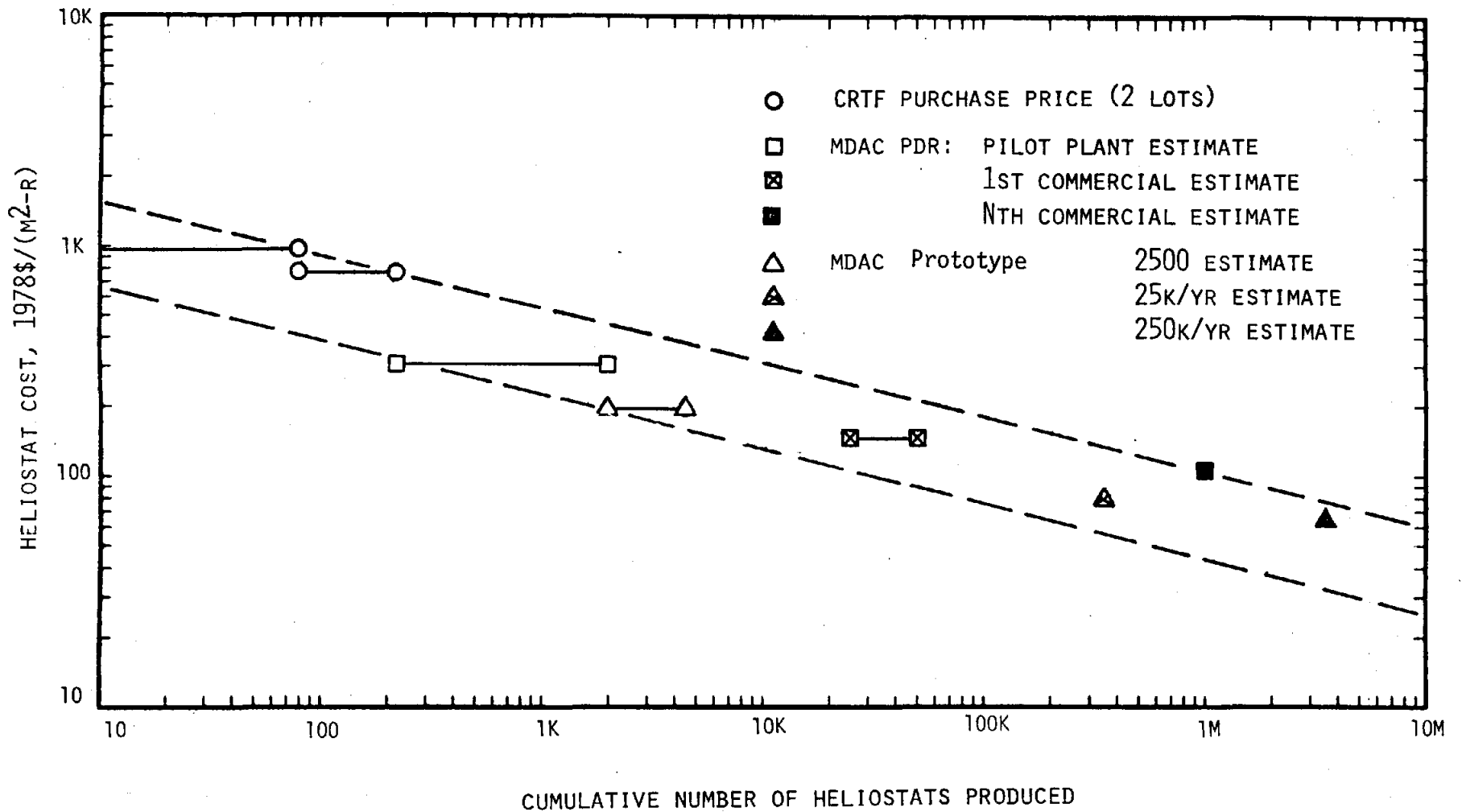
Figure 23. Trend Line for Heliostat Cost Estimates

The figure is a log-log plot titled with axes:
- Y-axis: HELIOSTAT COST, 1978$/(M²-R), ranging from 10 to 10K
- X-axis: CUMULATIVE NUMBER OF HELIOSTATS PRODUCED, ranging from 10 to 10M

Legend:
- O CRTF PURCHASE PRICE (2 LOTS)
- □ MDAC PDR: PILOT PLANT ESTIMATE
- ⊠ 1ST COMMERCIAL ESTIMATE
- ■ NTH COMMERCIAL ESTIMATE
- △ MDAC Prototype 2500 ESTIMATE
- ◮ 25K/YR ESTIMATE
- ▲ 250K/YR ESTIMATE

In designing the central receiver systems, each contractor developed a commercial plant with minimum cost and maximum performance as the primary goals. A pilot plant was designed that represented the characteristics of the proposed commercial plant. DOE's basic requirements for these plants are outlined in Table VIII.

TABLE VIII

DOE SYSTEM REQUIREMENTS

Design Point	Commercial Plant	Pilot Plant
	100 MW$_e$* (Best Sun Angle 950 W/m^2 Insolation)	10 MW$_e$* (2 pm Worst Sun Angle 950 W/m^2 Insolation)
Power Operating From Storage	At Least 70% Of Net Output	At Least 7 MWe
Solar Multiple = $\frac{\text{Max. Power Collectable}}{\text{Design Point Power To Turbine}}$	1.7*	Not Specified
Hours of Storage	3*	3
Plant Availability During Sunlight Hours	90%	90%
Operational Lifetime	30 Yrs	30 Yrs
Site Characteristics	Specified** (Nominally Barstow)	

*Could be altered by contractor with justification
**Survival conditions given, operational limits to be determined by contractor

All the systems generate steam in the receiver, use thermal storage,and incorporate a dual admission turbine. Consequently, the output steam quality of all proposed receivers was similar. The output steam quality of the storage subsystem did vary among the contractors; however, the only resultant difference was that the admission conditions for the turbine varied with the storage system. For these reasons, any combination of the various receiver, storage, and electrical power generation subsystems could be used with minor modifications.

Honeywell--A downward-facing cavity on a tower located approximately one half radius south of center is the distinguishing feature of the Honeywell concept (Figure 24). Sunlight is redirected from a circular field into the aperture of the receiver. The heliostat consists of multifaceted

focused mirrors supported by a steel framework. The individual heliostats are controlled in a coordinated manner by a central computer. Feedwater is converted to steam within the receiver using conventional proved drum boiler technology built to ASME code standards. The steam generated is piped directly to the dual admission turbine or to a sensible heat storage if it is not needed immediately. Two stages of storage are employed: a high-temperature stage consisting of a molten salt stored in separate hot or cold tanks (depending on the state of charge), and a low-temperature stage where energy is stored in a combination of heat transfer fluid and rocks. The bulk of the energy is stored in the low-temperature stage. The quality of steam produced from storage is lower than the charging steam; therefore, the storage steam is injected into the turbine downstream from the main turbine inlet so that steam conditions will match the expansion line characteristics of the turbine. Layout of the Honeywell 100-MW$_e$ plant is illustrated in Figure 25. As shown, four modules would collect energy, and the output of each module would be collected in a single storage and turbine plant facility.

Martin Marietta--The north-facing cavity design concept which evolved is depicted in Figure 26. Martin Marietta tradeoff studies indicate that the optimum size collector-receiver module is roughly the size of their proposed pilot plant. Fifteen modules would be required for a 150-MWe commercial plant. Martin Marietta stated that the modular concept contributed to achieving the high performance goal of the commercial plant by providing "maximized optical performance, thermal conversion efficiency, system reliability, and operational flexibility."
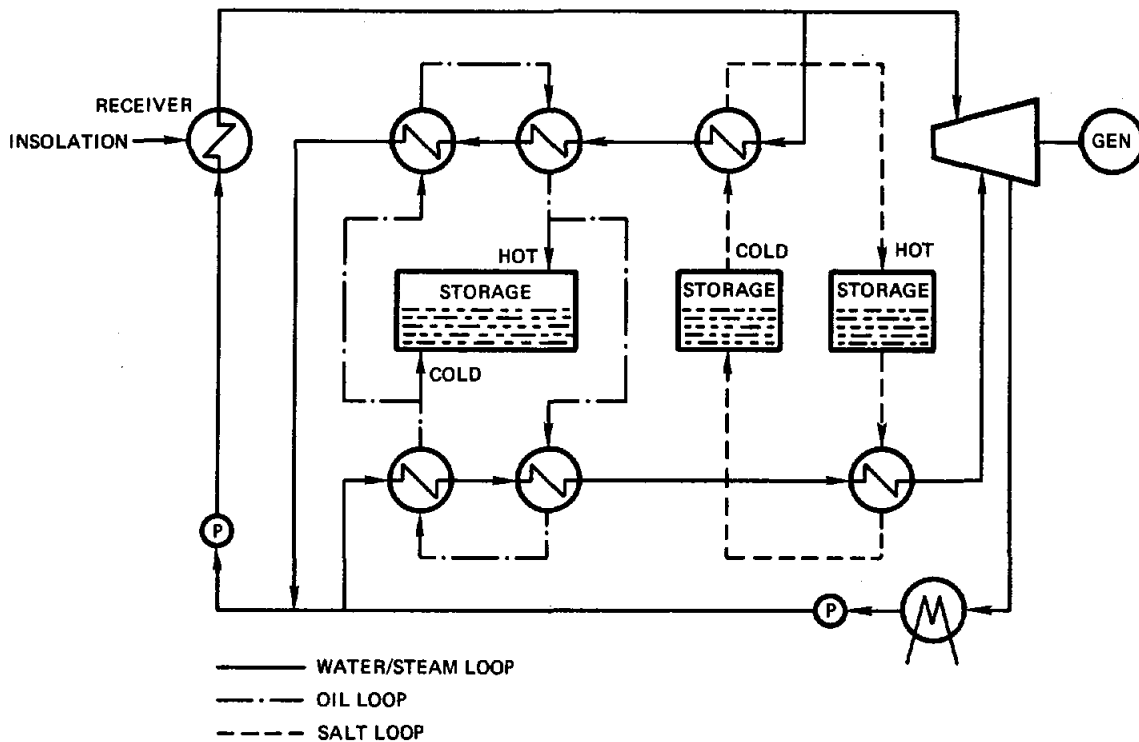
Figure 24. Honeywell Baseline Concept

59
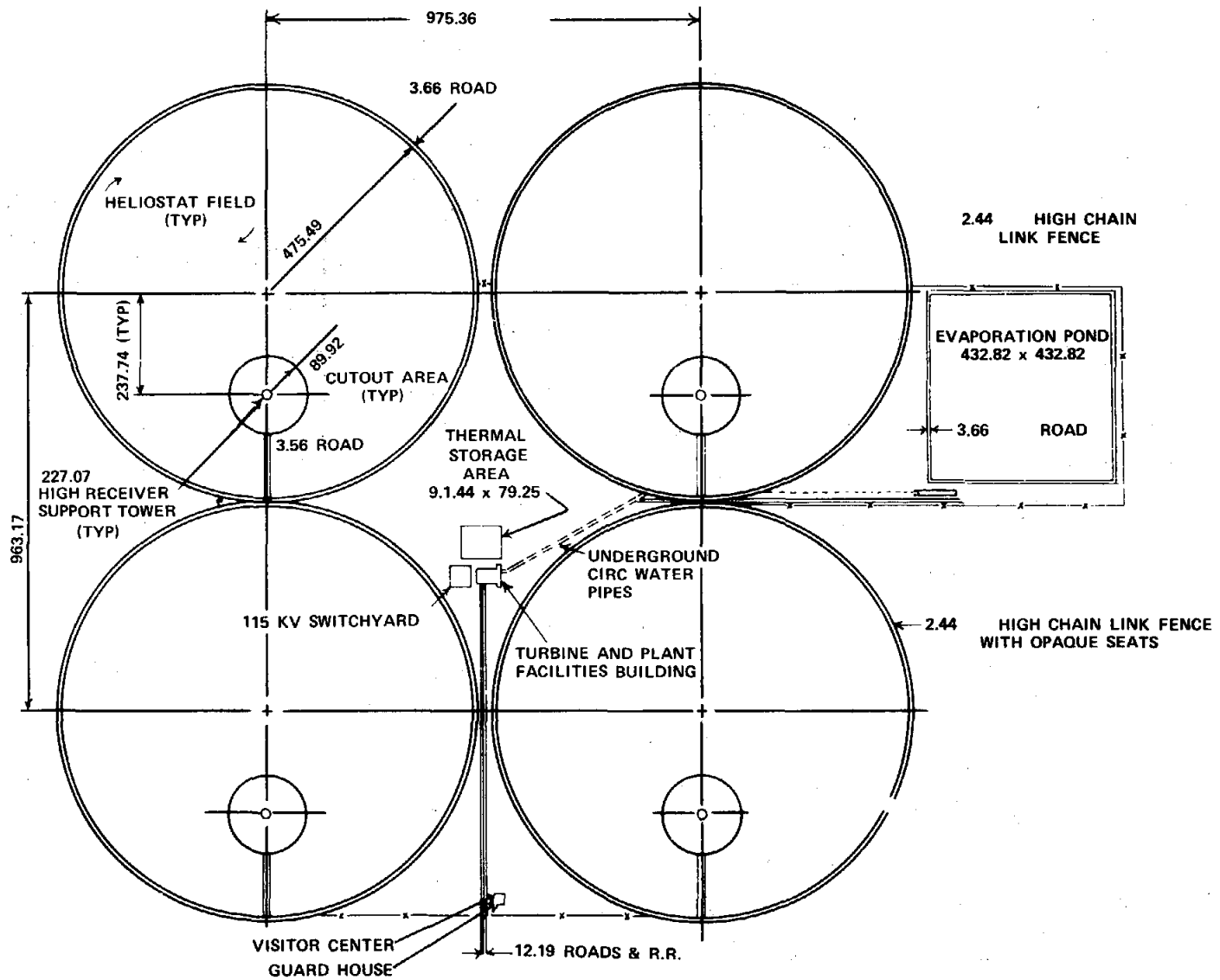
Figure 25. Honeywell Commercial Plant Layout

(a) Commercial Plant Plot Plan

(b) Collector Module

(c) Electric Power Generation Plant

(d) Thermal Storage Subsystem
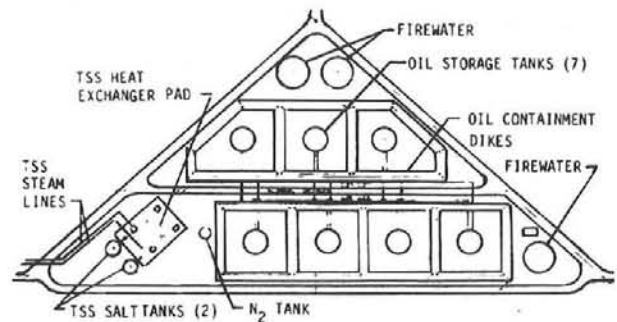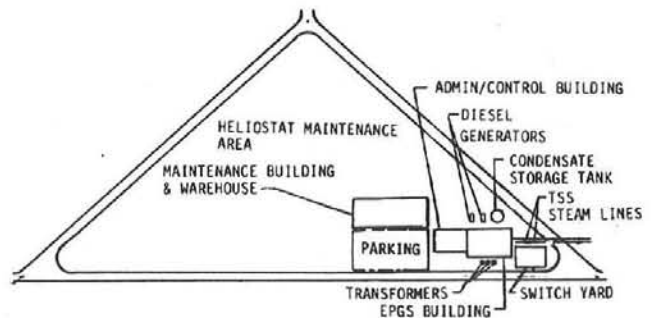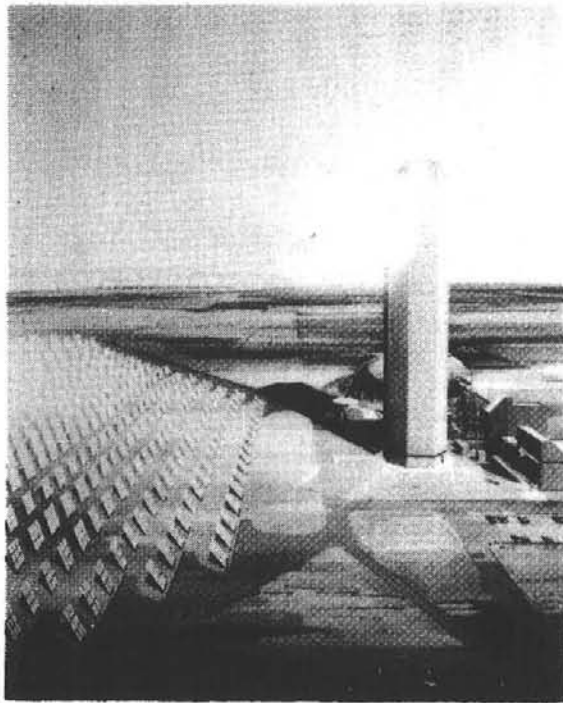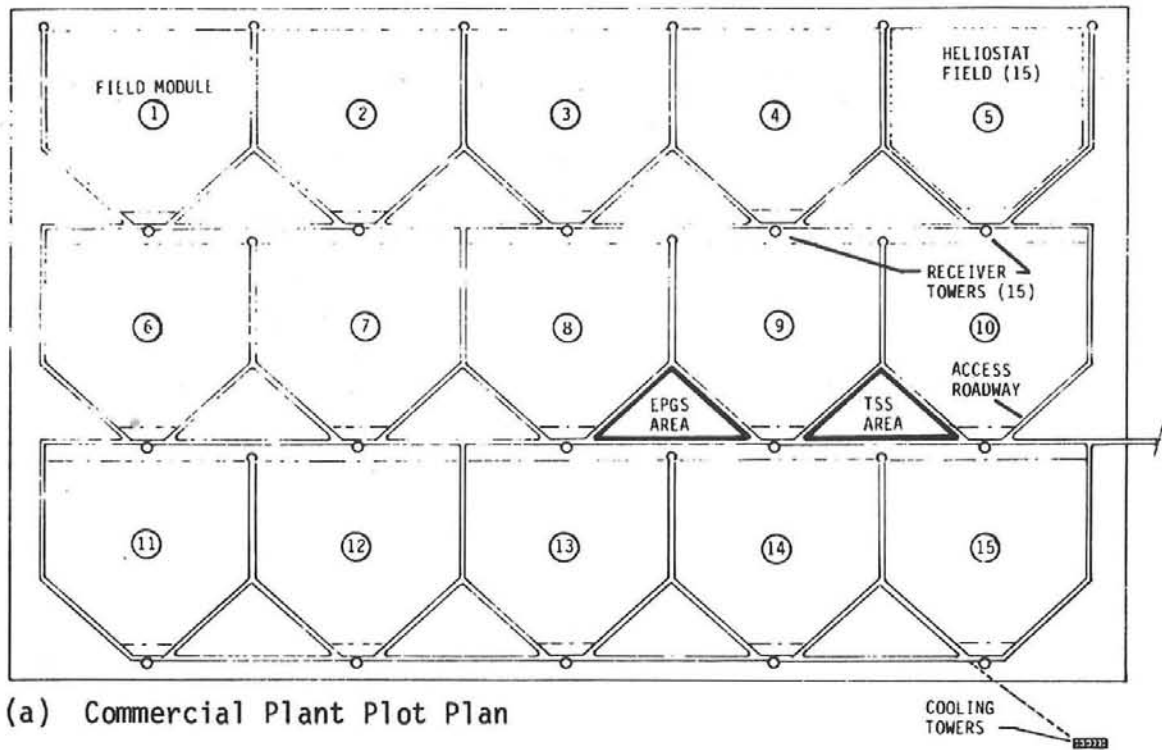
Figure 26. Martin Marietta Baseline Plant Schematic

61
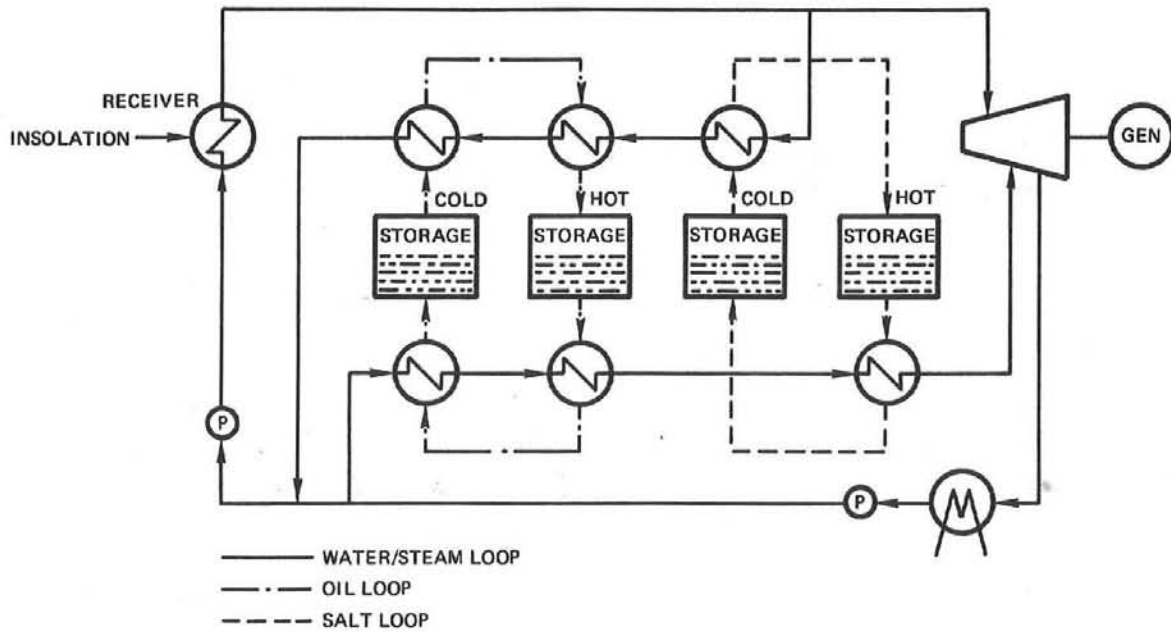
Figure 27. Martin Marietta Plant Configuration

A flow diagram of the commercial plant is shown in Figure 27. Concentrated sunlight enters the north-facing receiver cavity and converts the feedwater to steam. The steam from the individual receivers is conveyed to the central thermal storage subsystem and/or to the electric power generation plant. A large drop in pressure [1.38 MPa] is caused by long pipe runs between the receivers and the EPGS. The multiple receivers do enhance the availability of the plant in that repairs can be made on components of a single module, while the plant operates at a moderately reduced capability.

A two-stage, sensible heat storage system was selected. The low-temperature stage contains a low-cost hydrocarbon heat transfer fluid. Since this fluid is temperature limited, a high-temperature stage is employed so that steam at higher temperature and pressure can be generated. Multiple tanks are used in both stages. One extra tank beyond the minimum necessary for the fluid volume and appropriate piping and valving is included so that hot and cold fluids are separated with a minimum of tankage.

McDonnell Douglas--The key feature of the concept, shown in Figure 28, is the modularized external absorber receiver. Although this receiver tends to have a lower efficiency than cavity-type receivers, it was determined that the lower receiver and lower tower costs would offset the expense of the additional heliostats required to produce a comparable output. Based on tradeoff studies, McDonnell Douglas believes that a single receiver module is optimum for the 100-MWe commercial plant. Closed-loop (in-line sensor) control was proposed for the pilot plant and open-loop control for the commercial applications.

62
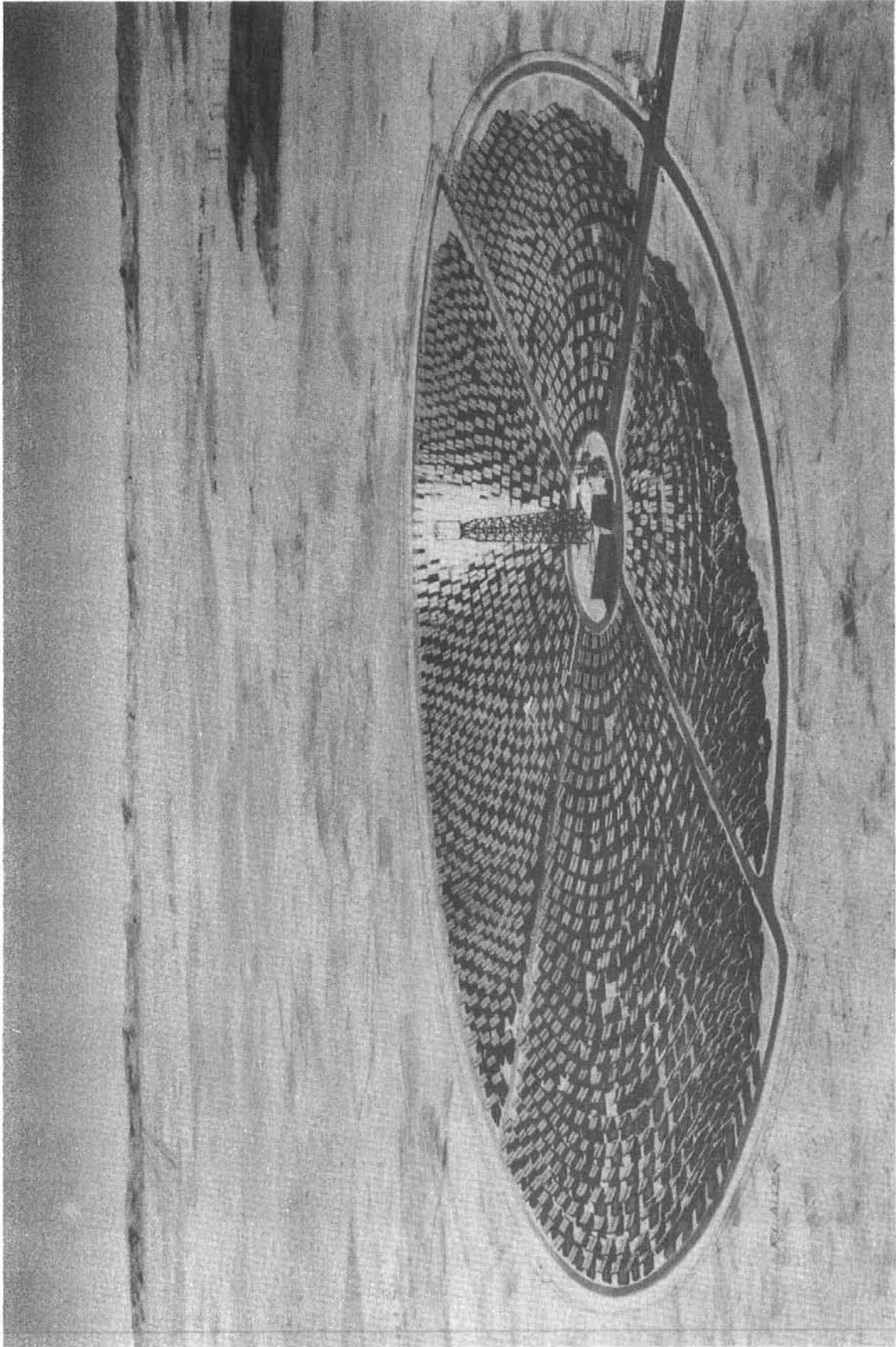
Figure 28. McDonnell Douglas 10-MW$_e$ Pilot Plant Design

63

In operation, insolation reflected from the collector subsystem is concentrated on to the outer surfaces of the 24-panel receiver. Six of the south-facing panels preheat the feedwater. The feedwater is then directed to the 18 remaining panels where individual panel flow control allows the feedwater to be converted into superheated steam in a single upward pass. (Each panel is coated with a high absorptivity material to reduce losses due to reflections.) The superheated steam from the receiver is piped either to the turbine/generator or to thermal storage. As in the Honeywell and Martin Marietta designs, a dual admission turbine has been selected.

The storage system is based on the thermocline principle where both the hot and cooler material are contained in a single tank and separated by a steep temperature gradient. With the hot fluid on top, this situation is stable due to the density difference in the fluid. A hydrocarbon-based heat transfer fluid is used as the heat transport media. Since this material is relatively expensive, much of the fluid is displaced by filling the tank with rocks. Because of temperature limitations of the heat transfer fluid, the quality of steam generated by storage is reduced, thereby reducing the thermal to electric conversion efficiency.

Comparison of Designs--A summary of the commercial plant characteristics for each design is given in Table IX. As shown, each contractor chose a slighty different optimum size plant for their baseline design. The one notable difference in the designs is the number of modules (i.e., the number of separate receivers) selected to produce the necessary thermal power.

TABLE IX

COMMERCIAL PLANT CHARACTERISTICS

	MARTIN MARIETTA	McDONNELL DOUGLAS	HONEYWELL
PLANT SIZE	150 MWe	100 MWe	100 MWe
SOLAR MULTIPLE	1.5	1.7	1.7
STORAGE AT 70% OF RATED	3.0 HR	6 hr	3 hr
NO. OF MODULES	15	1	4
NO. OF HELIOSTATS	23,310	22,914	20,220
HELIOSTAT AREA	40.83 m^2	37.9 m^2	40.0 m^2
REFLECTIVE AREA	9.55 x 10^5 m^2	8.7 x 10^5 m^2	8.09 10^5 m^2
DENSITY	0.20	0.24	0.29
HEIGHT TO APERTURE CENTERLINE	90 M	268 M	237 M
RECEIVER EFFICIENCY	0.945	0.90	0.875
AUXILIARY POWER			
RECEIVER	12 MWe	12 MWe	18 MWe
STORAGE	7.8 MWe	6.1 MWe	9.5 MWe
ANNUAL ENERGY	578,450 MWHe	446,000 MWHe	

After studying the optimizations performed by the contractors, it became evident that the best module size is highly dependent on the specific concept selected (e.g., field layout and tower design). It is also clear that differences in piping layout philosophy and presumed importance of atmospheric attenuation greatly influence the choice of module size. At that point in the development, the optimum module size could not be fully defined. However, selection of the concept based on commercial applications is not strongly influenced by the exact module size.

Table X illustrates the commercial plant design point and annual efficiencies. Annual efficiency calculations were not required for the commercial plant. If Honeywell had made the calculation, the overall efficiency would be similar to that of McDonnell Douglas. The optical performance of the pilot plants is discussed in Table XI.

TABLE X

COMMERCIAL PLANT DESIGN POINT EFFICIENCIES

	HONEYWELL	MARTIN MARIETTA	McDONNELL DOUGLAS
DESIGN POINT (NOON)	EQUINOX	JAN (NOV)	EQUINOX
COSINE	0.93	0.93	0.85
REFLECTIVITY	0.90	0.91 (.69)*	0.91 (.91)*
SHADOWING AND BLOCKING	0.99	0.99	0.98 (.92)
ATTENUATION	0.93	0.96	0.95 (.95)
RECEIVER INTERCEPTION	0.98	0.97 (.83)	0.96 (.96)
RECEIVER	0.88	0.94	0.90 (.90)
CONVERSION	0.39	0.37 (.32)	0.38 (.38)
PARASITIC	0.89	0.93	0.89 (.90)
OVERALL (EXCLUDING COSINE)	0.24	0.27 (.19)	0.25 (.18)

*Annual efficiencies

TABLE XI

YEARLY* OPTICAL PERFORMANCE OF PROPOSED PILOT PLANTS

	McDONNELL DOUGLAS	MARTIN MARIETTA	HONEYWELL
COSINE	.82	.87	.86
OPTICAL LOSSES			
TOWER SHADOW (%)	0.2	0.7	1.3
MIRROR SHADOW (%)	4.2	4.9	3.1
BLOCKING (%)	0.9	1.5	0.7
SPILLATE (%)	1.0	3.3	2.6
MIRROR EFFECTIVENESS** (W/m^2)	672	692	703

*Collection of energy above 15° sun elevations
**Average yearly power input to receiver per m^2 of heliostat

Pilot Plant--Southern California Edison Company (SCE), in a consortium with the Los Angeles Department of Water and Power (DWP) and the California Energy Commission, has joined the U. S. Department of Energy (DOE) to build and operate the nation's first solar thermal central receiver electric generating facility connected to a utility grid.

This 10-MW pilot plant, which is based on the design selected from the first-generation water/steam program, will be located in the Mojave Desert adjacent to SCE's Cool Water Generating Station in Daggett, approximately 12 miles southeast of the city of Barstow, California, and will begin operation in 1981. The solar portion of the facility will be owned by DOE, and the non-solar portion will be jointly owned 80% by SCE and 20% by DWP. The total cost of this project is currently estimated at $123 million.

A Visitor's Information Center is planned that will be in close proximity to the pilot plant. The center, scheduled to be completed in late 1979, will contain exhibits depicting the operation of a solar thermal central receiver power plant, solar energy products and services, and our energy problems, along with alternate energy sources.

Subsystems developed by McDonnell Douglas Astronautics Company provided the technical basis for the design of the 10-megawatt solar pilot plant. In August 1978, DOE selected McDonnell Douglas and Martin Marietta companies for contract negotiations for Phase I of the collector system (heliostats).

Under this phase, each company will build three prototype heliostats to be tested at the Central Receiver Solar Thermal Test Facility (CRTF) in Albuquerque, New Mexico. Final award for the pilot plant heliostats will be made based upon test results and final firm-price bids. Also in August 1978, McDonnell Douglas was selected by DOE for contract negotiation as the Solar Facilities Design Integrator (SFDI) which includes the design, fabrication, and integration of all solar facility plant subsystems except the collectors.

The plant design for the collector field calls for approximately 1600-1800 heliostats with a reflective area of approximately 40-45 m^2 per heliostat. The heliostat tracking control will require 75-kilowatts of power for operation; and when all heliostats are simultaneously moving to the stowed position (face-down, horizontal), the power usage is 450-kilowatts. The signal for vertical and horizontal heliostat tracking control is developed from the calculation of the azimuth and elevation positions for each heliostat as a function of time, mirror position, and target. Azimuth and elevation drive motors then obtain the calculated position using digital encoders for position feedback.

The collector field will surround the receiver tower with the tower set off-center in the southern portion of the field. The field is an elliptical arrangement about 488 m at the minor axis and 701 m at the major axis. The total land area for the pilot plant has been set at 526 x 10^3 m^2.

The vertical solar flux density curve impinging on the boiler will be constant over the mid 60% of the panels and taper off to zero flux at both ends. Pointing accuracy is specified as 1.5m rad. The receiver/boiler will be a once-through design with rated steam conditions of 515°C and 10.45 MPa. The diameter of the external surface boiler will be 7.01 m and the height 12.5 m. The boiler will consist of twenty-four identical tube panels, each of which will contain seventy .0127 m O.D. nickel alloy steel tubes. The tower itself will be constructed of steel and elevate the boiler to a height of 73.8 m to the bottom of the receiver tubes.

A thermal storage system will be provided to extend the plant's usefulness at night and will be capable of providing 277°C steam at 2.76 MPa. This will allow the turbine-generator to operate at 70% of rated output (7-megawatt) for approximately 4 hours. The storage energy, excess collected during the day, will be used to heat a high-temperature oil and crushed granite rock system. A thermocline sensible heat storage concept will be employed.

A master control system concept was derived from design features of each of the four Department of Energy contractors. The control system will be similar in design to that found in conventional power plants.

The electrical plant generating system will be designed and provided by SCE and DWP and will consist of the turbine-generator, cooling tower condenser, feed-water heaters and pumps, associated equipment, and a control room. The turbine will have dual steam inlets to accept steam from either the receiver directly or from the thermal storage system. A wet evaporative cooling tower will be provided for condenser cooling requirements.

The pilot plant is being designed to provide full output (10-MW net) for four hours on the worst solar day (December 21st) and eight hous on the best solar day (June 21). Any additional steam flow in excess of turbine-generator requirements will be routed to the thermal storage system for use during evening and other periods of insufficient sunlight.

The heliostats are being designed to operate in winds up to 15.6 m/s, at which point they would be driven to their horizontal stowed position. In the stowed position, the heliostats will be capable of withstanding a 40.2 m/s wind.

Currently under investigation is mirror maintenance as a function of time, weather, and mirror position. Minimal erosion of the mirror surfaces is anticipated based on recent studies and historical data. Stowing of the heliostats during high winds will deter erosion. The glass surface of the heliostats is not expected to be susceptible to problems of chemical erosion and all metal will have a protective coating.

Advanced Water/Steam Receiver Program

The advanced water/steam receiver program will reexamine water/steam receiver designs. The program is intended to increase the body of knowledge within this category of receivers and to examine new or improved designs which may be more cost effective than the Barstow design for repowering, process heat, or stand alone solar applications.

Three receiver contracts are being funded as part of this program: Combustion Engineering (CE), Martin Marietta (MM) with Foster Wheeler as subcontractor, and Babcox and Wilcox (B&W). Two categories of receivers are being studied and conceptually designed. Martin Marietta and Babcox & Wilcox are using steam pressures in the 9.5 MPa to 12.5 MPa range and steam temperatures from 480°C to 538°C; Combustion Engineering is using steam conditions from 13.8 MPa and 538°C to super critical.

For water/steam receivers to be competitive with other advanced receiver candidates (salt, sodium, or Brayton), they must be coupled to the most cost effective solar plants. To define these solar plants for the given steam conditions, all promising candidates for thermal storage and turbine-generators systems must be considered. General Electric (GE)is being funded as part of this program to define the possible combinations of receiver and thermal storage steam conditions which can be used with existing steam Rankine turbines. GE will study non reheat and reheat turbine cycles consistent with receiver steam conditions in the range of 50 to 250 MW_e and define storage steam conditions necessary to produce 90, 80, and 70% of nameplate rating for each of the turbines.

Sandia will synthesize complete plants by taking the cost and performance data developed by the contractors and conceptually designing total plants, including the thermal storage system. After the costs and performance of each major subsystem are defined, the most effective water/steam plant(s) will be determined by mixing and matching the various subsystems using the STEAEC and BUCKS computer codes. The cost/performance of the total concepts as they develop will be compared with those of the other storage coupled systems.

Currently, the receiver contractors are still optimizing their receiver designs. Therefore, the following receiver descriptions must be considered only as initial baseline designs. All three receiver contractors will use parametric analysis techniques to examine, modify, and optimize the initial designs.

Combustion Engineering (CE)--The CE initial baseline receiver produces 16.5 MPa/538°C steam with a 510°C reheat steam temperature and has a thermal power rating of 490 MW$_t$. A 12.4 MPa, 538°C/520°C steam receiver as well as a super critical receiver will be considered. The receiver, a single module with an external configuration, is being designed to accept a peak thermal flux of approximately 0.80 MW$_t$/m^2. The receiver contains one controlled circulation (pumped) recirculation boiler with a single drum. The economizer, evaporator, and super heater panels are located on the receiver such that the flux absorption rates are matched to the fluid flow and metal temperature capabilities of the boiler. The evaportor panels are located in the highest heat flux areas; the super heater panels are located in the lowest. Two configurations for steam reheat are being considered (Figures 29 and 30): a tower-mounted reheater located lower on the tower than the receiver, and a "live" steam reheater. The "live" steam reheater uses excess high-temperature and pressure steam to reheat the steam from the high-pressure turbine before it is introduced into the Intermediate turbine. The low-temperature reheating steam can be used to charge storage or heat feedwater.
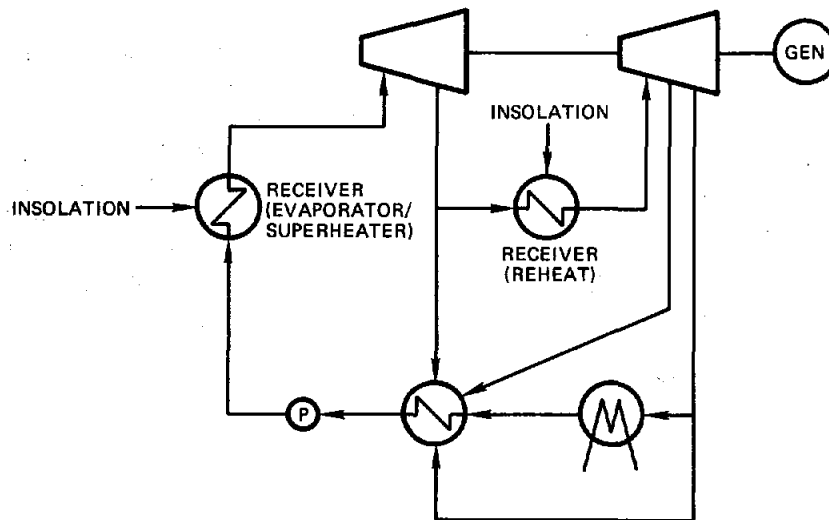
Figure 29. Solar Reheat (Storage Not Included)
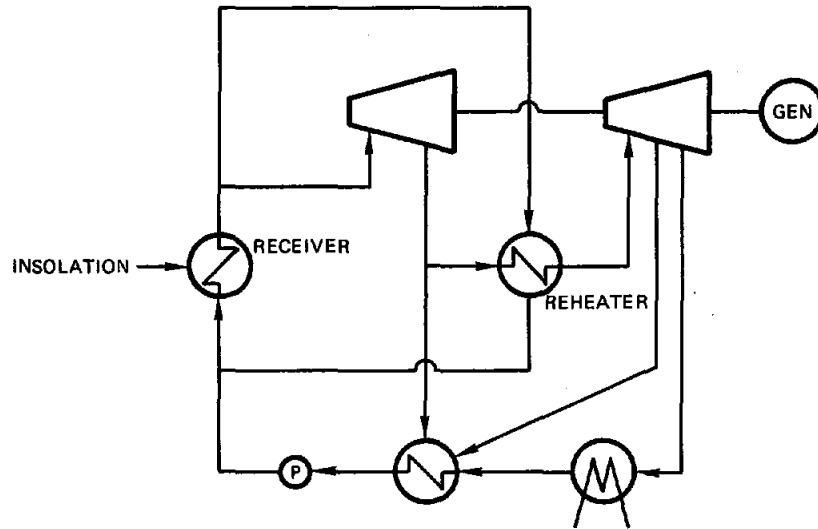
Figure 30. "Live" Steam Reheat (Storage Not Included)

Martin Marietta (MM)--The Martin Marietta initial baseline receiver will produce steam at 10.5 MPa and 516°C at ground level. Other steam conditions are also being evaluated to determine if they are economically competitive. The system design point size is 550 MW_{th} at summer solstice; 300 and 800 MW_{th} systems are being sized to establish any economics of scale. The receiver is a single drum natural circulation steam generator of the four-aperture-cavity type as shown in Figure 31. Each cavity receives energy from one quadrant of the collector field. This configuration allows for doublesided heating of the superheater and some boiler panels located on the sides of the cavities. The objective is to maximize the fatigue cycle lifetime of the tubes in the high-temperature superheater panels by minimizing the circumferential tempera-ture difference. The solar flux directed toward the back wall of the cavity causes one sided heating of the lower temperature boiler panels. The arrange-ment of the panels within the cavities is designed to provide the necessary apportioning of energy for boiling and superheating for any day of the year and for partial cloud obscurations.
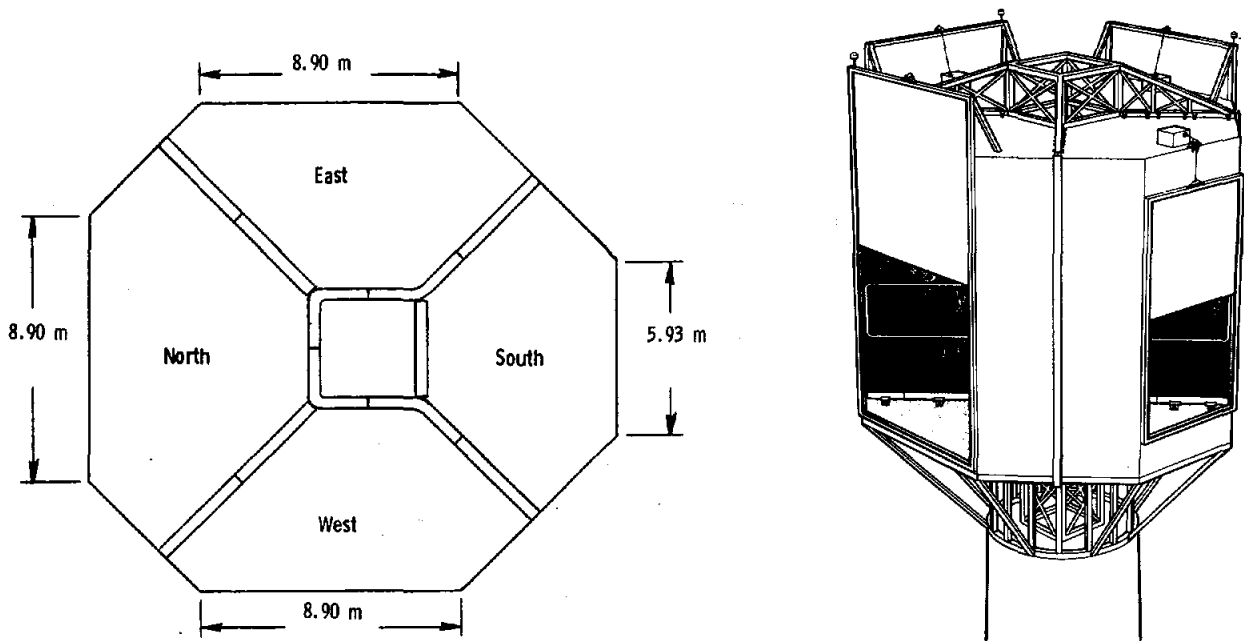
Figure 31. Martin Marietta Advanced Receiver

The collector field and receiver design will be optimized to produce a minimum cost system for power at the base of the tower. This optimization determines the size of the apertures, the size of the receivers, the distribution of the boiler and superheater panels within the cavities, and the distribution of the heliostats within the field. The receiver size and field aiming strategy are designed to keep the solar flux below a critical level at all points on the receiver tubes. The net result is a field with a large north quadrant, small south quadrant, and intermediate size east and west quadrants.

Babcox and Wilcox--The Babcox and Wilcox initial baseline receiver produces 10.5 MPa 510°C steam with a thermal power rating of 420 MW_t. Other steam conditions and thermal power sizes will be considered. The receiver is a single module with an external cylindrical configuration that is designed to accept a peak thermal flux of approximately 0.75 MW_t/m^2. The receiver contains two pump-assisted recirculation boilers, one on the west side and the other on the east (Figure 32). Although there are two separate steam drums, the evaporator portions of each boiler are interconnected. The superheaters of each boiler are independent and consist of three superheat passes with two stages of attemperations for temperature control. B&W has developed and applied for a patent on a unique arrangment of evaporator tubes and superheater membrane panels in which the low-temperature evaporator tubes are used to screen the superheater panels such that the incident flux of 0.75 MW_t/m^2 is reduced to ~ 0.2 MW_t/m^2. This proposed method reduces the heat flux or superheater a panel to an acceptable or desirable level without increasing the receiver size or weight. The screen tubes will be cooled by subcooled or nuclear boiling which absorbs most of the incident heat. One row of screen tubes can reduce the heat flux by 30% to 70% depending on tube size and spacing (Figure 33).
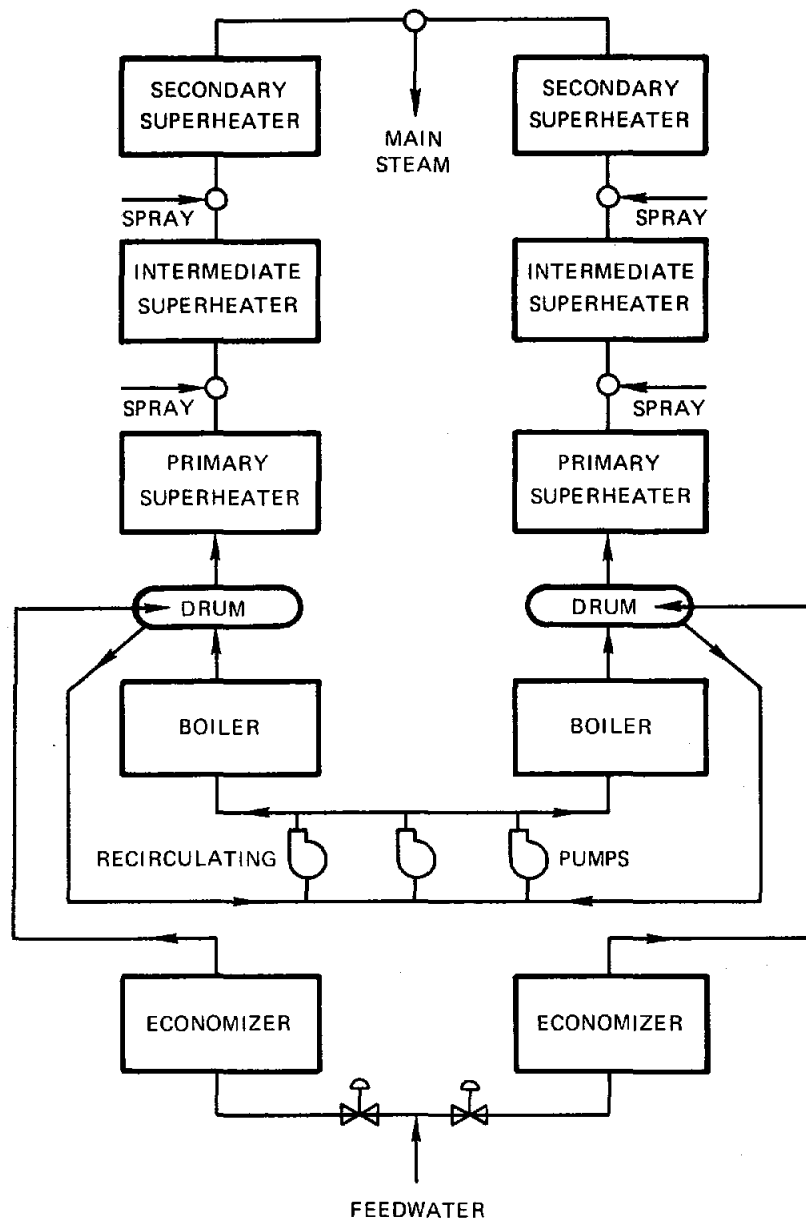
Figure 32. Babcock and Wilcox Schematic Flow Diagram
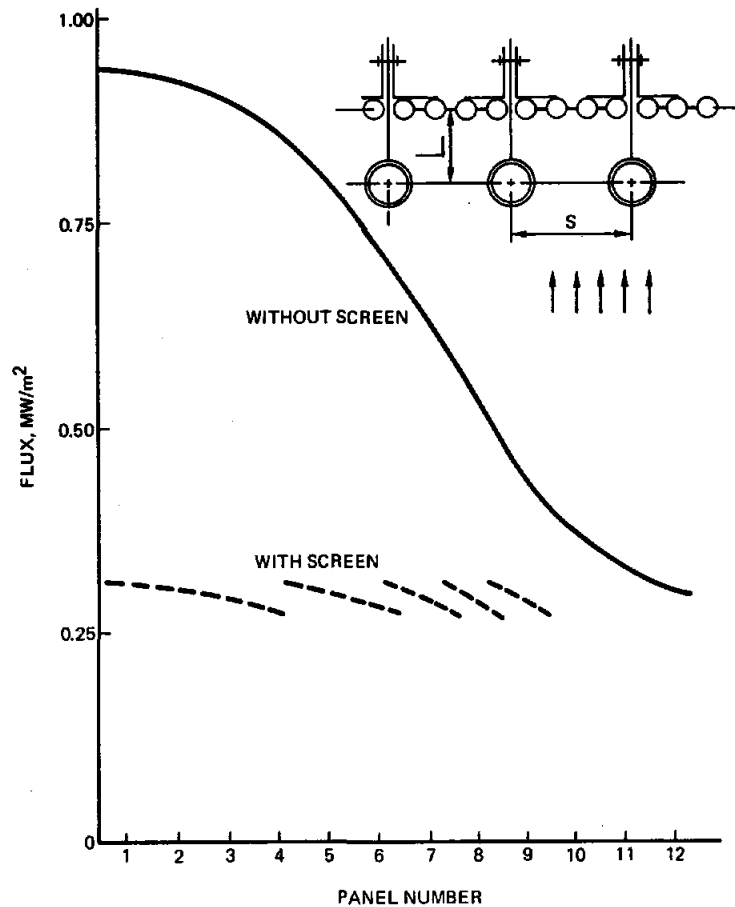
Figure 33. Comparison of Panel Peak Heat Flux Distribution
Without and With Screen Tubes

The collector field is a surround type with the tower/receiver positioned
to obtain an approximate ~ 2.5 to 1 circumferential flux variation on the
receiver. B&W is expending considerable effort designing the receiver to be
reliable and very tolerant of insolation variations due to cloud passages
over the collector field.

Brayton Systems

Boeing, Dynatherm, and Sanders have conducted studies on designs which
incorporate a Brayton cycle turbine. The Boeing studies were supported
both by EPRI and as part of the DOE Advanced Central Receiver program. The
Dynatherm and Sanders programs emphasized receiver design.

Boeing--The Boeing system uses a closed Brayton power conversion cycle
and sensible heat storage to provide extended operation after sunset and
buffering for the thermal cycle during insolation dropouts. A schematic of
the system is shown in Figure 34; an artist's conception of the plant in
Figure 35, and a plant layout in Figure 36.
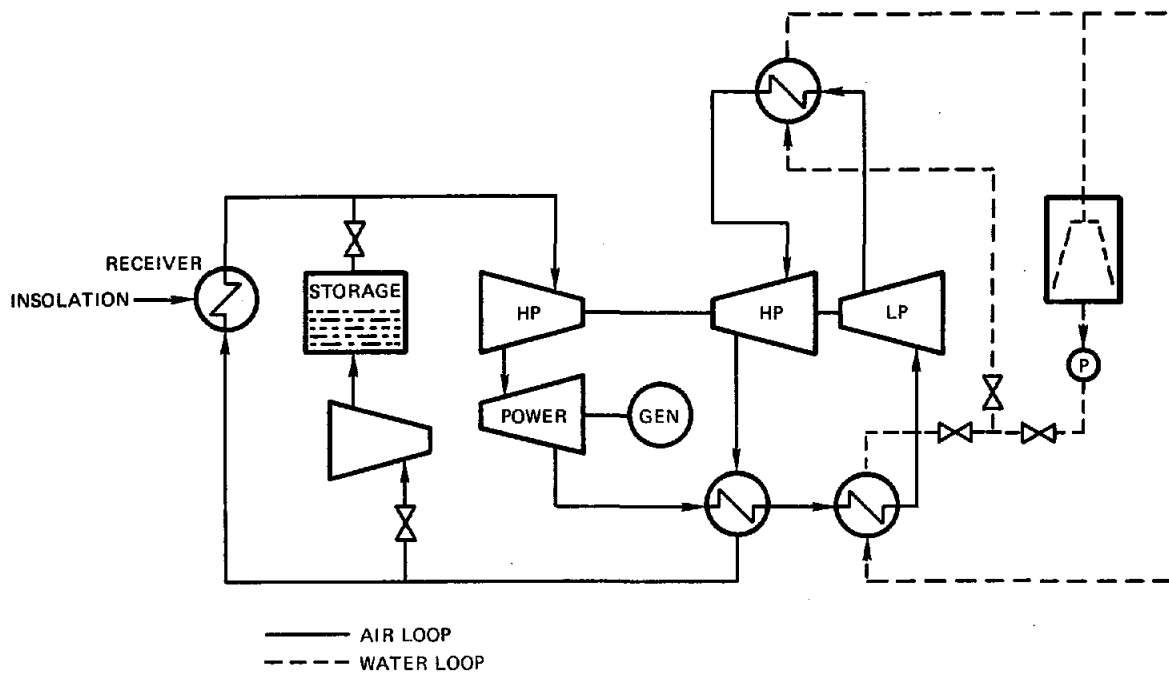
Figure 34. Schematic of Boeing Brayton System
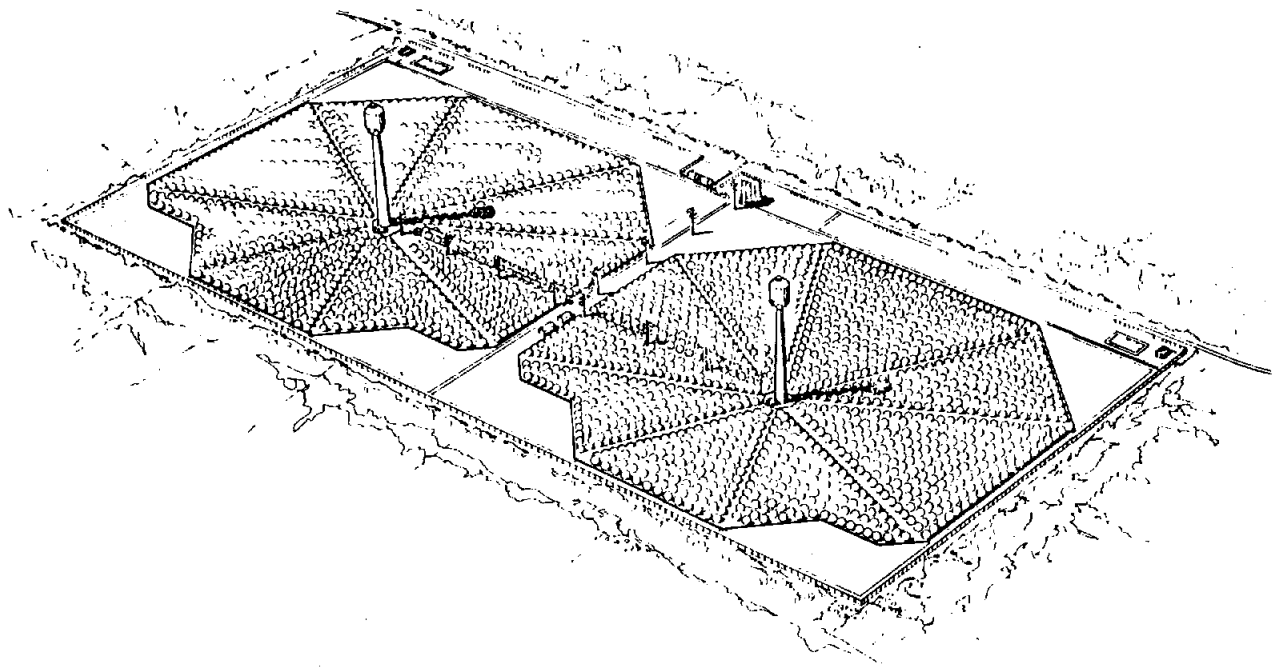
Figure 35. Boeing Designed 150 MW$_e$ Plant
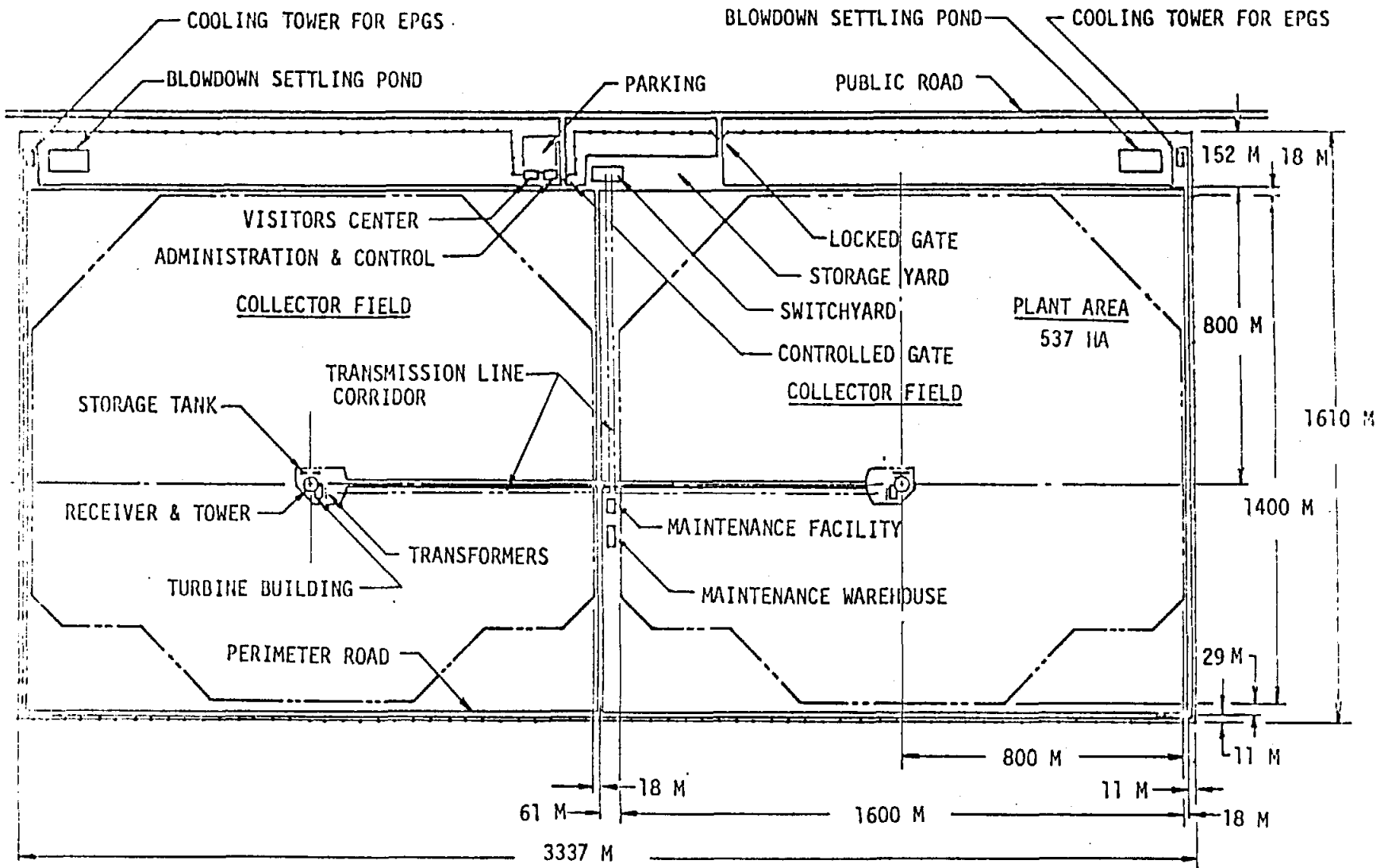
Figure 36. 150 MW_e Solar Plant Arrangement

In this system, the insolation is reflected and concentrated into the interior of the four-aperture receivers mounted on 200-meter concrete towers. The flux is directed by the collectors onto the heat exchanger panels (3) which ring the interior of the receiver. Heat exchanger tube spacing is designed to minimize circumferential temperature gradients by using the relatively high reflectivity of the cavity insulation, which reflects the sunlight onto the back (outer) side of the tubes.

The heat exchangers transfer the thermal energy to a pressurized, gaseous working fluid (air or helium) that is circulated by the storage compressors and the high- and low-pressure compressors of the electric power generation system turbine. The flow of the working fluid is controlled by the master control system which modulates the flow through valves in addition to controlling the inventory in the system. The heated working fluid is either ducted to storage or ducted into the high-pressure and power turbines. The power turbine drives a conventional 13.8 kv air-cooled generator. A portion of the working fluid is constantly cleaned by a filter; makeup fluid for the conversion cycle is filtered and supplied to the turbine through an inventory control system. Waste heat from the conversion cycle is rejected through conventional wet cooling towers.

Depending on the operating strategy, insolation levels, and power output requirements, thermal energy can be stored by diverting all or part of the working fluid into the sensible heat (brick), storage subsystem. The storage subsystem may be simultaneously charged while the turbine is operating, and has been sized to permit three hours of operation at turbine nameplate rating when fully charged. During insolation dropouts, or as insolation power declines in the afternoon, energy is recovered from the storage subsystem by reversing the flow of gas through the tank to provide maximum turbine inlet temperature. The storage subsystem also supplies thermal energy to the turbine after sunset in the same manner. Working fluid filtration during charge and discharge is accomplished by filters which remove any particulates from the storage media. The principal characteristics of the system are summarized in Table XII.

This concept is predicted to have an overall energy conversion efficiency* of approximately 17% when generating from the receiver. When generating from storage, the overall efficiency is approximately 14%. In the combined generation mode (using both the receiver and storage as heat sources), the conversion efficiency is approximately 16%. Figure 37 shows the breakdown of these efficiency values.

The sensible heat storage concept is well suited for this type solar power plant. It uses available materials, known technology, and has very low maintenance requirements; however, it is relatively costly. Use of the storage subsystem is directly affected by the available insolation and the plant utilization policy, e.g., amount of incident insolation stored, system load duration profile, and plant net power output. The design of an optimal storage policy was beyond the scope of this study. However, based on the ·

---

*Efficiency is defined as the ratio of plant power output to the thermal power intercepted by the collector field.

TABLE XII

PRINCIPAL CHARACTERISTICS OF THE BOEING BRAYTON SYSTEM

Characteristic	Value or Description
Plant	
Type	Two 75 MW_e Modules
Power Output	150 MW_e Gross; Approx. 132 MW_e Net
Annual Electricity Production	495,586,000 KWh (based on 1976 Barstow (insolation)
Area	5,370,000 m^2
Module	
Number of Heliostats	10,480 (9.5 m diameter)
Reflective Area	687,000 m^2
Tower	200 m, reinforced concrete
Receiver	4-apertures, 5.0 m x 4.0 m; cavity-type with 43 heat exchanger panels
EPGS Efficiency*	42.2%
EPGS Inlet Pressure*	3.45 MPa
EPGS Turbine Inlet Temp*	815°C
Storage Media/Mass	Alumina (Al_2O_3)/5.04 x 10^6 kg
Storage Time	3 Hours @ 75 MW_e
Master Control	Highly automated; redundant computers and data buses.
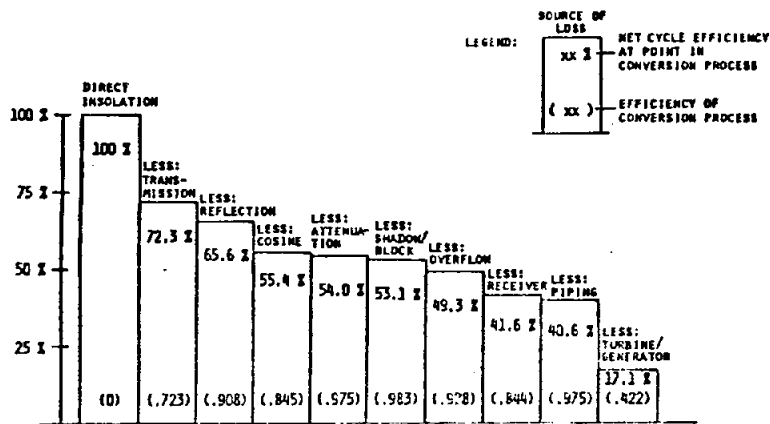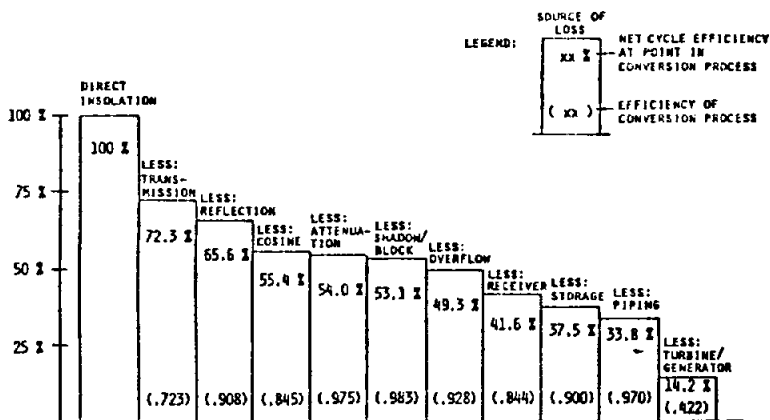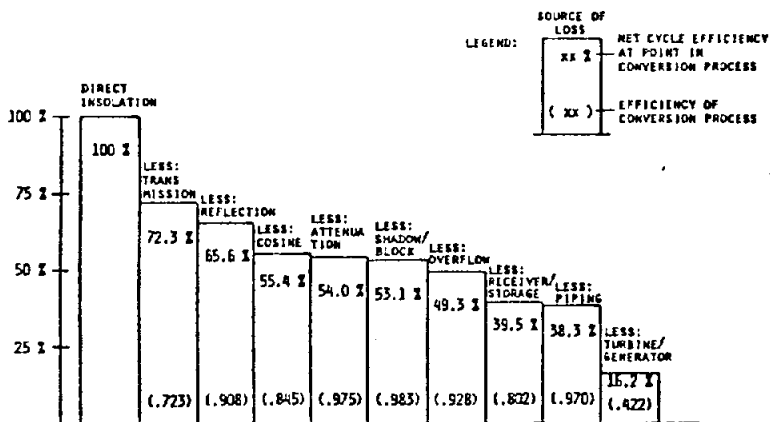
*At design point

Figure 37. Power Conversion Losses

1976 Barstow insolation, variable breaker closing times and plant power output levels, the average monthly storage utilization is approximately 2.9 hours, or about 96% of design capacity. A total of 123,525,200 kWh were generated from storage. Based on the 1976 Barstow insolation, the predicted plant availability, and the variable power levels and breaker closing times discussed above, the plant is expected to produce 480,497,100 kWh's per year. This output is shown on a monthly basis in Figure 38.

Boeing, under EPRI funding, designed and fabricated a 1 MW$_t$ experiment which was successfully tested at the CRTF. Engineering feasibility of the concept has been demonstrated.
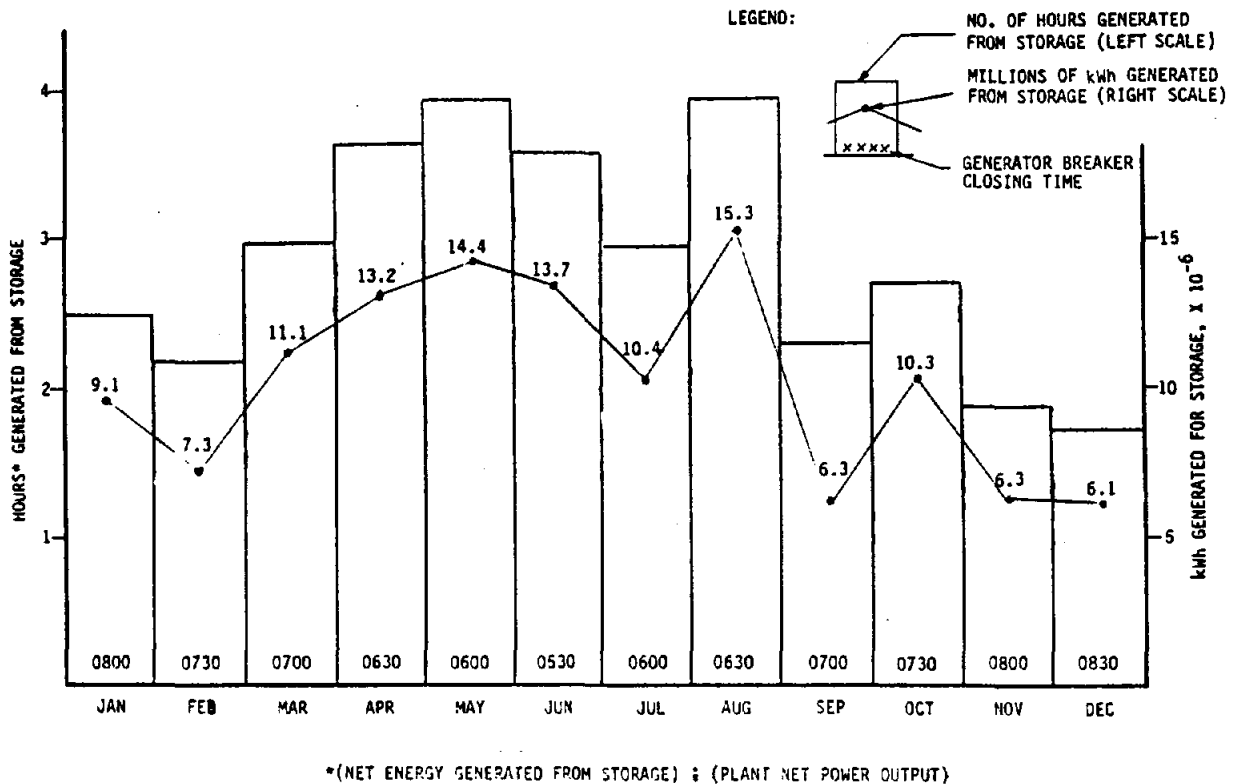
Figure 38. Boeing Storage Subsystem Performance

Dynatherm--The Dynatherm Corporation has proposed a Brayton cycle electric power generation system that uses sodium heat pipes in the receiver. The receiver configuration, shown in Figure 39, is a cavity-type receiver for a north field collector layout. The size shown is for a 10-MW$_e$ power plant. The solar energy is incident on the nine panels at the back of the cavity. The panel configuration is shown in Figure 40. Each panel uses 637 sodium-filled heat pipes to conduct the heat into the compressed air passage. A schematic of the heat pipe is shown in Figure 41. The energy would be collected at about 810°C and would heat the air to about 816°C. Theoretical and experimental work on the heat pipes has been performed to verify the capability of each pipe to absorb 13 KW$_T$, which corresponds to a conductance of about 420 watts T/°C.
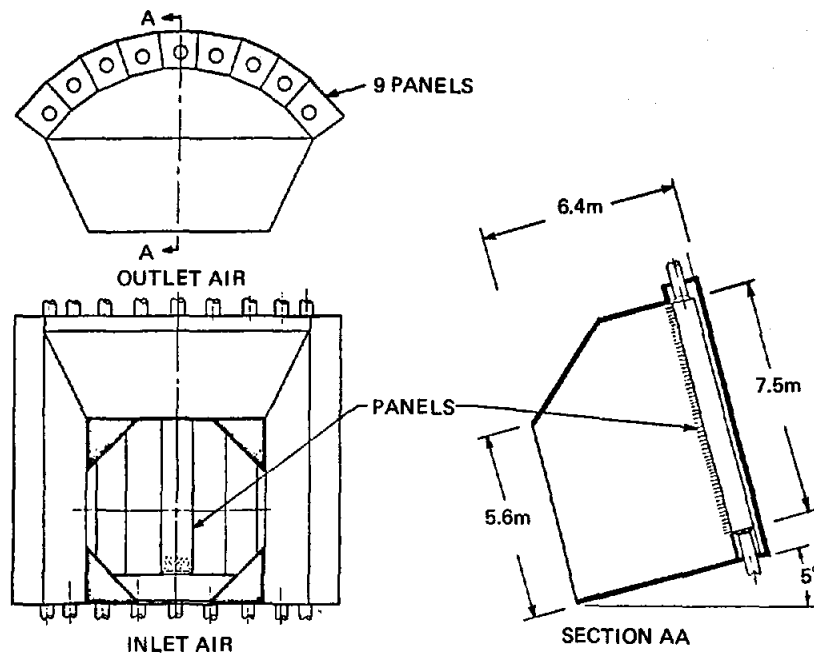
Figure 39. Dynatherm Cavity Receiver Configuration
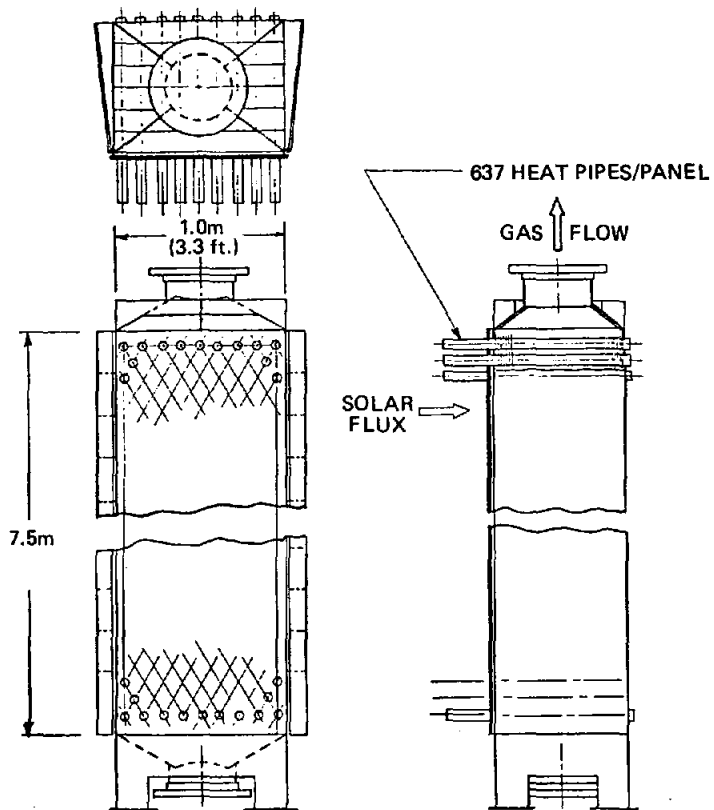
Figure 40. Dynatherm Panel Configuration

80

COLLAR

REFRACTORY

(114mm)
PITCH

~800mm

~300mm

60mm

HEAT PIPE

FINS

BACK PLATE

FRONT PLATE
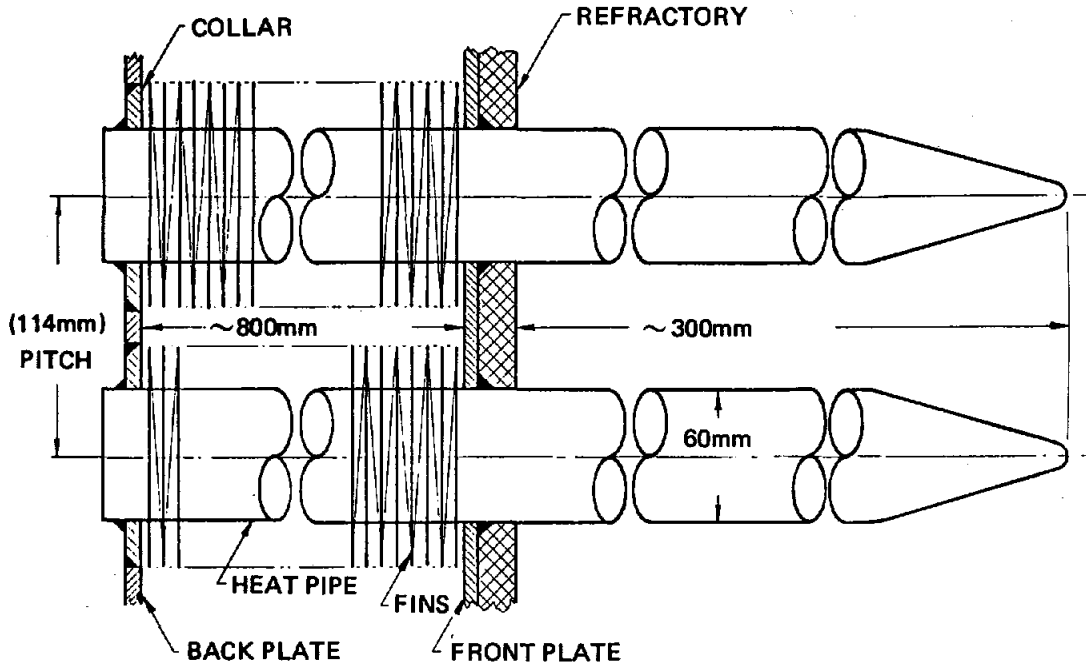
Figure 41. Dynatherm Heat Pipe Schematic

A regenerative Brayton cycle turbine is used for power generation. The entire EPGS is located at the top of the receiver tower to shorten the pipe runs to reduce costs. The efficiency of the EPGS would be about 33% with a possibility of upgrading to 38% by turbine redesign. A schematic of the EPGS is shown in Figure 42. A bottoming cycle could be used in conjunction with the plant to get the system up to efficiencies of about 46%. Dynatherm is working on this receiver concept as part of a contractor team headed by Bechtel for developing a hybrid system.

RECEIVER

INSOLATION

P = .10MPa
T = 16°C

P = .59MPa
T = 815°C

P = .61MPa
T = 450°C

GEN

P = .11MPa
T = 490°C

P = .10MPa
T = 275°C

REGENERATOR

P = .61MPa
T = 235°C
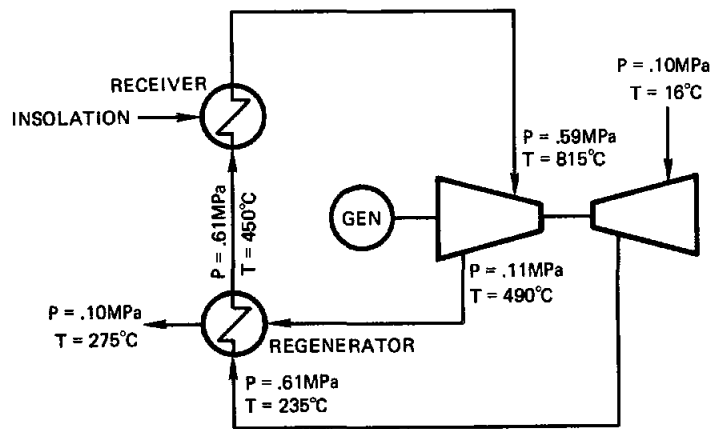
Figure 42. Dynatherm Regenerative Open Air Cycle

81

Sanders Associates--The Sanders system concept is based on a Brayton cycle turbine. The entire energy collection, storage and electric power generation system is located at the top of the tower (Figure 43). The special features of this concept are:

1. Very high temperature collection system 1000°C.

2. A cycled, modular energy storage system.

3. No waste heat rejection equipment.

4. Relatively high efficiency in coverting thermal energy to electric power (>40%).

The system, shown in Figure 44, consists of a solar receiver, several energy storage checker stoves, and a turbine for power generation. The heat transfer fluid in all parts of the system is air.
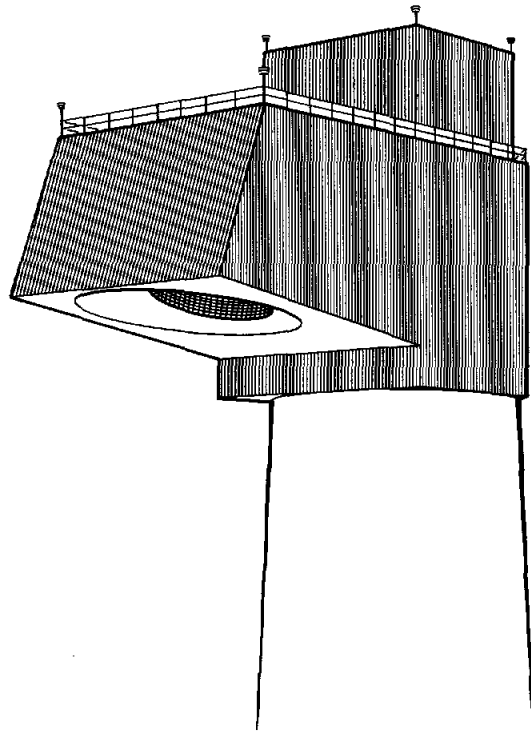
Figure 43. Sanders Brayton Cycle Receiver

ENERGY COLLECTION SYSTEM
(SOLAR ENERGY STORAGE)

POWER GENERATION

RECEIVER
INSOLATION
1090°C
STORAGE
650°C

GEN

1090°C
STORAGE
150°C

650°C
STORAGE
150°C

POSITION I

POSITION II   POSITION III
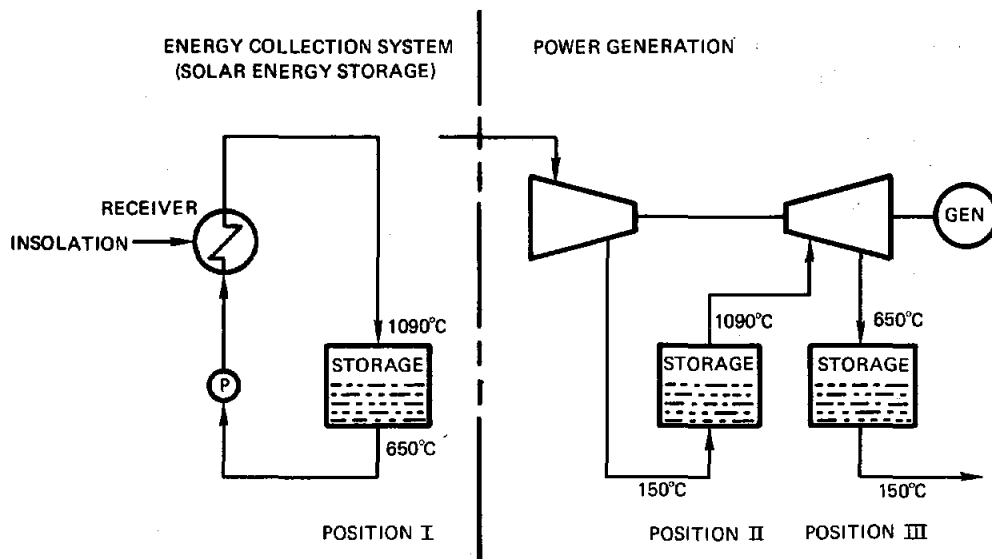
Figure 44.   Schematic Layout of System

The receiver is a vertical cavity type with ceramic honeycomb as the solar collection surface. The honeycomb is cooled by passing air through the matrix of cells. The air enters the honeycomb at 650°C and is heated to a temperature of 1100°C. The heated air is circulated between the receiver and the first checker stove using a fan. The air in the receiver is at ambient pressure and the aperture is open to the atmosphere. Although this is an open system, the air is not intended to exchange with the outside air. Note that the recirculating air entering the chamber is at 650°C, so any air that escapes represents an energy loss. Obviously, some air will escape; the extent of this convection loss is still being evaluated.

The storage subsystem consists of four identical modules, called checker stoves. Each module is alternately charged from the receiver and later discharged by the power generation subsystem. A portion of the charging energy is also supplied by exhaust heat from the turbine. The checker stove is a tank that is filled with firebrick or other high temperature material. The bricks are arranged to allow minimal pressure drop through the stack. A thermocline develops in the length of the stove as it is being used, and therefore the temperature of the exiting gas is relatively uniform.

Three of the stoves are in use at any given time, with the fourth being used to buffer mismatches in energy flow in the system. The flow of air is switched between the stoves so that they functionally occupy three different positions in the system. The stove at Position I is charged with the hot air exiting the receiver at 1100°C. The stove cools the air to 650°C by heating the bricks. When all of the bricks are heated to 1100°C,

the airflow is switched so that the stove occupies Position II. Compressed air leaving the turbine compressor enters the stove and is heated from 150°C to 1100°C. When the stove is depleted (cooled to about 150°C) it is switched to occupy Position III. In this position the stove functions as a recuperator as it cools the 650°C turbine exhaust to about 150°C. When the stove is charged to 650°C, it is returned to Position I to complete the charging.

The advantage of this system is that charging and discharging takes place at the pressure that fits into that part of the system cycle requirements. The highest pressure in the system is only 413 KPa so there are no high-pressure requirements for the tanks. All of the heat transfer in the system is by direct contact and no heat exchangers are used in the system.

The high temperature and effective recuperative in the system allows a thermal-to-electric conversion efficiency of perhaps as high as 50%, which is better than will be achieved by steam Rankine cycle systems. This efficiency is achieved without the use of cooling tower heat rejection system which simplifies siting and environmental problems.

Sanders designed and fabricated a .25 MW_t receiver experiment which was tested at the Georgia Technology Advanced Components test facility. To date, tests have been limited to one half of maximum power.

Molten Salt Systems

As part of the Advanced Central Receiver program, Martin Marietta developed a conceptual design for a central receiver which uses salt as the heat transport fluid. In addition, Sandia Laboratories is developing a direct absorption receiver that also uses salt.

Martin Marietta--The 300-MW_e 11 hours of storage system consists of nine heliostat fields (Figure 45), each containing 7711 heliostats that direct the solar energy to the receiver located at the top of a 155-meter tower. The system is shown schematically in Figure 46. The receiver is a cavity with four apertures (Figure 31). Inside the cavity the solar flux is absorbed on panels constructed of 0.038 m Incoloy tubes welded to 0.41 m x 0.0064 m wall pipe headers at the top and bottom. The panels (two for each wall) comprising the square center section are defined as back walls and are each 1.8 m wide x 14.8 m high. The panels comprising the diagonal walls of the receiver are of uniform 1.83 m width but of differing heights. The molten salt enters the receiver at 288°C and leaves at 565°C. The flowrate of the salt is controlled to maintain a constant salt exit temperature. The molten salt is pumped to the steam generator and/or the storage subsystem. The hot salt pumped to the steam generating system is used to heat boiler feedwater and make 510°C, 16.5 MPa superheated steam for the steam turbine/ generator. During the process, the hot salt is cooled to 270°C and then pumped to the bottom of the thermal storage tank and/or back to the receivers. During periods when solar insolation is insufficient for rated operation, energy is extracted from the storage subsystem and used to supply heat to the steam generator. Thermal energy is stored as sensible heat in cylindrical flat-bottomed tanks, each of which is designed to operate in a thermocline mode. The tanks are 23.8 m in diameter and 26.8 m high. The API tanks are specially insulated on the inside to allow use of carbon steel and to minimize
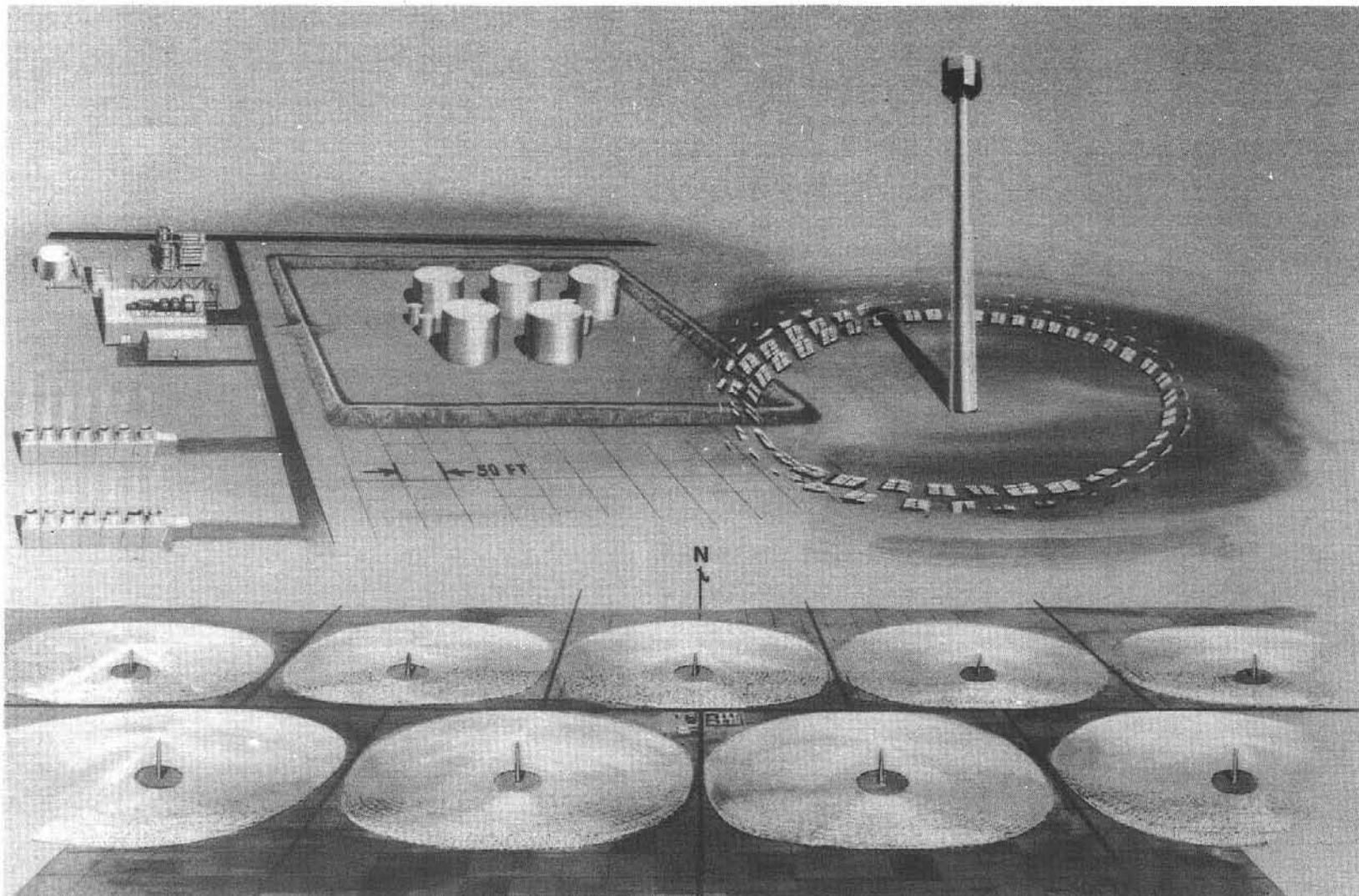
Figure 45. Artist's Concept of Martin Marietta System

heat loss and thermal stress. Each storage tank is complete with its own cantilever-type hot salt pump and sump. The storage tanks area is completely enclosed by a dike that would contain the total volume of working media in the event of an emergency.
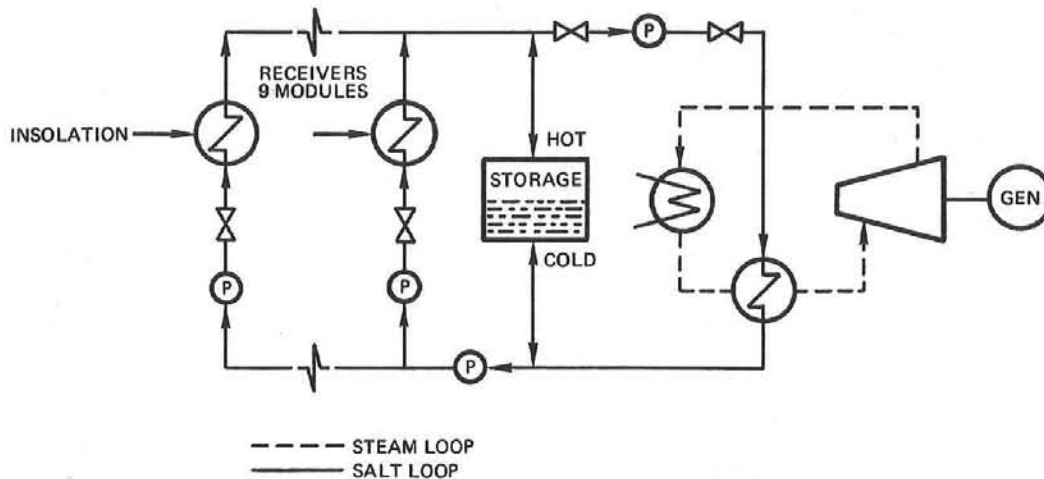
Figure 46. Martin Marietta System Schematic

The heat exchangers required to transfer the heat from the molten salt to the water stream consist of a superheater, reheater, two boilers, and two preheaters. The relatively low-pressure molten salt is on the shell side of the exchangers and the high-pressure water/steam is on the tube side. The hot molten salt at 563°C flows through the superheater and reheater in parallel and then through the two boilers in parallel followed by the two preheaters in series. Steam is produced out of the superheater at 16.5 MPag, 510°C, and at 3.45 MPag, 510°C from the reheater.

The turbine cycle consists of the turbine, feedwater heaters, condensate pumps, drain pumps, boiler feed pumps, and all associated piping. The main cycle parameters, based on the results of the parametric analysis, are throttle conditions of 16.5 MPag and 510°C with reheating to 510°C and a turbine backpressure of .0085 MPa. After an allowance for auxiliary loads of approximately 35 MWe, the unit will produce a net output of 300 MWe.

Yearly system performance was evaluated using the Solar Thermal Electric Annual Energy Calculator (STEAEC) program with the 1976 Barstow weather data tape. Major yearly performance results are listed in Table XIII.

TABLE XIII

STEAEC OUTPUTS

Yearly Energy to Collector Field	7 439 000	MWht
Yearly Energy Incident on Receiver	4 663 000	MWht
Yearly Available Energy in Molten Salt	4 239 000	MWht
- To Turbine	2 730 000	MWht
- To storage	1 509 000	MWht
Yearly Energy to Turbine from Storage	1 484 000	MWht
Yearly Gross Electricity from Turbine	1 849 000	MWhe
Yearly Net Electricity from Turbine	1 726 000	MWhe
Yearly Auxiliary Energy Purchases from Grid	16 000	MWhe

The STEAEC output indicates that the system has a capacity factor of 0.649; that is, it could have produced 64.9% of the power of a plant operating at full load for 24 hours per day, 365 days per year, at Barstow, California, in 1976. This assumes that plant downtime is negligible and that maintenance is performed at night after plant shutdown. Figure 47 shows the stairstep for the design point of 1200 hours on June 21.

Direct Absorption System--Research on a rather novel direct absorption central receiver concept started at SLL in 1973. Unlike more conventional receiver designs where the energy is first absorbed on a metal or ceramic surface and then conducted to a heat transport fluid, the concentrated light is absorbed directly into a black, low vapor pressure, molten salt flowing down the walls of the receiver. Figure 48 shows an external version of a direct absorption receiver for an offset central heliostat field. Cavity configurations have also been investigated. The system is otherwise similar to the salt system being studied by Martin Marietta.

2634.0 MWt - NORMAL INSOLATION (950 W/m^2) X TOTAL HELIOSTAT AREA

0.3% | 2626.1 MWt - NORMAL INSOLATION X WORKING HELIOSTAT AREA

10.0% | 2362.5 MWt - REFLECTED FROM HELIOSTATS (COSINE = 1)

14.4% | 2023.1 MWt - REFLECTED, NO HELIOSTAT SHADING OR BLOCKING
(COSINE < 1)

1.2% | 1999.6 MWt - REFLECTED, NO TOWER SHADOW

0.0% | 1999.6 MWt - POWER DIRECTED AT RECEIVERS

1915.7 MWt - MAXIMUM ATTENUATED POWER AT RECEIVERS   4.2% | 1915.7 MWt

3.6% | 1846.7 MWt - POWER INCIDENT ON RECEIVERS

1.0% | 1828.2 MWt - POWER ABSORBED IN RECEIVERS

4.7% | 1743.2 MWt - POWER FROM RECEIVERS AFTER CONDUCTION, CONVECTION,
IR LOSSES

0.8% | 1729.5 MWt - TOTAL POWER AVAILABLE FROM RECEIVERS

972.1 MWt - STORAGE HEAT INPUT

757.4 MWt - CYCLE HEAT INPUT

56.5% | 329.3 MWe - GROSS OUTPUT

8.9% | 300.0 MWe - NET OUTPUT

Figure 47. Design Point Stairstep (1200 hr, 21 June)
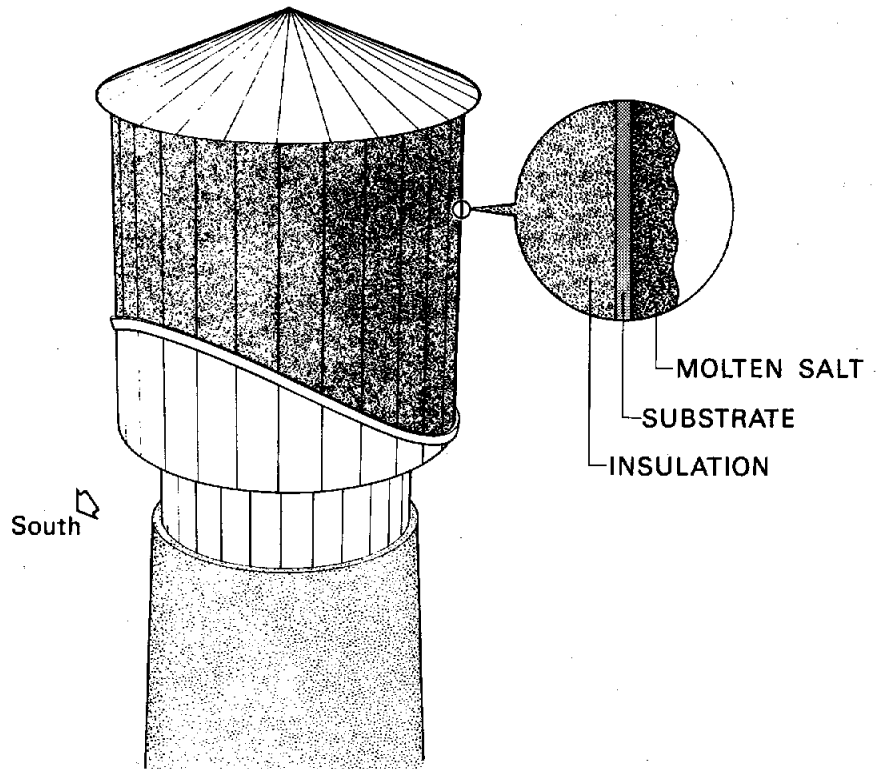
Figure 48. Direct Absorption Receiver

The potential advantages of direct absorption are:

1. Increase in flux density - Since the energy is absorbed directly in
   the heat transfer fluid, flux density is not limited by heat transfer
   and thermal stress constraints. Full advantage can thus be taken of the
   high concentration capability of central receiver configurations.

2. Absorber surface area can be reduced - This reduction is possible
   because of the high flux capability and results in the following:

   (a) Radiation and convective losses are reduced (in proportion to
       area reduction), and thereby receiver efficiency is improved.

   (b) Receiver weight and cost are reduced in relation to area.

3. Peak and average receiver temperatures are reduced - Unlike other
   concepts wherein the energy is first absorbed on a surface and then
   conducted to a lower temperature heat transfer fluid, the highest
   temperature in the direct absorption receiver is that of the fluid
   itself. Temperatures are typically 40-150°C lower, which results in a
   further reduction of radiative and convective heat losses.

4. <u>Thermal stress and creep-fatigue problems are reduced</u> - Because there are no absorber tubes, this major constraint on receiver design and lifetime is removed. In addition, the following operational advantages result:

   (a) Since the receiver can tolerate the high rates-of-change of flux which can occur during cloud passage, no special heliostat array controls are needed to limit flux rates of change.

   (b) Because of low thermal mass and inherently fast response, energy losses during startup, shutdown, and cloud transients are minimized.

5. <u>Design and fabrication of the absorber surface maybe simplified</u> - The absorber is reduced to a simple substrate (such as sheet metal or chain mesh) whose function is to provide a surface down which the fluid can flow. Complex welded tube arrays and manifolds tailored to flux distribution, requirements for pressure integrity, and concerns about surface absorptivity or internal scale buildup are thus avoided. The resulting reduced cost and weight per unit area of absorber surface, when coupled with the minimized total area, substantially reduces receiver cost and weight.

At this point in development, the principal uncertainties associated with the concept are:

1. High-temperature stability of the direct absorption fluid is not firmly established. Based on tests at SLL and Martin Marietta, mixtures of sodium nitrate and potassium nitrate look very promising, but stability data at the temperatures of interest is still limited.

2. Corrosion rates and effects on containment materials are also not well established for the high-temperature portions of the system. Only limited data is available for materials of interest under the envisioned use conditions. Tests to date show Incoloy 800 to be a good, conservative candidate, while certain stainless steels are possible lower cost alternatives.

3. Because of uncertainties on stability and corrosion, the nature and required rates of fluid maintenance which may be required have not been determined. Tests indicate that reactions with air proceed very slowly, and straightforward maintenance methods have been identified.

4. It is presently unclear whether direct absorption can be used in an external receiver configuration because of possible wind entrainment of salt droplets. Small scale tests thus far are inconclusive. Further tests are planned under more representative conditions.

5. The feasibility of the direct absorption process has yet to be demonstrated on a reasonably large scale under representative conditions. Efforts are under way on a 3-MW$_t$ experiment to demonstrate feasibility at CRTF.

If the concept looks sufficiently attractive R&D participation by one or more industrial contractors will be solicited.

Sodium Systems

General Electric and the Energy Systems Group developed conceptual designs of central receiver systems which incorporate sodium as the working fluid. These studies were conducted as part of Phase I of the advanced central receiver program and resulted in two very similar designs. General Electric is now funded under phase II of the advanced central receiver program to continue to develop the concept. In addition to these activities, sodium was selected as the working fluid for the IEA project in Europe. The details of each of these programs are presented in the following sections.

General Electric--The results of a parametric study led to the selection of the commercial plant configuration described in Table XIV and shown schematically in Figure 49. In this configuration, a 360° field of enclosed heliostats focuses sunlight onto a cylindrical receiver located at the top of a 190-meter, slip-formed-concrete tower. The receiver, shown in Figure 50, is 16 meters in diameter, 16 meters high, and comprised of 24 individual absorber panels, each 2 meters wide and 16 meters long. The absorber panels are cooled with sodium that enters through a tube header located at the vertical midpoint of the panels and flows upward and downward. The flow to each panel is controlled by an individual electromagnetic (EM) pump, ensuring precise sodium flow control, and therefore good absorber panel temperature control. Cold sodium entering the panel at the midpoint provides maximum cooling capacity at the location of highest solar flux. The hot sodium exits each absorber panel through upper and lower exit manifolds at 593°C and is mixed at the inlet to the downcomer, which conducts the hot sodium to the base of the tower.

TABLE XIV

G.E. SODIUM CENTRAL RECEIVER SYSTEM

Subsystem	Description
Receiver/Collector	GE Enclosed Heliostat 360° Field Configuration Single Sodium Loop 593°C Sodium from Receiver
Storage	Low Pressure Field-Assembled Vessels Separate Hot and Cold Storage Vessels
Electrical Power Generation	Steam Conditions 166 MPa/593°C/593°C (with Feedwater Heating above Cold Reheat Point)
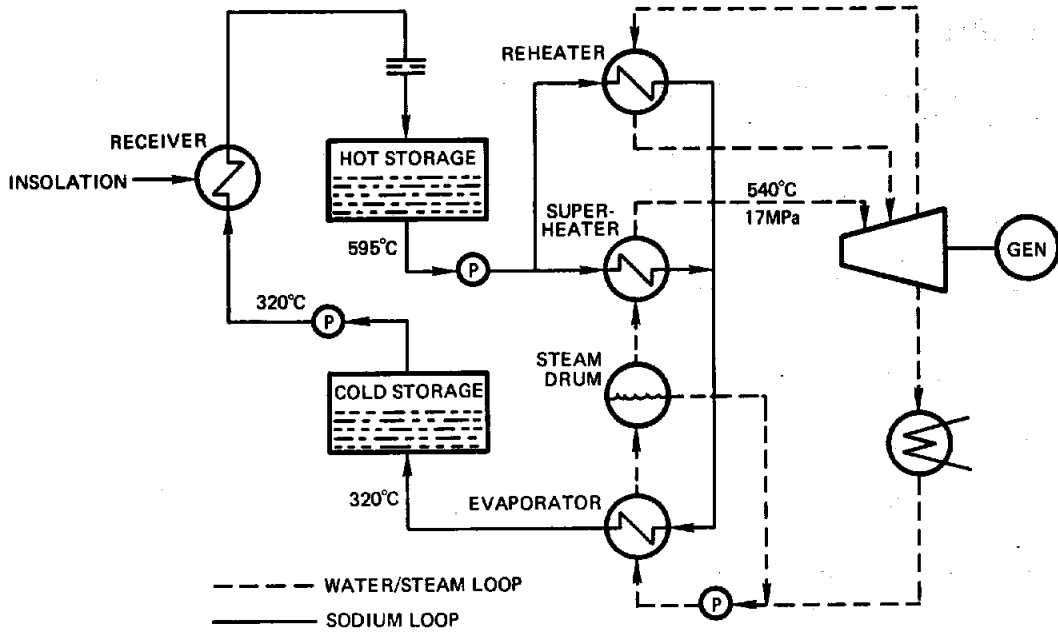
Figure 49. Commercial Scale Sodium Plant Proposed By General Electric
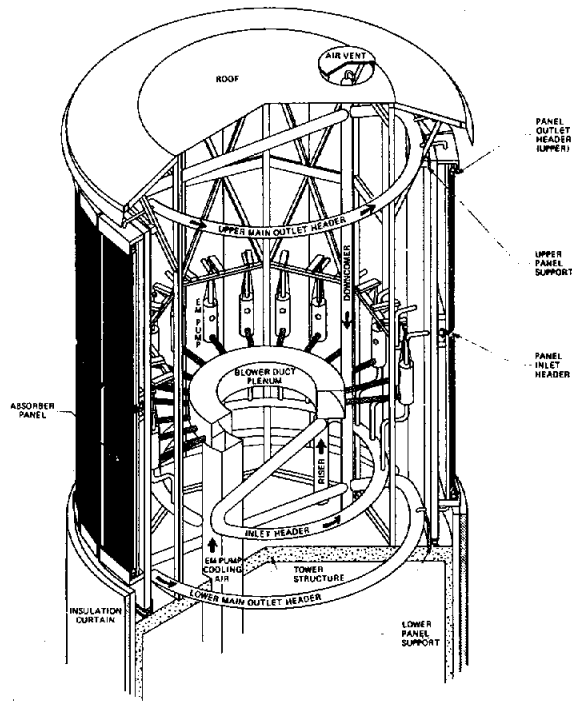
Figure 50. General Electric Sodium Receiver

An insulating curtain (shown in the lowered position) is used to reduce thermal losses from the receiver during shutdown periods. When the receiver is in operation, the curtain is lowered below the base of the receiver and serves as a shield to protect the upper portion of the tower and receiver/tower attachment structure from radiant flux spillage.

The hot sodium at the base of the tower is throttled through valves to reduce its pressure from 1.5 to 0.2 MPa. This is done to permit the use of low-pressure piping and storage vessels, which results in a substantial cost savings.

The storage subsystem consists of six separate hot and cold spherical storage vessels, each 18.3 m in diameter. The hot, low pressure sodium flows to the hot storage vessels and is then pumped to the steam generator as required to supply the steam demand for the turbine. In this arrangement, the storage vessels effectively decouple the sodium flow to the steam generator from the sodium flow in the tower, simplifying the operational and control characteristics of the system.

The steam generator section of the plant consists of three separate components: an evaporator, a superheater, and a reheater. Sodium at 593°C enters the hot side of the superheater and reheater to provide steam at 593°C. The flow to each of these components is controlled to satisfy the dynamic heat balance. At the exit of each of these components, the sodium streams are joined and fed to the evaporator where water from the feedwater train is heated and evaporated. The sodium exits the evaporator at 321°C and flows to the cold leg storage vessels.

On the steam side of the plant, water from the condenser operating at two inches of mercury is pumped through a series of feedwater heaters, a deaerator, and then through additional feedwater heaters to the steam generators. The steam generator design used in this study is based on the hockey-stick design developed in the Clinch River Breeder Reactor Program. The feedwater enters the evaporator and passes into a steam drum and moisture separator. Steam then passes to the superheater where it is heated 538°C, the turbine throttle inlet temperature. The steam then expands through the high-pressure turbine from inlet conditions of 16.6 MPa and 538°C to 2.88 MPa and 299°C. This steam is then passed through the reheater where its temperature is again raised to 593°C for introduction to the reheat turbine. The exhaust from the reheat turbine flows to the low-pressure turbine where expansion down to the condenser backpressure of two inches of mercury takes place.

Control of the plant is executed at three integrated levels: individual subsystem, master control, and manual control. Individual subsystems exert automatic controls which regulate the functions within key subsystems; examples are control of the feedwater flow rate to the steam generator in response to steam demand from the turbine and control of sodium flow through the absorber panels to maintain adequate panel cooling and an 1100°F sodium exit temperature as the solar flux varies. The master control subsystem integrates the functions of the individual subsystems, regulates plant output in accordance with utility demands, and regulates the plant during emergency conditions. Manual control can supersede the master control subsystem under any operating condition.

The temperature levels and environment dictate the use of Incoloy 800H and stainless steel 316H in hot leg components. These materials are available, and fabrication technologies are well developed. The other materials required for construction of the commercial plant are even more readily available. A summary of the materials selected for use in the commercial plant conceptual design is presented in Table XV.

TABLE XV

SUMMARY OF CONCEPTUAL DESIGN MATERIALS SELECTION

Component	Material
Cold Leg Piping	Carbon Steel
Hot Leg Piping	Stainless Steel 316H
Absorber Panels	Incoloy 800H
Storage Tanks (Hot)	Stainless Steel 316H
Storage Tanks (Cold)	Carbon Steel
Superheater and Reheater	Incoloy 800H
Evaporator	2-1/4 Cr - 1 Mo

The overall plant performance at the design point (noon on the summer solstice) is shown in Figure 51. Of the 1067 MW of solar power that would be available normal to the heliostat field reflective surface, 414 MW would reach the receiver. After accounting for reflection, radiation, and convection losses, the power into the sodium is 369 MW. In addition, a small amount of pumping power is added in the sodium circuit which increases the power level to 371 MW. Of this power, one-third is used to charge storage, and two-thirds goes to the steam generator. The 248 MW of steam produces 110 MW of electricity with a 44.5 percent steam cycle efficiency. The auxiliary power requirement for the whole plant is 10 percent of the gross generation capacity. Accounting for the auxiliary power requirement yields a net generation capacity of 99 MW$_e$.

Figure 52 shows the diurnal variation in net power output over the design point day. The minimum in the curve occurs at noon because the auxiliary pumping power is greatest at noon and decreases with decreased insolation. The maximum power output is achieved during operation from storage with the receiver shut down. The net electric energy available from the plant on the design point day is 1554 MW$_e$h.

94
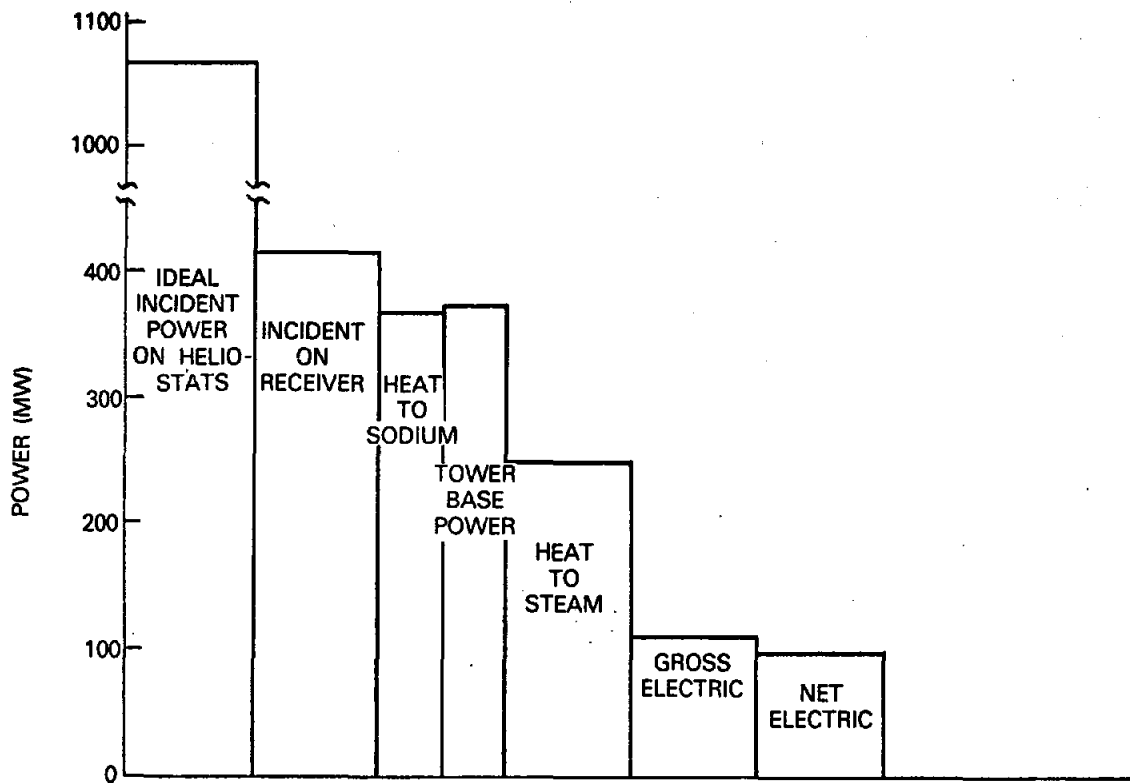
Figure 51. Plant Performance
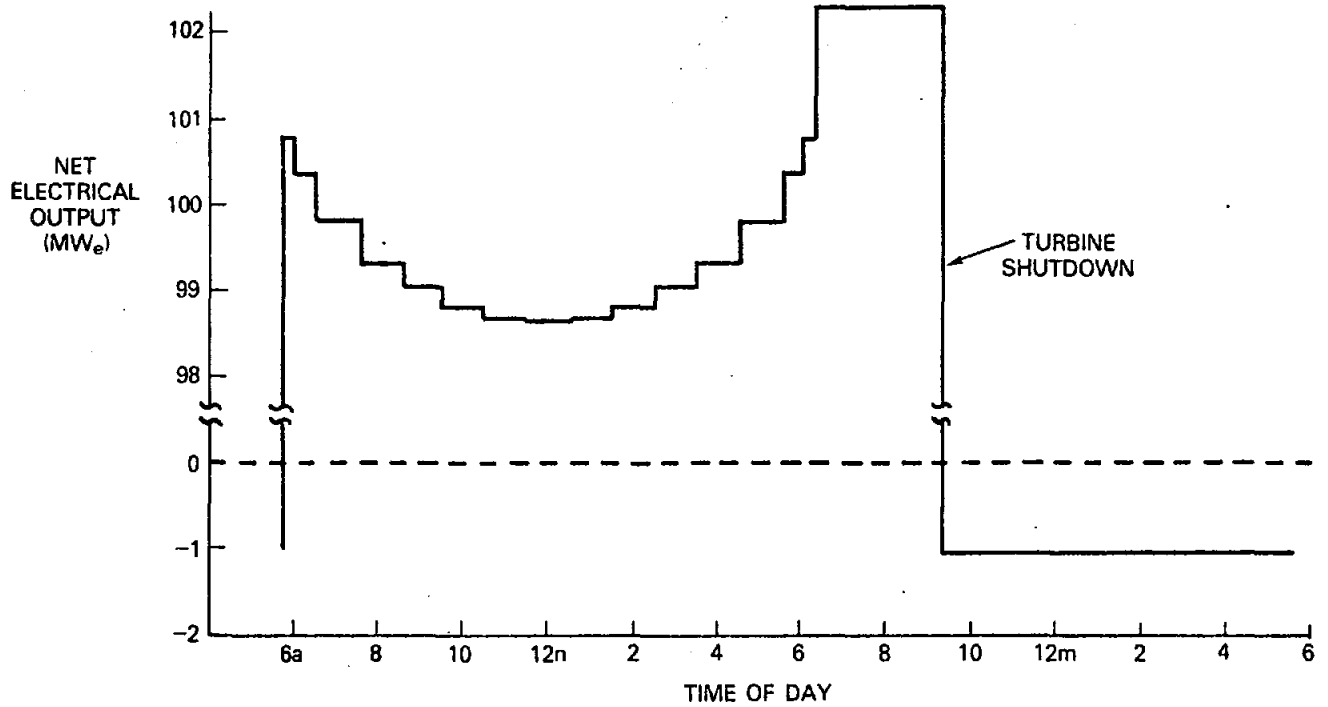
Figure 52. Daily Variation in Output

Energy Systems Group--The baseline sodium configuration proposed by
the Energy Systems Group is depicted in Figure 53. Sodium is pumped up
to the receiver where it is heated, and then it flows down the tower,
through a pressure reducing device, and into a large, hot storage tank
that is located at ground level and whose size is made to meet a specific
thermal energy storage capacity requirement. From this tank, the sodium
is pumped by a separate pump through a system of steam generators, wherein
heat is transferred from the sodium to water. The steam generator system
consists of a separate superheater and reheater operating in parallel and an
evaporator unit operating in series with the other two units. The steam
generated in the steam generators is fed to a conventional "off-the-shelf,"
high-efficiency turbine. The steam loop operates in a conventional Rankine
cycle with the steam generators serving the same purpose as a conventional
boiler. Performance data for 100 and 281-MW$_e$ central receiver
systems are presented in Table XVI.
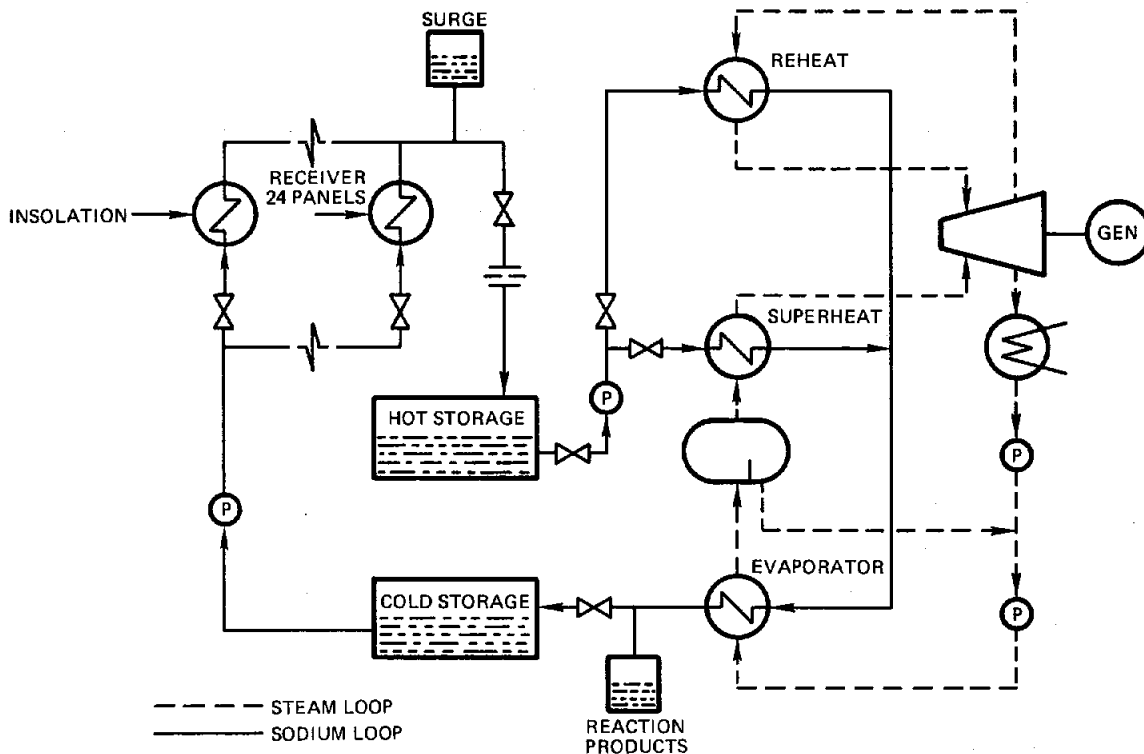
Figure 53. Energy Systems Group Sodium System

TABLE XVI

ESG ADVANCED CENTRAL RECEIVER BASELINE DATA SUMMARY

System	Parameter	Units	Configuration	
			Final Advanced Baseline	Optimum Advanced Baseline
Electric	Net Power	MWe	100	281
	Gross Power	MWe	112	312
	Cycle Efficiency	%	43.1	43.2
Receiver	SM		1.50	1.50
	Nom. Thermal Power	MWt	260	723
	Max. Thermal Power	MWt	390	1084
	Receiver Temp. - In	°C	288	288
	Receiver Temp. - Out	°C	593	593
	Flow Rate	10^6 kg/hr	3.66	10.2
	Receiver Midpoint EL	m	174	268
Storage (100% Power)	Operating Time	hr	3	3
	Energy	MWt-hr	812.5	2400
	Quantity	10^6 kg	7.6	23
	Volume	10^3 m^3	9.5	28.2
EPG	Turbine in Press.	MN/m^2	12.4	16.5
	Superheater Temp.	°C		
	Reheater Temp.	°C		
Collector	Mirror Area	km^2	0.692	1.99
	No. of Heliostats		14,106	40,660
	Overall Efficiency	%	24	24

The system incorporates an external cylindrical receiver concept on a single tower (174 m to the receiver centerline) and an all-sodium, two-tank thermal storage system. The receiver consists of 24 flat panels arrayed to form a right circular cylinder with a diameter of 16.1 m and a height of 16.1 m. The design lifetime of the receiver is 30 years although it is anticipated that panels may be replaced from time to time. The average maximum temperature reached by the receiver panels is 608°C. The sodium flow rate is 3.66 x 10^6 kg/hr. The collector field, consisting of 14,106 heliostats, surrounds the tower, which is located to the south of the field center (north biased field). Net power output is 100 MW_e with a daytime parasitic power requirement of 12 MW_e, which reduces to 6 MW_e during the storage operation because neither the collector field or the receiver feed pump is required. The collector field mirror area is 692,000 m^2, with a total incident power of 657 MW_t (based on insolation of 950 w/m^2). The total incident power required for direct operation at 100 MW_e is 409 MW_t, which gives a plant net efficiency of 24.5% and a cycle efficiency of 43.2%.

The thermal storage subsystem contains the hot and cold storage liquid sodium tanks, a pump, a pressure-reducing device, and interconnecting pipe. Liquid sodium from the cold storage tank at 288°C is pumped by the receiver feed pump through the receiver where the sodium is heated to 593°C. The sodium flows from the receiver down the tower through a pressure-reducing valve to the hot storage tank. The pressure-reducing device reduces the tower static head so that the storage tank operates at atmospheric pressure with an inert cover gas such as argon. The liquid sodium from the receiver subsystem is stored in the hot storage tank at energy rates up to 390 MW_t, which corresponds to a flow rate of 3.66 x 10^6 kg/h. The sodium is pumped from the hot storage tank at energy rates of up to 250 MW_t, or 2.34 x 10^6 kg/h, to the steam generator units where steam is produced at 538°C and 12.4 MPa. (The steam generator units consist of an evaporator, a superheater, and reheater units.) Sodium from the evaporator returns to the cold storage tank, completing the circuit.

During the day, sufficient hot sodium is accumulated in the hot tank for 3.25 hrs of operation at 100% rated power. With this storage arrangement, plant operation is always from storage. The steam conditions provided are the same regardless of whether the receiver loop is operating.

An anti-siphon system and surge tank prevent the sodium from draining from the receiver on loss of pump power. The anti-siphon device also prevents backflow in this event which would draw hot sodium into the cold header and riser.

The storage tanks are 30.5 m in diameter with a height of 13.6 m for the hot storage tank and 12.3 m for the cold. The hot tank, which operates at 593°C, is made of stainless steel; the cold tank (288°C) is made of carbon steel. A summary of the materials proposed for the ESG design are presented in Table XVII.

TABLE XVII

ESG MATERIALS SELECTION

SUMMARY OF CONCEPTUAL DESIGN MATERIALS SELECTION	
Hot Leg Piping	Stainless Steel 304
Cold Leg Piping	Carbon Steel
Hot Leg Pump	Stainless Steel 304
Cold Leg Pump	Carbon Steel
Absorber Panels	Stainless Steel 304
Storage Tank (Hot)	Stainless Steel 304
Storage Tank (Cold)	Carbon Steel
Evaporator	2 1/4 Cr - 1 Mo
Superheater	Stainless Steel 304
Reheater	Stainless Steel 304

The electric power generating subsystem is a conventional system with a tandum compound, double-flow turbine with reheat, wet cooling system with forced draft cooling towers, and six feedwater heaters using turbine extraction steam. The gross cycle efficiency is 43.1% with 7.0 kPa condenser back pressure. A steam drum between the evaporator unit and the superheater insures that dry steam enters the superheater. Maximum guaranteed generator output is 112,000 kW, and at the VWO (valve wide open) rated conditions, the generator output is 116,741 kW.

IEA Small Solar Power Plant Demonstration (SSPS)--The SSPS-Project consists of two 500-kW$_e$ plants: a central receiver and a distributed receiver. The plants will be constructed adjacent to each other on a site in. the Province of Almeria, Spain. The project is under the direction of the International Energy Agency (IEA), Paris, France, and is performed by the DFVLR acting as Operating Agent on behalf of ten IEA member countries: Austria, Belgium, Germany, Greece, Spain, Sweden, Switzerland, USA and - during Stage 1 of the Project - Italy and United Kingdom. The United States funding was 22% in the design phase and is planned to be about 22% in the hardware phase.

According to IEA goals the main objective of the SSPS Project is to demonstrate within about two years the technical feasibility of operating in an interconnected grid as well as in stand-alone mode. Both plants, therefore, are demonstration plants of a pilot character rather than test facilities.

In October 1978 the CRS-Consortium, headed by the German company Interatom, presented the final design (Table XVIII Stage 1). This design is characterized by

- a heliostat field of 160 Martin Marietta third-generation heliostats, using curved mirror facets in five different focal lengths, delivering 4.2 MW through the aperture (equinox noon),

- a cavity type sodium receiver with an aperture of 3 x 3 m using a tube bundle arranged as a vertical half cylinder. Outlet temperature of sodium is 530°C,

- a one-loop heat transfer system with a hot and a cold sodium storage tank and a steam generator. According to the basic SSPS requirement all components of the sodium loop are proven technology,

- A condensating steam turbine (10 MPa, 500°C) with three bleeding points,

- a control system similar to conventional power plants with an operator in the control loop.

The design as described above was more costly than the funding available from the participating countries. Therefore, cost reduction possibilities are being investigated both by the Operating Agent and the contractor. As a result

- the design point insolation was changed from 700 to 920 w/m^2, which resulted in a field of 100 heliostats, delivering now 2.7 MW$_{th}$ energy input into the cavity instead of 4.2 MW$_{th}$,

- energy storage capability was reduced from 2 MWh to 1 MWh,

- design lifetime is now 10 years instead of 30 years,

- a less sophisticated prime mover will be selected and proposed.

According to current planning the hardware phase (Stage 2) of SSPS Project will start on June 1, 1979. Manufacturing, erection and acceptance will be accomplished within 24 months. Accordingly, CRS plant can be put into operation in the summer of 1981, together with the distributed collector system (DCS), the second part of the SSPS project.

Hybrid Systems

Bechtel, the Bureau of Reclamation, Energy Systems Group, and Martin Martietta are developing hybrid designs. These studies were initiated early in 1979, and the first phase will be completed late in 1979.

TABLE XVIII

CENTRAL RECEIVER SYSTEM (CRS)

SPECIFICATION	STAGE 1 FINAL DESIGN			STAGE 2 DESIGN
POWER OUTPUT	500 KW_e at 700 w/m^2			500 KW_e at equinox noon -------- (920 w/m^2)
POWER DELIVERY	Utility grid Substitute load			--------
ENERGY STORAGE	Equivalent to 2 MWh Available up to 24 h after fully charged, To be loaded under full, partial, zero el. output			Equivalent to 1 MWh --------
OPERATIONAL MODES	Insolation only Insolation and storage Storage only			--------
OPERABILITY - Insolation [W/m^2] - Wind [km/h] - Earthquake - Hail [mm]	FULL 1100 18 0.03 m/s^2	REDUCED (50%) - 50 0.3 m/s^2	SURVIVAL - 144 0.6 m/s^2 19 at 20 m/s	--------
AVAILABILITY	95% at 700 w/m^2 or more			(open)
LIFETIME	30 years			10 years (Heliostats 30 years)
LAND USE FACTOR	~20%			--------
COOLING	Evaporative water cooling Max. 1.5 liter over 15 hours			--------
SAFETY PRECAUTIONS	Emergency power Defocussing Devices Independent safety instrumenta- tion Alarm and protection systems			--------
SERVICE INTERVALS	Equiv. to stationary industrial equipment			--------

Bechtel

The power system will use a gas turbine/ heat recovery steam generator (HRSG)/steam turbine combined cycle to generate electricity from both solar and fossil fuel energy. Solar energy will be used to preheat the combustion air to temperatures in the 816-1093°C range. Fossil energy will be used in the combustor units to boost this temperature to the gas turbine inlet temperature in the 1093-1316°C range.

Variation in solar energy input caused by clouds, time of day, or year can be compensated for by supplying additional fossil energy to the combustor to maintain gas turbine inlet temperature. It is anticipated that the time response of this compensation is sufficient to preclude the requirement for any energy storage subsystem, which would result in capital cost savings.

The concept will use an elliptically-shaped field of tracking heliostats to focus the incident insolation into a multi-cavity receiver atop a tower. An artist's conception of the proposed 100-MW$_e$ commercial-scale plant is shown in Figure 54. The combined cycle plant is shown at the base of the tower. Riser and downcomer piping is contained within the tower structure.
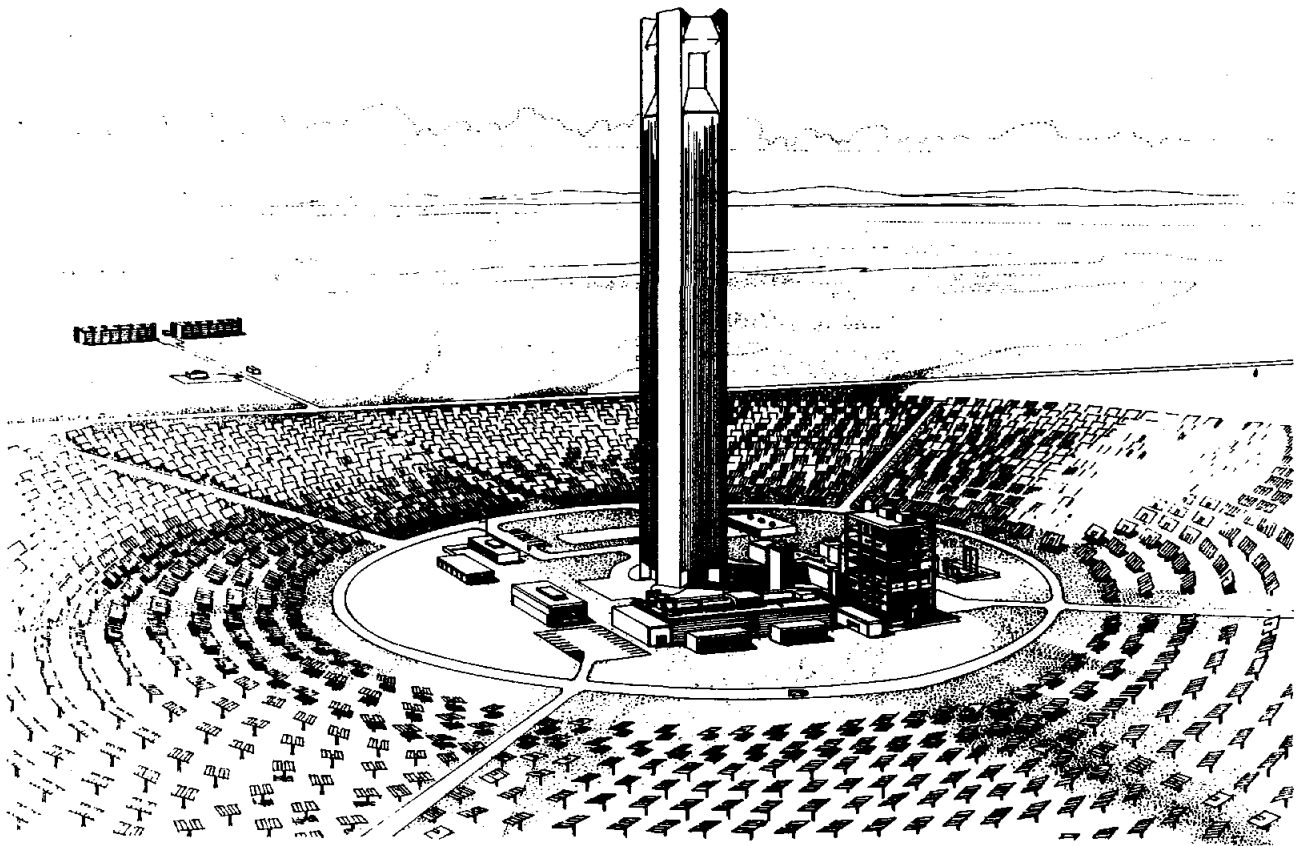
Figure 54. Bechtel Hybrid System

102

Two alternative systems have been designed based on the same concept, but using different temperature levels for the receiver discharge and gas turbine inlet temperatures. The "baseline" design is a lower temperature design that represents a more conventional technology. The "advanced" version is a higher temperature design that is several years further removed from commercialization. The baseline and advanced designs are capable of achieving commercial readiness by the mid and late 1980's, respectively.

Design and performance data of the baseline and advanced systems are summarized in Tables XIX and XX for hybrid mode operation using distillate oil as the fossil fuel. The baseline design, Figure 55, uses a 1093°C inlet temperature combined cycle plant similar to designs for which orders could be placed today. The 816°C outlet temperature gas receiver for the baseline design is a multi-cavity heat pipe receiver. This combined cycle plant has a thermal energy input to net electric output efficiency of 43.5%, a considerable improvement over steam Rankine cycle or Brayton cycle efficiencies when operating on fossil fuel. The solar energy thermal input to the combined cycle is 56.3% at the design point. On an annual average daytime basis this fraction is 31.2%. If two hours of average nighttime operation is assumed, the solar input fraction is 26.4%. For a plant capacity factor of 45%, this input represents a solar capacity factor of 12.7%.

TABLE XIX

BECHTEL HYBRID DESIGNS

	Baseline Design	Advanced Design
Reflective area per heliostat, m^2	38.6	38.6
Number of heliostats	5682	7095
Field arrangement	elliptical, south offset tower	
Receiver type	multicavity	multicavity
Absorber type	heat pipe	ceramic tube
Height of aperture above ground level, m	175	196
Riser pipe diameter, m	1.52	1.22
Downcomer pipe diameter, m	1.83	1.83
EPGS pressure ratio	12:1	12:1
Net power, hybrid mode, MWe		
Gas turbine	68.4	64.7
Steam turbine	31.6	35.3

TABLE XX

BECHTEL HYBRID SYSTEM PERFORMANCE

	Baseline Design	Advanced Design
Solar receiver outlet temperature, C(F)	816	1093
Gas turbine inlet temperature, C(F)	1093	1316
Fossil fuel	distillate oil	distillate oil
EPGS thermal to net electric conversion efficiency, %	43.5	47.7
Design point solar capacity fraction, %	56.3	71.9
Annual avg. daytime solar fraction, %	31.2	40.8
Assumed avg. nighttime operation on fossil fuel, hrs	2	2
Annual avg. solar fraction, %	26.4	34.5
Plant capacity factor, %	48	48
Solar capacity factor, %	12.7	16.6
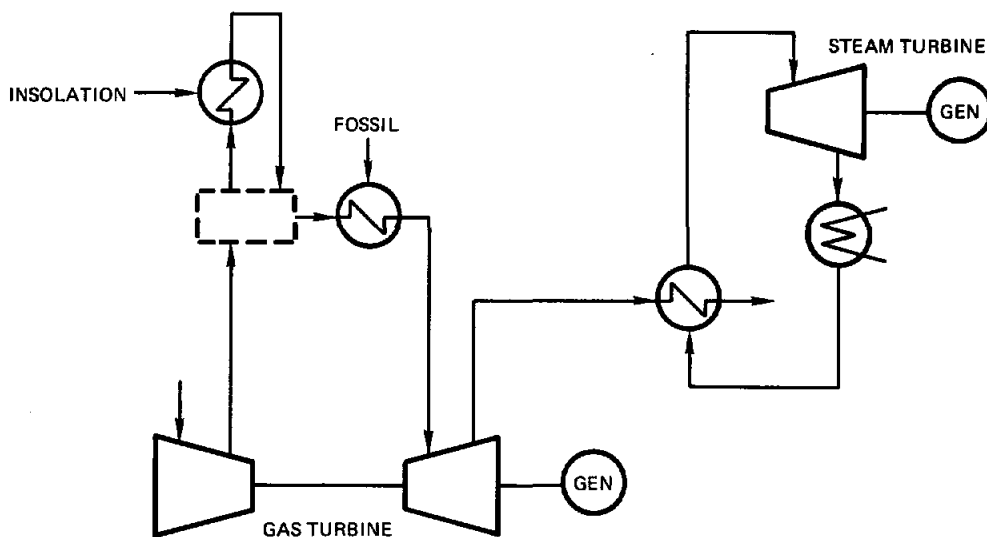
Figure 55. Bechtel Hybrid System

As an alternative to the baseline design, the advanced design uses a 1316°C inlet temperature to the combined cycle plant, corresponding to designs estimated to be available in the mid- to late-1980's. The 1093°C outlet temperature gas receiver would be a cavity ceramic type. The 1316°C advanced combined cycle plant has a thermal energy input to net electric output efficiency of 47.7%, resulting in considerably greater fossil fuel savings. The solar energy fractions at the design point and on an annual basis are also considerably increased relative to the baseline design.

Bureau of Reclamation Solar/Hydroelectric Grid Study

A twelve month study of the economic and technical feasibility of combining solar thermal electric generation with the Bureau of Reclamation (Bu Rec) hydroelectric grid in the Southwest was initiated on February 1, 1979, through an interagency agreement between DOE/SAN and Bu Rec/Boulder City, NV.

Some of the issues to be addressed are:

1. What are the effects of irrigation, recreation, and other water flow level requirements?.

2. What configuration of solar plant (size, inclusion or absence of storage) is compatible with the hydroelectric grid?

3. What level of solar penetration is economically feasible?

4. Where are appropriate solar sites?

5. What is the expected busbar electricity cost using a representative calendar year for insolation and water flow?

6. What is the sensitivity of costs and system performance to extremes of water flow and insolation?

7. What are the interface requirements between a solar and hydro system?

8. What are the barriers to implementation of such a system?

Energy Systems Group

The Energy Systems Group is developing a liquid-sodium-cooled central receiver/sodium heater hybrid system. The basic subsystems are identified in Figure 56. Liquid sodium transports the thermal energy absorbed at the receiver to steam generators located at ground level. During periods of non-solar operation, energy will be supplied by a fossil-fueled sodium heater. The steam is supplied to a conventional turbine-generator set. The sodium system can operate at temperatures of 593°C or more to generate steam at 538°C. A thermal storage/buffer system is designed to operate at the same high temperatures so that steam conditions are unchanged during operation. The buffer provides a smooth transition between solar and non-solar operation.
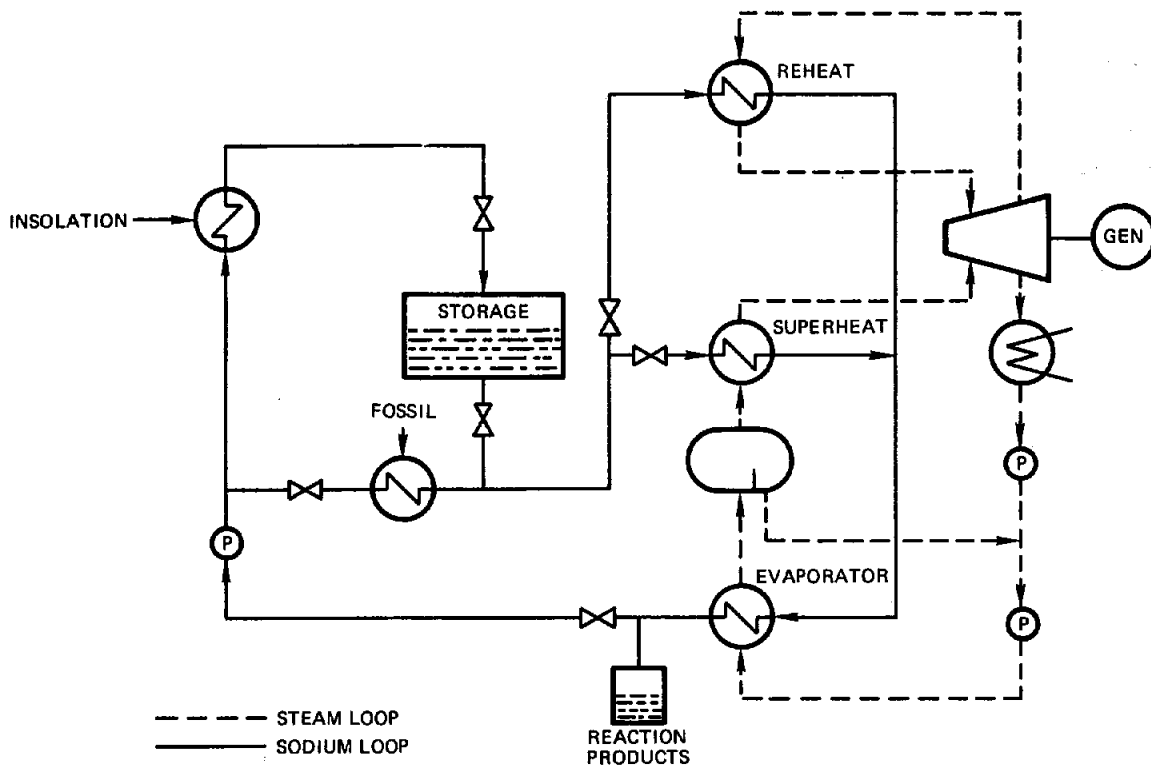
Figure 56. ESG Buffer Storage Design

At noon the solar receiver supplies 80% and the fossil-fired sodium heater 20% of full power; at night the fossil-fired sodium heater supplies fuel power. Steam, which is generated at 538°C in the steam generator, passes through the turbine generator to develop the 100-MW$_e$ net plant output.

The solar receiver and fossil-fired sodium heater can be connected either in parallel or series. Two options also exist for the series connection: the solar receiver can be connected in series either upstream or downstream of the heater. Based on the foregoing, the receiver and heater, connected either in series or parallel, are designed to furnish the required thermal energy with a constant sodium inlet and outlet temperature of 288°C and 590°C, respectively. In the series configuration, the sodium enters the downstream component at 288°C and leaves the upstream component at 593°C.

Variations in the solar receiver thermal energy output, because of the diurnal variation in absorbed thermal power, will be made up by the fossil-fired sodium heater to provide a constant net electrical plant output of 100 MW. As the receiver output drops, the heater output is increased. In the series arrangement, load changes are adjusted by varying

106

the temperature rise across the components. Conversely, with the parallel arrangement, load changes are made by varying the sodium flow through the components. At some specified minimum load in the solar receiver, the receiver will be shut down and all the power will be generated by the sodium heater. For the baseline reference design, the receiver is sized to develop 80% of full power at noon during the summer solstice.

For the parallel mode of operation, the sodium flow must be proportioned between the receiver and heater in order to maintain a constant temperature rise across the units. If the receiver is operating at 75% of full load, sodium flow is proportional so that the heater provides the 25% balance of the heat load.

The advantages of the parallel configuration are:

1) System is able to respond more rapidly to load changes than series arrangement

2) Components experience small thermal fatigue effects since the axial ΔT remains approximately fixed at all loads

3) Easier to control than series arrangement

4) A minimum of thermal buffering is required

Two options exist for designing the plant with a series configuration The receiver can be piped upstream of the heater or connected downstream. In either case, for full-load turbine operation, the sodium flow rate through the two components is maintained constant, and the temperature rise across each component is varied in direct proportion to its input. Either component may be required to operate at full power by itself, and therefore both components must be designed for the full 288°C temperature rise, which is the same temperature design conditions for these components when they are connected in parallel.

The life of sodium systems is determined by the number and magnitude of the thermal and mechanical stress cycles they receive. For this reason, sodium systems are generally designed to minimize the number of thermal cycles, unless there is a compelling economic or technical reason to do otherwise. With the series arrangement, components are subjected to more thermal cycling than with the parallel arrangement, since the sodium flow is fixed and the temperatures are varied with the load. In addition, more severe temperature transients are generated in the heater and receiver when connected in series.

Martin Marietta

The Martin Marietta hybrid system, shown in Figure 57, uses a salt-cooled, cavity-type solar central receiver coupled to a fossil heat source. A steam Rankine cycle [12.4 MPa, 510°C, reheat] is used in the electric power generation system (EPGS). The solar and fossil portions of the system are in parallel so that each can be run independently. Combinations of the solar system and coal, oil, or gas-fired fossil systems are being compared on the basis of capital expense and fuel cost in the intermediate and baseload regimes.
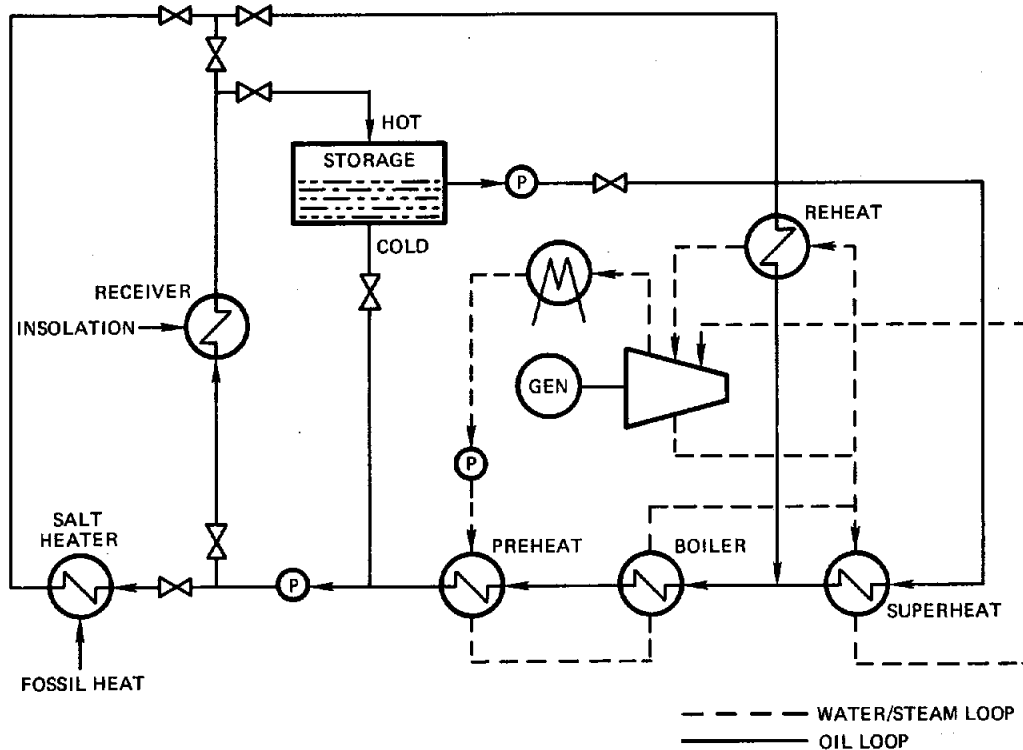
Figure 57. Martin Marietta Hybrid System

The heat transfer medium for the solar receiver is molten draw salt (NaNO3, KNO3). The salt is also used as a sensible heat storage medium in multiple hot [566°C] and cold [288°C] tanks or in a thermocline tank system. When steam is required, hot salt from the receiver or storage is run through a heat exchanger. The fossil salt heater would be used to thermally charge the storage system from which steam would be generated in times of reduced insolation.

The molten salt storage system and an enlarged collector field provide an economic means of storing solar energy so that baseload capacities and significant (0.65) fossil fuel displacement can be achieved. The fossil heater serves as a backup system for cloudy days (to guarantee capacity credit for the system) or to extend operation beyond what would be available even on sunny days in the winter. Economic trade-off studies are being performed to determine the amount of storage (3-12 hours) necessary to minimize electricity costs for various operating scenarios (baseload or intermediate).

Line focus solar central power systems fall into two categories: central linear receiver and distributed linear receiver systems. SRI International is preparing a conceptual design of the former; BDM Corporation and General Atomics are developing the distributed receiver systems. Performance and cost improvements may be possible for the line focus systems based on alternate subsystem technologies similar to those investigated points focus technology. In order for DOE to compare the proposed concepts a "Point Focus Strawman" has been prepared. Performance of the strawman is based upon the McDonnell Douglas 100-MW$_e$ water-steam design.

BDM Corporation

The BDM design team is proposing a two-stage collector field configuration, wherein the majority of the field is operating at relatively low temperatures, using state-of-the-art pertroleum-based, high temperature working fluids. A smaller portion of the field will be using high-temperature, newly developed, collector fluids that would superheat the saturated steam produced by the low-temperature collector field.

The low-temperature solar array would operate at an outlet temperature of 316°C and would require slightly less than 90 x 10^{4}m^2 of aperture. The working fluid is a relatively inexpensive petroleum based oil. Sensible storage would be interconnected in parallel with the low-temperature array. Because the working fluid is relatively inexpensive, capital expenditures are reduced, and since the solar array would be operating at a lower temperature, the overall collection efficiency can be slightly higher than that of the high temperature array. The energy captured by the low-temperature array would be used to produce saturated steam in the boiler, which would then be forwarded to a superheater driven by the high-temperature solar array. The high-temperature array will also use a more costly fluid in reduced volumes, and would operate with an outlet temperature of 400°C. Only about 19 x 10^{4}m^2 of aperture would be required to superheat the steam. The relatively small storage volume would be connected in parallel between the superheater and the high-temperature array. Steam generated in the boiler would be superheated and then forwarded to a single-admission steam turbine.

Both of the systems would have a 6.4 m aperture linear parabolic trough (initial baseline design). The basis of the trough design will be a 6.4 m wide adaptation of the T-700, a 2.1 m linear parabolic trough manufactured by Solar Kinetics of Dallas, Texas (Figure 58). The T-700 has an aluminum structure and a glass-enveloped, black chromium -coated, steel receiver tube.

General Atomics

The proposed line focus system is illustrated in Figure 59. The system uses 7.4 x 10^{5}m^2 of mirror surface mounted on collector modules. The
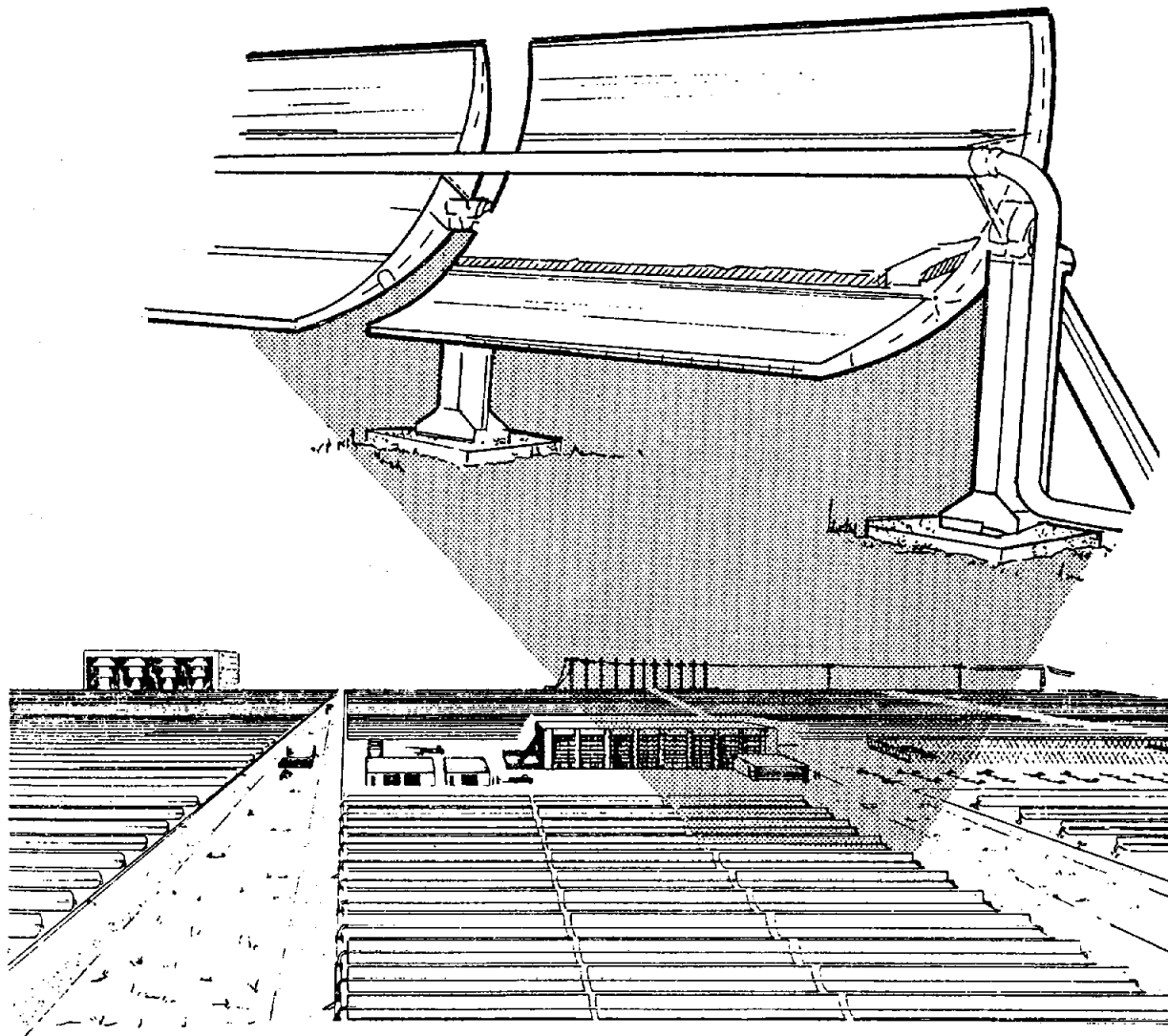
Figure 58. Schematic Diagram of Proposed BDM Line Focus Systems

stationary mirror surfaces are arranged so that the concentrated insolation (factor of 49) is focused on a movable receiver. The collector modules are arranged in 91-m long east-west rows to minimize optical end losses, to facilitate the headering and transport of the heat collection fluid, and to permit ready isolation of one row for maintenance.

The proposed heat transfer fluid is a eutectic mixture of 46 mol percent sodium nitrate and 54 mol percent potassium nitrate ("draw salt"). Draw salt has the virtues of good volumetric specific heat, moderate pumping power requirements, low vapor pressure, acceptably high operating temperature, and modest cost. In addition, the salt may be passed either into storage or to a salt-to-steam generator, thereby eliminating the need for a separate fluid for thermal storage. Further, under another program, GA is presently constructing a test unit to demonstrate the operation of the receiver with molten salt.

110
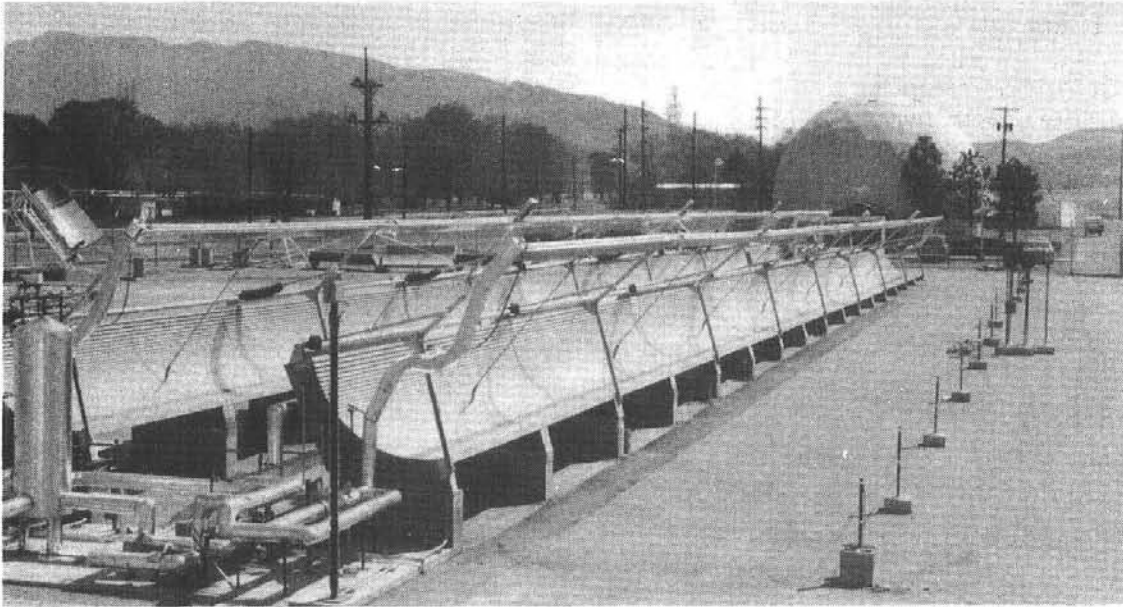
Figure 59.   GA Design At Sandia Laboratories, Albuquerque

The operating temperatures of the line focusing system will be determined from system optimization studies in which the major factors will be total plant cost, receiver thermal losses, salt flow rates and associated pumping losses, salt decomposition rate, storage requirements (volume and pressure) and overall plant efficiency, which is related to steam pressure and temperature. The baseline concept has inlet and outlet salt temperatures from the receiver of 292°C and 568°C respectively.

The high outlet temperature from the receiver allows steam to be produced at 583°C and 16.6 MPa in the once-through steam generator and at 538°C and 2.7 MPa in the reheater. The power cycle uses reheat not only to achieve high plant efficiency but also to prevent excessive (and hence corrosive) moisture from leaving the low-pressure steam turbine. The power conversion uses three steam turbine stages and achieves a net plant steam-to-electricity efficiency of 41.6%. The steam equipment is fully representative of existing technology. The overall sun-to-electricity efficiency for a 950 W/m^2 incident insolation is approximately 14% for the GA design.

The thermal baseline storage system is a multiple system with two hot tanks and two warm tanks. Thermal losses in storage are small. There is only a small difference between steam conditions when operating directly and when operating from storage. Accordingly, the baseline power recovery from storage is 420 MW_e-hr, which can be withdrawn at rates up to full plant capacity of 100 MW(e).

111

The plant is arranged with the power conversion equipment approximately in the center of the collector field as illustrated in Fig. 60. The primary concern of the arrangement is to keep the electric generating equipment close to the thermal storage to minimize thermal transport losses and piping runs. The evaporative cooling towers are outside the field and downwind (prevailing) so that incident solar radiation and the mirror surfaces are not impaired by moisture drift. The illustrated arrangements are conceptual, and particular site requirements such as the main slope, location of rail and roads, prevailing wind direction, and cooling water supply will impact any final design.
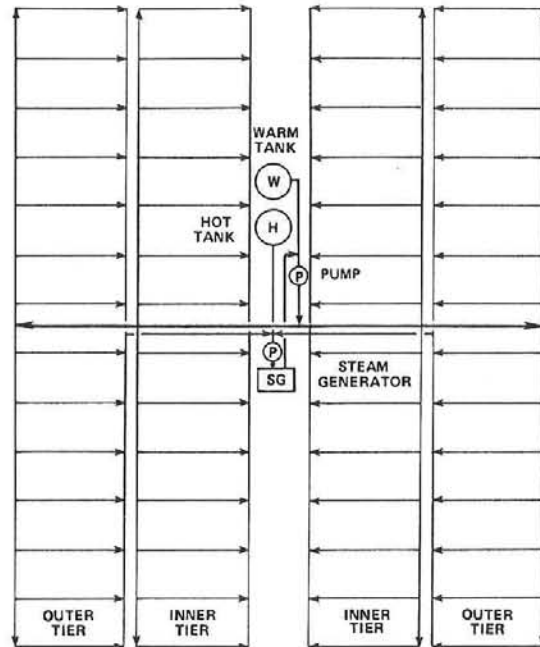
Figure 60. Reference HTS Piping Arrangement

SRI

The line focus system being studied by SRI is shown in Figures 61, 62, and 63. Drawsalt is used as the working fluid in order to create a system that is safe, one that can be built from available hardware with a minimum of new design, and one that can readily be integrated into current steam-generating plants. The design was optimized within certain constraints, such as the size of cranes for installation and existing towers for support. The heliostat and receiver performances for the proposed system are based on a study made by FMC and SRI in Contract E(04-3)-1246.

112
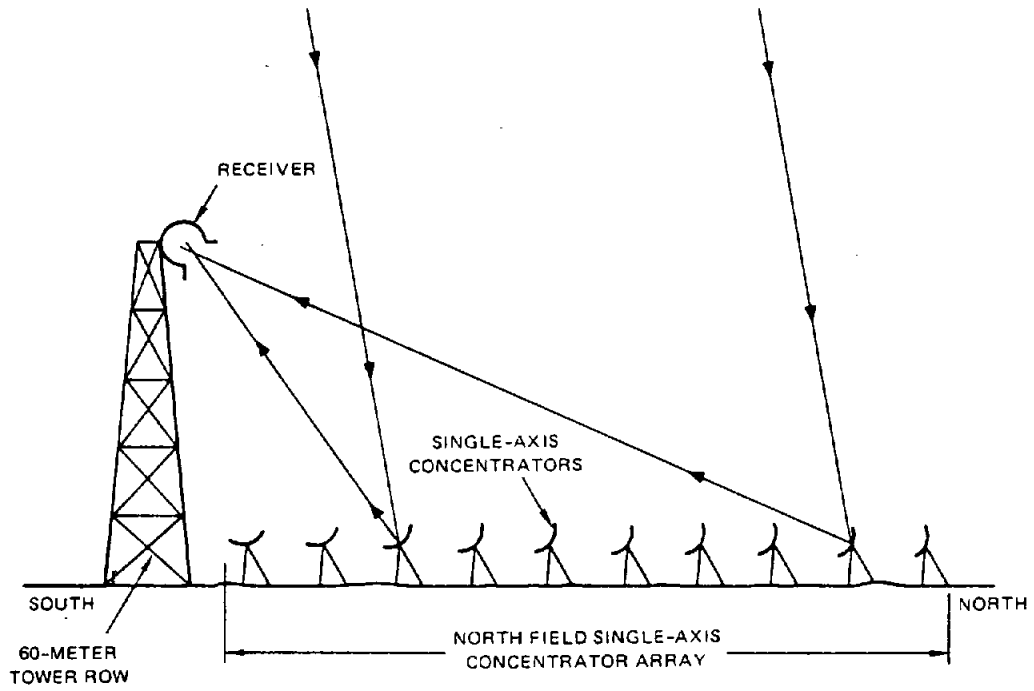
Figure 61. SRI High-Temperature, Line-Focus, Central Receiver System
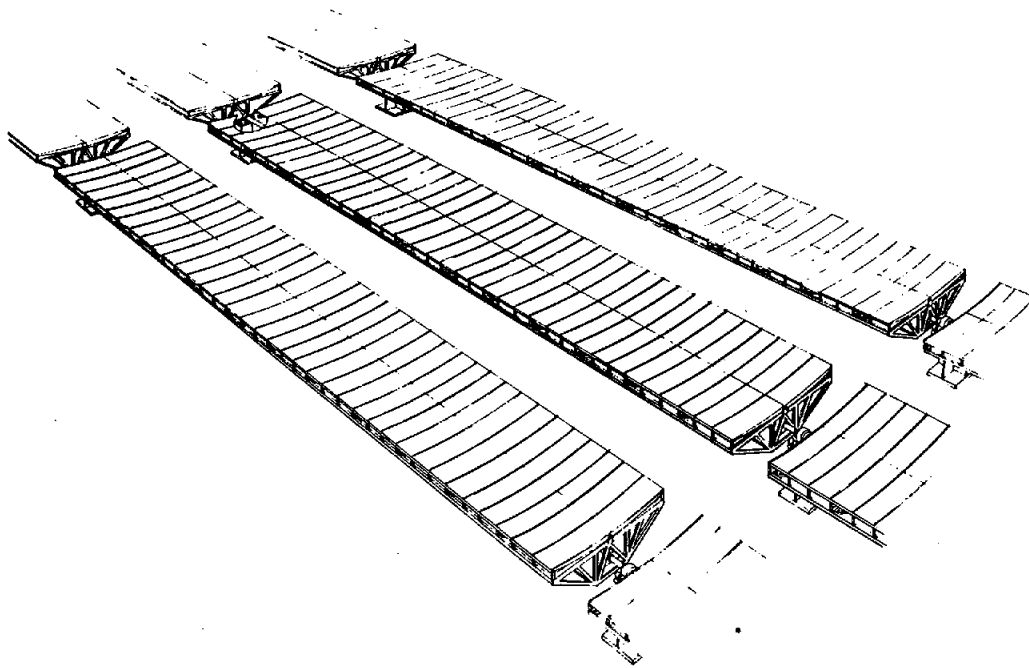
Figure 62. Artist's Sketch of SRI Concentrators
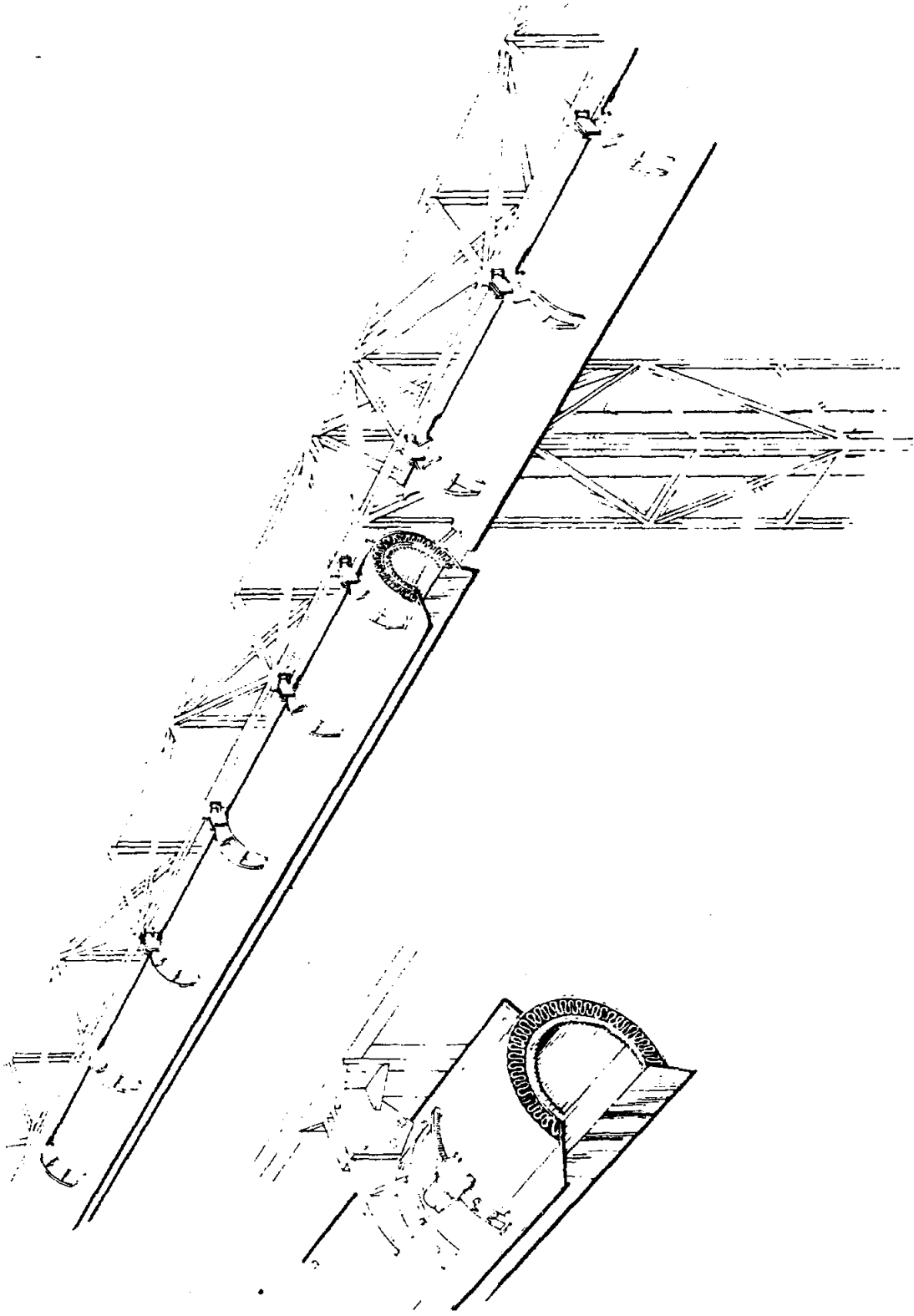
Figure 63. High-Temperature, Line-Focus, Central Receiver

Figure 64 shows a plot of the heat rate from the receiver versus the time of day to produce the required electrical power. The cross-hatched region in the figure shows the energy for direct operation, while the remainder of the heat under the curve goes to storage. Direct operation could be continued longer on the equinox day than is shown, which would result in greater overall system performance than is projected. The solar multiple of the design is 2.1, versus 1.7 for the central receiver strawman; this reflects the fact that the line focus central tower system can operate long into the evening. Table XXI shows the characteristics of the present design, together with those of the strawman design.
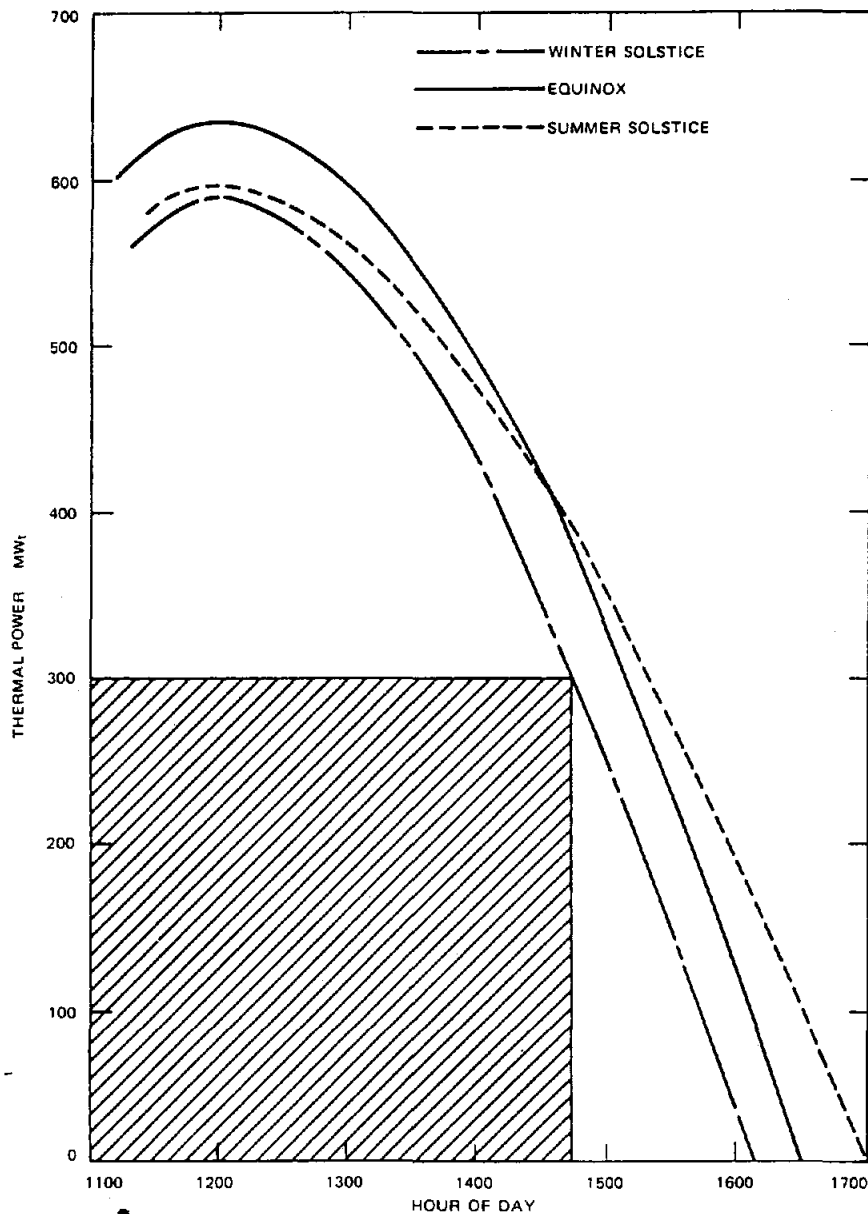
Figure 64. Thermal Power From Receiver Versus Time Of Day

TABLE XXI

DESIGN CHARACTERISTICS

Strawman	Present Design
System	
100-MW electrical steam Rankine cycle	100-MW electrical steam, Rankine cycle
Solar multiplier, 1.7	Solar multiplier, 2.1 as a result of assumed load factor, 0.4 on 100-MW_e rating
6-hour storage @ 70 MW_e	6-hour storage @ 70 MW_e
Physical	
0.78 x 10^6 m^2 heliostat area	1.005 x 10^6 m^2 heliostat
Plant Design	
Identical	

The baseline design is a cavity-type linear receiver 1.8 m in diameter with a 1.2 m aperture mounted on a 61-m tower. The 16.240 m of receiver heat the salt from 260 to 566°C. Towers are spaced at 45.6 m intervals, with a distance of 45.6 m between rows. Fiber-reinforced concrete heliostat modules 12 m long, with 3 m x 3 m reflective panels are arranged in 36 m rows. Forty six thousand eight hundred linear feet of heliostats are required.

Materials

A major concern with materials and heat transport fluids used in solar applications is the response of the material to the diurnal temperature cycling. This factor must be taken into account by the designers. Materials studies are being done to provide experimental data in critical areas.

116

Heat Transport Fluids

Table XXII summarizes the thermophysical properties of the proposed heat transport fluids. Advantages and disadvantages of the fluids from the materials standpoint are summarized in Table XXIII. Depending upon criterion, any of the fluids may be selected. Societal factors, variations in component materials supplies, economies of scale, potential system improvements and individual preferences can affect selection.

TABLE XXII

PHYSICAL PROPERTIES OF SELECTED HEAT TRANSPORT FLUIDS

Fluid	Thermal Conductivity w/m·°K	Viscosity Pa - s	Specific Heat (J/kg °K) x 10^{-3}	Density kg/m³
Liquid Water (.101 MPa, 373K)*	0.21	3.05×10^{-4}	4.18	960
Steam (.101 MPa, 811K)*	0.019	2.86×10^{-5}	2.13	0.27
Sodium (811K)*	21.9	1.96×10^{-4}	1.26	819
Helium (.101 MPa, 811K)*	0.008	3.34×10^{-5}	5.19	0.192
Air (.101 MPa, 811K)*	0.013	4.18×10^{-5}	1.03	0.456
50 w/o $NaNO_3/KNO_3$ (811K)*	0.19	1.0×10^{-3}	1.59	1740

*Condition for fluid properties

Salt--Sodium nitrate/nitrite and potassium nitrate salts have been proposed as primary heat transfer and thermal energy storage media for numerous solar energy systems. They are inexpensive, abundant and readily available, and exhibit suitable thermal properties. The two nitrate based salt systems most commonly alluded to are "draw salt" (50% $NaNO_3$ and 50% KNO_3 by weight) and "Hitec" (53% KNO_3, 40% $NaNO_2$ and 7% $NaNO_3$ by weight). These two salt compositions are commercially available and have found widespread industrial use for heat treatment and heat transfer applications (see Table XXIV).

TABLE XXIII

RELATIVE FLUID MATERIALS PROPERTIES ADVANTAGES-DISADVANTAGES

Fluid	Advantage	Disadvantage
1. Water/Steam	- Extensive user experience	- High pressures require heavy piping
	- Ready sources of components	- Receiver control and design complicated by phase change
	- Very near term technology†	- Low gas phase heat transfer coefficient
	- Flexible P-T properties and direct couple to turbine	- Low gas phase energy transport density
		- Enthalpy-temperature properties of water/steam difficult to match to storage media
2. Liquid Sodium	- Extensive materials data base	- Potential for <u>dramatic</u> materials cost reductions appears low (some reduction in component cost possible thru redesign).
	- Extensive component development and test programs	
	- High thermal conductivity and energy transport density imply small receivers	
	- Very near-term technology†	
3. Molten NaNO$_3$ KNO$_3$ eutectic	- Inexpensive raw materials	- Minimal large system experience at the proposed operating temperatures. None for power generation
	- Intermediate energy transport	
	- Potential for the use of inexpensive materials and low cost component designs.	- Many detailed questions require answers; e.g., long-term decomposition, trace impurity effects, compatibility under thermal cycling, containment corrosion.
4. Air-Helium	- Minimum environmental impact with catastropic failure	- Most development required for temperatures $\geq$ 815 °C
		- Low energy transport density

NOTES: Comments for 1-3 assume 565 °C max working fluid temperature

†Solar thermal cycling environment effects upon thermal-hydraulic performance of materials is the major materials unknown.

TABLE XXIV

REPRESENTATIVE APPLICATIONS OF NITRATE BASED HEAT TRANSFER SALTS (HTS)

Date	Location	Inventory of HTS, kg	Temeprature Salt °C	Steam Generation Rates kg/hr
1959	Elizabeth, N. J.	75,000	400 to 480	10,000
1969	Selkirk, N. Y.	20,000	430 to 480	4,545
1969	Stickney, Ill.	220,000	400 to 480	22,727
1969	Morris, Ill.	165,000	400 to 480	20,454
1971	Kearney, N.J.	220,000	400 to 480	22,727
1971	Texas City, Tx.	220,000	400 to 480	22,727
1974	Stickney, Ill.	67,000	400 to 480	6,364
1975	Stickney, Ill.	75,000 1,062,000	400 to 480	10,455

The major concerns for the solar application are (1) the compatibility of molten salts with potential construction alloys, and (2) the thermal stability of the molten salt at elevated temperatures and in representative gas environments. Published experimental or operational experience with molten nitrate salts near or above 538°C was not available; therefore, screening experiments were initiated at Martin Marietta Aerospace, Sandia Livermore, and Sandia Albuquerque to evaluate the relative stability of candidate containment alloys. To date, these studies have been encouraging in that Incoloy 800 was identified as a potential high temperature alloy for use at 538-593°C; and 1018, Cr5-1Mo, and Cr9-1Mo alloys were identified for use at temperatures below 454°C. Short-term experiments (< 6 months) performed by Martin Marietta have shown that the following assumptions can be used in equilibrium calculations to represent the behavior of draw salt in a closed system at 565°C: (1) ideal solution behavior, (2) ideal gas behavior, and (3) nitrate → nitrite + oxygen is the only reaction of importance. Martin Marietta predicted decomposition rates of less than 2-5% per year from these experiments. Additional experiments will be conducted to certify these alloys in a high-temperature molten salt system for 30 years.

Since solar systems employing nitrate/nitrite salts would require large quantities of material, it is highly desirable to use commercial-grade starting materials. However, the impurity levels in the most inexpensive commercial-grade salts are generally high. The common impurites are chlorides, sulphates,

and carbonates. If necessary, the means for controlling the salt purity are available. On-site reprocessing and purification may be a reasonable approach for (1) the initial purification of commercial grade salt and (2) the on-stream clean-up of salt during operation.

While nitrate salts are an abundant commodity, there is a concern regarding availability of production capacity if large quantities are required. Thus, the continued identification of candidate non-nitrate salt systems is of value, in that in addition to relieving the potential burden on present domestic production capacity, alternate salt compositions also may provide for superior stability at high temperature, less corrosive behavior, and lower life cycle cost.

Liquid Sodium--The broad technology base that has been developed in liquid-metal fast-breeder reactor (LMFBR) programs in this country and abroad over the past 25 years can be applied in the design, materials selection, and construction of components for solar central-receiver systems (see Table XXV). Information relative to the thermal-hydraulic performance of sodium-heated steam generators, the reliability and performance of large sodium pumps, flow meters, and valves, and the necessary sodium-purity control and monitoring equipment is readily available and directly applicable to the development of solar-power systems. Except for specific environmental characteristics such as thermal cycling, the criteria for selection of materials for a sodium-cooled solar-power system are similar to those in LMFBR systems, i.e., the materials must possess adequate strength at high temperatures, compatibility with the sodium and water/steam environments, and on the water side, resistance to chloride and caustic stress-corrosion cracking. Special LMFBR requirements such as resistance to swelling and embrittlement under neutron irradiation and some of the high reliability requirement can be omitted in the present application. Also, the potential reduction in thermal shock transients to sodium/water heat exchangers in a solar plant may reduce mechanical design requirements and cost without reducing necessary quality control and assurance.

Sodium is a chemically reactive element that must be contained in an oxygen free (parts per million range) system. In suitable systems, the oxides of structural metals are chemically reduced or removed by traces of sodium oxide "flux." Alloy elements are then subject to solution in the molten sodium. Although the equilibrium solubility is rapidly approached, corrosion rates are typically very low (4×10^{-7} to 4×10^{-6} M/yr. at 590 and 704°C, respectively).

The compatibility of sodium with candidate structural materials has been extensively studied in support of liquid metal cooled nuclear reactor development. AISI 304 and 316 stainless steel and Incoloy 800 are considered suitable for long term use at sodium temperatures up to 538°C, based on studies concentrated in temperature ranges below 593°C but including work up to 815°C. The stainless steels and Incoloy 800 have relatively low yield strengths and have a propensity for self-welding and galling, which is abetted by the cleaning action of liquid sodium; therefore, hardsurfacing materials,

TABLE XXV

LIQUID METAL RECTOR EXPERIENCE

Facility	Location	Power (Mwt)	Coolant	Component	Material	Temperature (°C)		Operation
						Design	Maximum Operational	
EBR-II	Idaho	45	Na	core vessel	304 SS	538	471	1964 to present
				piping	304 SS	538	471	
				IHX shell	304 SS	538	471	
FERMI	Michigan	100	Na	core vessel	304 SS	538	440	1963 to 1966
				piping	304 SS	538	440	
				IHX shell	304 SS	538	440	
SEFOR	Arkansas	24	Na	core vessel	304 SS		437	1968 to present
DFR	Scotland	60	NaK	core vessel	321 SS*		415	1962 to 1967; 1969
				piping	321 SS		415	
				IHX shell	321 SS			
Rapsodie	France	24	Na	core vessel	316 SS*		538	1967 to present
				piping	316 SS		538	
				IHX shell	316 SS			
SRE	California	20	Na	Core vessel	304 SS	875	554	1957 to 1964
				piping	304 SS	648	554	(>37,000 hr)
				IHX shell	304 SS	648	538	
HNPF	Nebraska	240	Na	core vessel	304 SS	538	507	1963 to 1965
				piping	304 SS	539	507	
				IHX shell	304 SS	539	507	
BR-5	USSR	5	Na Primary NaK secondary	core vessel	321 SS*		449	1959 to ?
				piping	321 SS		449	(38,000 hr to
				IHX shell			427	July 1967)
EBR-1	Idaho	1.4	NaK	core vessel	347 SS		321	1951 to 1963
				piping	347 SS		321	
				IHX shell	A-nickel		304	
SNAP 2 (DR & ER)	Al	0.06	NaK	core vessel	316 SS	704	648	~3000 hr EACH
				piping	304 SS	704	648	
				IHX shell	316 SS	704	688	
SNAP 8 (DR & ER)	Al	0.6	NaK	core vessel	316 SS	760	704	S8ER · 10,000 hr
				piping	316 SS	760	704	S8DR · 1500 hr
				IHX shell	316 SS	760	676	To present
SNAP 10 (FS-3,	Al	0.03	NaK	core vessel	316 SS	565	543	FS-3 · 10,000 hr
FS-4)	Al	0.04		piping	316 SS	565	543	FS-4 · 1,000 hr
ARE	Tennessee	2.5	Na	core vessel	Inconel		704	220 hr
				piping	Inconel			

*Materials listed are the nearest US alloy composition.

such as the cobalt-nickel alloys, have been used for years on the contact surfaces of valve discs and seats to achieve acceptable wear and bearing properties.

Sodium-heated steam generators represent conventional state-of-the-art technology. For example, there has been a great deal of concern expressed over the chloride stress-corrosion cracking susceptibility of the stainless steels and Incoloy 800. However, adequate performance of these materials in contact with steam and water depends on adequate control of water purity. Since these materials, particularly the stainless steels, are in use in some superheaters and reheaters, that use demonstrates that water purity can be maintained. It is assumed that designs for central receiver steam generator systems will provide for such water chemistry control.

Air and Helium--Materials property limitations govern the maximum operating temperature of Brayton cycle systems. In the maximum temperature range of combustion gas turbines (1000°C) metallic or ceramic liners are used. These are cast, non ductile materials, which require a minimum of machining. Blades are subjected to the highest loads and require the greatest corrosion resistance. Fifteen to twenty per cent of total engine cost is for the hot-stage blades and vanes.

At the highest proposed gas turbine operating temperatures (1400°C) materials such as silicon carbide (SiC) have been suggested for use. There is no data base upon which long-term performance can be estimated for these materials because high-temperature structural refractories are a new technology. In addition, optimized fabrication, non destructive examination, and proof testing techniques required for use of large ceramic components must be addressed. This situation exists for both homogenous silicon carbide and composite materials, i.e., SiC-coated substrates. In the temperature range 750-1000°C, high nickel and cobalt based alloys such as Haynes 188, Nimonic 263, and Inconel 617 are used. Cobalt-containing materials are difficult to weld under the best circumstances and require post-weld heat treatments.

Iron-base alloys dominate the 550-750°C range, the 12% Cr Mo V steels being typical examples, for stationary applications (gas turbines). At the low end of this temperature range, austenitic stainless of modified 18 wt% nickel 8 wt% chromium composition is commonly employed. Table XXVI and XXVII present information for an abbreviated list of very high-temperature materials.

In anticipated solar central receiver applications, the most data is available on turbines and hot and cold leg piping. Performance information is lacking on high-temperature heat exchanger materials, fabrication of very large heat transfer surfaces, and the resistance of light weight castable insulation to pressure. Hot corrosion, the nemesis of combustion gas turbines should be minimized in a closed air Brayton cycle.

Water--A prime design guide has been the ASME Boiler and Pressure Vessel Code. Section I of the code, Power Boilers, seems to be applicable to the design of a solar receiver in which steam (or another vapor) is generated. However, there are conditions of loading and service unique to solar systems

122

TABLE XXVI

MAJOR ELEMENTS CONTAINED IN SELECTED HIGH TEMPERATURE ALLOYS (wt %)

Alloy	C	Mn	Si	Cr	Ni	Co	Mo	W	Cu(a)	Ti	Al	P(a)	S(a)	Fe	Other	UNS.[†]
304L S.S.	0.03(a)	2(a)	1.0(a)	19	10							0.045	0.03	Bal	P .045(a),	S30403
316L S.S.	0.03(a)	2(a)	1.0(a)	17	12		2-3					0.045	0.03	Bal	P .045(a),	S31603
Incoloy 800	0.10(a)	1.5(a)	1.0(a)	21	32.5	-	-	-	0.75	0.4	0.4	-	0.015	Bal	Cu 0.75(a)	N08800
Inconel 600	0.15(a)	1.0(a)	0.50(a)	15.5	Bal	-	-	-	0.50	-	-	-	0.015	8.0	Cu 0.5(a)	N06600
Inconel 601	0.05	1.0(a)	0.25	23	61	-	-	-	1.0	-	1.4	-	0.015	Bal	Cu 1.0(a)	N06601
Inconel 617	0.1(a)	-	-	22	Bal	12.5	9.0	-	-	-	1.3	-				-
Inconel 625	0.1(a)	0.5(a)	0.5(a)	21.5	Bal	-	9.0		-	0.2	0.2	0.015	0.015	5.0(a)	Cb (3.7)	N06625
Haynes 188 sheet	0.10	1.25(a)	0.35	22	22	Bal	-	14	-	-	-	-	-	3.0(a)	0.04 La	R30188
Hastelloy X	0.10(a)	1.0(a)	1.0(a)	21.2	Bal	2.5(a)	9.0	0.6	-	-	-	0.04	0.03	18.5		N06002
Hastelloy N	0.06(a)	0.8(a)	1.0(a)	7.0	Bal	0.2(a)	16.5	0.5(a)	0.35	-	0.5(a)	0.5	-	5.0(a)	0.5Al + Ti(a), B 0.01(a)	N10003
* %	-	98		89	70	97	0	38		38	8	-	33			

[*]1977 Percent of USAD Demand met by imports.
(a)$_{max}$
[†]Unified Numbering System for Metals and Alloys

TABLE XXVII

GENERAL INFORMATION FOR SELECTED HIGH TEMPERATURE MATERIALS

MATERIAL	RELATIVE COST $/kg	WELDING*	FABRICATION	COMMENTS
304L S.S.	1.0	Good	Good	Commonly Available - Max Temp 1050
Incoloy 800H	5.48	Fair to Good	Fair to Good	Inconel Welding
Inconel 600	8.80	Good	Good	For use in severely corrosive environments
Inconel 601	8.05	Fair to Good[†]	Fair to Good	Improved over 600; better high temperature properties
Inconel 617	14.87	Fair to Good[†]	Fair to Good	Improved over 625; very good high temperature mechanical properties; not presently coded at high temperatures; 12.5%-Co
Inconel 625	11.75	Good	Fair	Aging (brittle) at high temperature (looses Cr and Ni); unacceptable for high temp. cyclic fatigue service
Haynes 25	51.24	Poor	Poor; Considerable Work Hardening	High cobalt content; not available in large quantities because of extreme shortage of Co
Haynes 188	43.80	Poor	Same as Haynes 25	Same as Haynes 25; requires less cobalt than Haynes 25
Hastelloy X	13.6	Fair	Fair	More expensive and not as good mechanical properties as Inconel 601

*Welding costs for Incoloy and Inconels are similar; three times higher for Haynes.
†Caution due to aluminum content; use proper filler welding product.

and very critical in their design. For example, Section I does not consider thermal cycles explicitly or implicitly because fossil fuel boilers do not normally sustain as many severe thermal cycles as are projected for solar receivers. There are other aspects of Section I which may also be questionable for solar applications and may require change for economic reasons.

A contracted program conducted by Foster Wheeler Development Corporation was aimed at the development of a set of interim design rules and standards applicable to the central receiver solar thermal power system components that generally fall under the scope of the ASME Boiler and Pressure Vessel Code. Test Programs and additional development work required in order to upgrade the interim standard were identified.

An ASME Solar Code Committee was formed in mid 1978 to evaluate materials test information and revise the code standards as appropriate for solar water receiver applications. To generate specific data for code standards, as well as supply other engineering design information, a number of experiments are under way. Argonne National Laboratory has begun a test program using 300 series stainless steel and Incoloy 800 which are internally pressurized and cyclically loaded along the tube axis. The goal of this program is to verify that combined compressive creep and fatigue which occur in solar boilers are much less damaging than the conditions of combined tensile creep and fatigue normally used as the worst-case condition for materials testing.

Further data is being generated by the testing of a prototypical external receiver panel at the DOE CRTF. Concurrent pilot scale testing of a five tube panel at the Sandia radiant heat test facility will provide scaling information. Other contracted work by Combustion Engineering seeks to experimentally determine critical heat flux levels for single-sided heated smooth bore and rifled tubing.

These programs, along with others, will create a supportive base of mechanical properties data, standards and design rules which will be applicable to the special conditions of solar water receivers.

Hydrocarbon and Silicone Fluids--Although hydrocarbon and silicone fluids (Table XXVIII) are not being considered in large scale central receiver schemes as the heat transport fluid, they are being considered for line focus systems and small power distributed systems as the heat transport fluid and in all systems as a potential thermal storage fluid. These "oils" offer advantages over the salt and sodium systems in that their freezing points are much lower, which eliminates costly heat tracing, and they are, when properly maintained, not corrosive to common materials of construction. However, their operating temperature limit at present is 400°C, and only the more expensive fluids can be used at these temperatures without massive fluid breakdown. The fluids under consideration have been used in the past as heat transfer fluids, not heat storage, and therfore there is a scarcity of information on long-term thermal stability in bulk. The tests run by manufacturers in the past have not been designed to simulate a thermal storage system nor has much research been done to develop stabilizers for these fluids. In general, the fluids that cost $200-800/m^3 have a 315°C temperature limit, the $800-2000/m^3 fluids a 370°C limit, and the $2000-5000/m^3 fluids perhaps as high as a 400°C limit.

TABLE XXVIII

HYDROCARBON AND SILICONE FLUIDS

Material	Maximum Operating Temperature °C
Caloria HT43	< 320
Sun 21 Oil	< 320
Therminol 55*	< 320
Therminol 66*	< 340
Monsanto MCS 1980*	< 400
Monsanto MCS 2067*	
Monsanto MCS 2046*	< 370
Syltherm 800	< 400

*Developmental materials

Although in general these fluids are not corrosive to common materials of construction, these same materials may be harmful to the fluid. For example, it has been shown that at temperatures in excess of 315°C, low carbon steel has a very significant impact on the degradation of paraffinic hydrocarbons (SAND79-8209).

An additional materials compatibility problem arises when these fluids are used in a tank filled with rock or iron ore. Here, the fluid has a certain amount of sensible heat but the bulk is maintained in the solid media. Such systems require a lower fluid inventory (hence lower fill costs) but typically generate higher percent fluid losses because of surface catalysis effects by the solid media. Tests have been conducted and are continuing at Sandia Livermore to ascertion the fluid loss rate for several classes of fluids in contact with several types of solid storage media. Only when accurate fluid loss data is generated can reasonable assessments be made as to the economy of higher storage temperatures with the higher priced oils and solid storage media.

Metallurgical Studies

Argonne National Laboratory is investigating specific elevated-temperature mechanical properties of materials used for critical components in solar central receiver power systems. Several general features of water/steam receiver operating conditions are likley to create difficult structural design problems. The first of these is the highly cyclic nature of the thermal loading of critical components. In addition, repeated thermal cycling of superheater or boiler tubing while under internal pressure can lead to incremental growth or ratchetting. The analyst must therefore design against structural failure caused by thermal fatigue and creep-fatigue interaction and must also avoid excessive deformation caused by incremental growth.

Steady-state operation of the boiler and superheater tubing will cause nonaxisymmetrically loading at elevated temperatures. In particular, during daytime operation the outer wall of the superheat tubing on the high-temperature side will experience a large compressive axial stress and a moderate compressive hoop stress. On the other hand, the inner wall on the high-temperature side will be subjected to a compressive axial stress and a small tensile hoop stress. In addition a comprehensive survey of available information on sodium effects on candidate materials for solar-thermal electric piping and steam generators is being conducted. The survey includes information on sodium effects on mechanical properties, sodium compatibility, mass-transfer effects, and friction, adhesion, and self-welding behaviors in a sodium environment. Recommendations for future testing will be included.

The balance of the program is concerned with mechanical-properties data generation in support of the ASME Code development. This work interfaces directly with a program being conducted by Foster Wheeler Energy Corporation entitle "An Interim Structural Design Standard for Solar Energy Applications." In the Foster Wheeler program, design standards and criteria are to be established for solar central receiver systems that will eventually lead to the development of a set of ASME Code rules for solar applications. A critical phase in this development is the formulation and execution of an extensive mechanical-testing program to generate the required design-limits data. This mechanical-testing program is to be conducted by Argonne National Laboratory. As an initial effort under this subtask, a test matrix has been developed for the high-cycle fatigue testing of Incoloy 800 boiler tubing under biaxial (constant internal pressure plus cyclic axial loading) conditions. In parallel with the high-cycle fatigue testing, biaxial low-cycle fatigue testing of Inconey 800 will be carried out with a test matrix similar to the test matrix will for Type 316H stainless steel. Available fatigue data for Incoloy 800 and 800H, totaling some 480 data points, have been collected and published.

The response of I800 to creep and fatigue loading conditions is also being studied at Sandia. Objectives are:

1) Identify how the stress history (creep, fatigue, aging) alters the way in which high-temperature microstructural changes occur. This understanding will allow better predictions of which compositions should be most suitable in applications such as solar receivers that have a strong high-temperature fatigue component in their stress history.

2) Assess the influence of welding heat affected zone microstructure changes on creep and creep-fatigue properties.

3) Establish how alloy chemistry and heat treatment affect the sensitivity of stress-strain-temperature-time relationships. Some sensitivity is anticipated since certain Alloy 800 compositions are known to undergo precipitation hardening. Testing will provide the stress-strain histories necessary for computer modeling.

Baseline low cycle fatigue (LCF) data on two heats of Alloy 800 have been generated between plastic strain ranges of 0.75 and 0.25%. Comparative behavior of the two heats is sought because one heat had a large grain size (ASTM 6) and the other a small grain size (ASTM 12). Cycles to failure, cyclic hardening behavior, and fractographic observations indicate that the small grained material may have a slightly longer fatigue life; more importantly, widespread crack initiation, which could aggravate steam-water corrosion, occurs in the large grained material. The preliminary conclusions from these tests have led to a recommendation that a maximum grain size of ASTM 10 be added as a specification for the Alloy 800 to be used in the Barstow receiver.

High cycle fatigue tests at 565°C are in progress. Three specimens under stress have been cycled through 10^8 cycles. A dominant feature of these tests has been the extent of the cyclic hardening. For instance, between stress limits of 196 MPa the initial plastic strain range was greater than 0.1%; after 10,000 cycles the plastic strain range was about 0.06%; and after 10^6 cycles some plasticity was still observed. Only after about 3 x 10^6 cycles was the behavior completely elastic. This indicates that a detailed structural analysis of the receiver over the period of its lifetime may require using stress-strain material properties which evolve over the entire life.

The mechanical behavior of I800 tubes with internal steam simulating the pilot plant conditions is being monitored. The tests have five objectives:

1. Generate typical monotonic and cyclic stress-strain curves for real tubes with two different alloy chemistries in the as received and "nominally" age hardened condition.

2. Investigate the variations in mechanical properties resulting from cyclic history, alloy chemistry, and age hardening.

3. Investigate the analytical significance of stress relaxation during the diurnal cycle.

4. Generate the best estimate duty cycle for material in the departure from nucleate boiling (DNB) region and another region farther up the tube that will be identified as the high temp-high strain (HT - HE) region.

5. Run a limited number of tube specimens through the estimated duty cycles with a) dry inert gas pressure and b) steam pressure to see if there are any surprises.

Martin Marietta, Denver, has conducted a preliminary test program which surveyed several alloys (A516, A387, 304, 316, 321, A286, IN800) with respect to general corrosion resistance in the molten salt environment. They also conducted stress corrosion tests on some of these alloys. However, all of these tests were conducted under no load or constant load/strain conditions on smooth specimens. Environmental degradation often does not manifest itself under these conditions; in addition, the design application requires environmental compatibility under both dynamic and cyclic loading.

To further evaluate IN800 and 316 SS, Sandia will conduct slow strain rate tests. These tests will allow a quantitative assessment of the following variables on stress corrosion cracking susceptibility:

1. Electrochemical potential
2. Temperature
3. Molten Salt Chemistry
4. Metallurgical Variables

Slow strain rate testing, with control of the electrical potential, allows an accurate and quantitative assessment of the stress corrosion cracking susceptibility of tough, ductile alloys of the type which will be used for the central receiver tubes. These test results will detect any decrease in the load-carrying capacity of the material due to environmental degradation (i.e., SCC). The corrosion fatigue susceptibility of the prime candidate material will also be assessed.

Stresses and temperatures anticipated for solar receivers are sufficient to induce nonsteady inelastic deformation in portions of the structure. Some of the alloys of interest for this application are likely to operate in, or close to, the creep range. Nonsteady thermal stresses produced by diurnal solar cycles will induce low-cycle fatigue behavior, and DNB effects in single-pass steam plants are likely to add high-cycle fatigue. Steady stresses due to fluid pressures and structural loads may induce creep and rachetting.

Elevated-temperature material behavior is partitioned by code procedures into rate-dependent "creep" and rate-dependent "plasticity" components. This partitioning is unsatisfactory because it is not physically justified; furthermore, predictions based upon the associated models are often less than satisfactory. Interaction between plasticity and creep behavior is not part of the partitioned theories. In reality, however, subsequent creep behavior following plastic deformation and subsequent plastic behavior following creep may differ considerably from the response with no prior deformation. The partitioning approach can be "patched" in order to approximate some coupled response; however, because of the many assumptions involved, designs based on such analyses must be extremely conservative if they are to be safe.

Experiments have been initiated which are designed to provide correlation between the mathematically required internal state variables and microstructure. True correspondence between the model parameters and the material microstructure is required if models are to be reliable and predictive. The deformation model which has been proposed was used to predict the metallurgical state achieved through various deformation histories. Metal specimens with these histories have been prepared and are currently undergoing metallographic analyses. An attempt will be made to relate the observed microstructure of these specimens to the state predicted by the model.

Receiver External Environment Characterization

The purpose of this program is to identify the critical factors in the environment external to the central receiver absorber tube and subsequently, if required, to evaluate the influence of such environment on the life of the tubes.

All of the central receiver designs propose containment materials on the basis of successful experience with other heat exchanger designs which employ the same working fluid inside the tubing, i.e., 1) water/steam, 2) sodium, 3) sodium nitrate/sodium nitrite salt, or 4) a closed cycle gas such as air or helium. In no case has such successful experience included the presence of desert air on the outside surface. Indeed, the typical atmospheres include neutral (non-oxidizing) flue gasses, very high purity water, and neutral or reducing products of combustion, all of which can be argued as less corrosive to some materials than ordinary air. Furthermore, desert atmospheres frequently contain dust, may contain "alkali," a coloquialism for the salt residues from evaporating natural waters. This environment must be evaluated to determine its potential for damaging the metals in the receivers.

The first goal of this project is to sample the air at Albuquerque and Barstow at suitable elevations to determine what it contains as dust and aerosols. Then this environment will be synthesized in the laboratory and accelerated tests will be conducted. A self-powered air sampler is being fabricated to permit air sampling over a sufficient period of time to yield a representative air characterization.

Heliostat Mirrors

In November 1978 a mirror deterioration problem with heliostat facets fabricated by McDonnell Douglas and Martin Marietta was discovered at the Heliostat Development Facility located at Sandia, Livermore. The facets in questions are installed on operating heliostats used for experimental purposes and had been exposed to the environment for varying periods of six to nine months. When discovered, the deterioration noticed had the appearance of small black spots, about the size of a pinhead, clustered in groups at different positions on the facets. For clarification, a facet is the term used to describe a reflector module including the silvered glass mirror, structural backing and environmental seals.

130

When the discovery was made, telephone calls were initiated to suppliers, heliostat designers, test facilities, and others involved in solar applications of silvered glass mirrors. When asked to closely examine mirrors in their possession, nearly all indicated seeing signs of deterioration. After collecting and collating the observers findings, several conclusions could be drawn.

1. The mirror degradation is not limited to any one mirror module design, fabrication method, mirror maker, type of glass, or geographic location.

2. The observed deterioration can be categorized three ways: (1) as black spots, (2) as darkened streaks, and (3) as silver delamination from the glass.

3. The heliostat mirrors installed at the CRTF in Albuquerque do not show similar signs of deterioration. These facets have a laminated glass construction and many have been exposed for more than two years.

An investigation into the causes revealed that: the prime cause of mirror deterioration is water in the liquid phase which is allowed to contact the back sides of the mirror for a significant length of time. Other general conclusions are:

• Stress - although adhesive shinkage and thermal cycling can generate significant stress in the module, the stress itself was not considered to be the direct cause of the deterioration. However, the deterioration may be stress induced or stress enhanced.

• Although the adhesives and sealants used in te modules examined could have been contributory agents in the deterioration process, there are available adhesives and sealants that would pose no treat to the mirrored surfaces.

• In general, air pollutants were not considered a problem unless the back side of the mirrors were exposed without any additional protection. Protective backing designed to keep out moisture should prevent the intrusion of air pollutants.

Currents efforts aimed at defining a solution involve module designs that either provide a hermetic seal or allow the module to dry out as rapidly as it absorbs moisture (a "breathing" design) and better or additional mirror backing paints to inhibit the permeation of water through to the silver layer.

TEST FACILITIES

Four solar test facilities are available for research or testing: the Sandia 5-MW$_t$ Central Receiver Test Facility (CRTF) in Albuquerque; the Georgia Tech 400-kW$_t$ Advanced Components Test Facility (ACTF) in Atlanta; the U. S. Army 30-kW$_t$ White Sands Solar Furnace (WSSF) in New Mexico; and the French CNRS 1000-kW$_t$ Solar Furnace in Odeillo. Photographs of these facilities are presented in Figures 65 through 68.
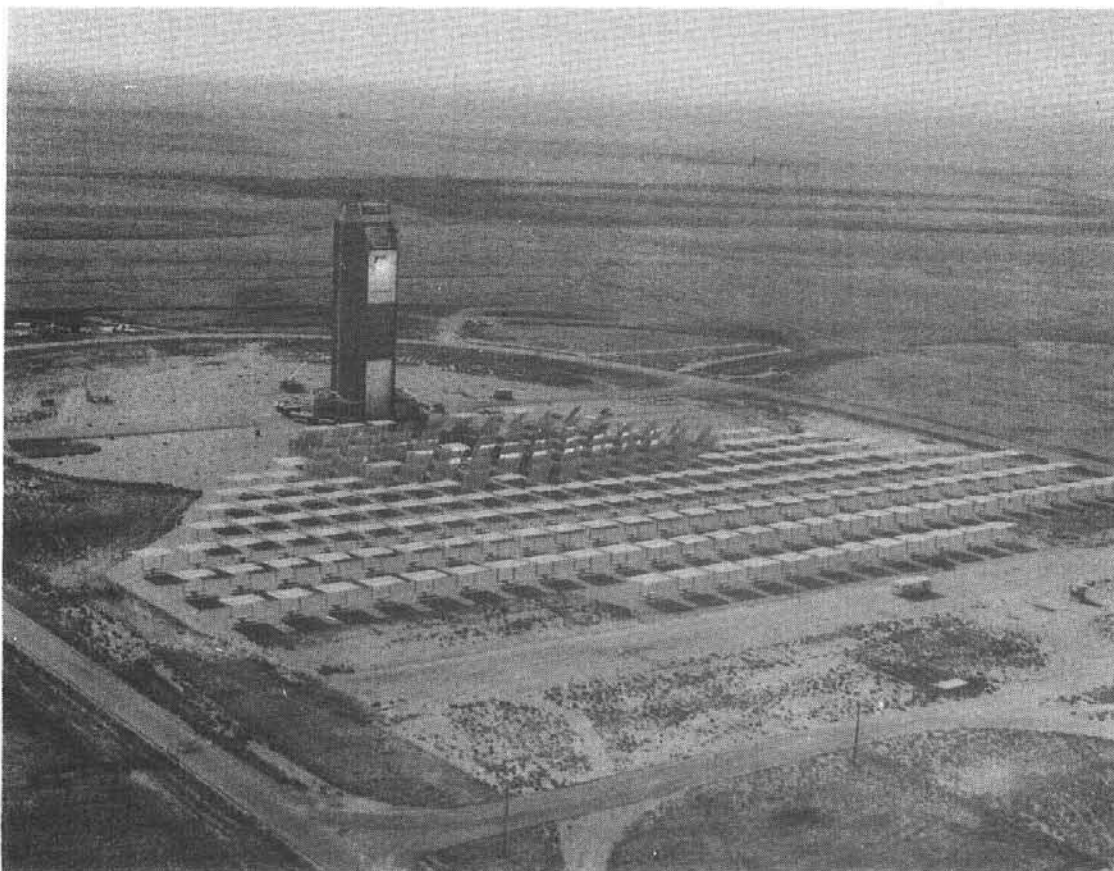
Figure 65. Central Receiver Test Facility
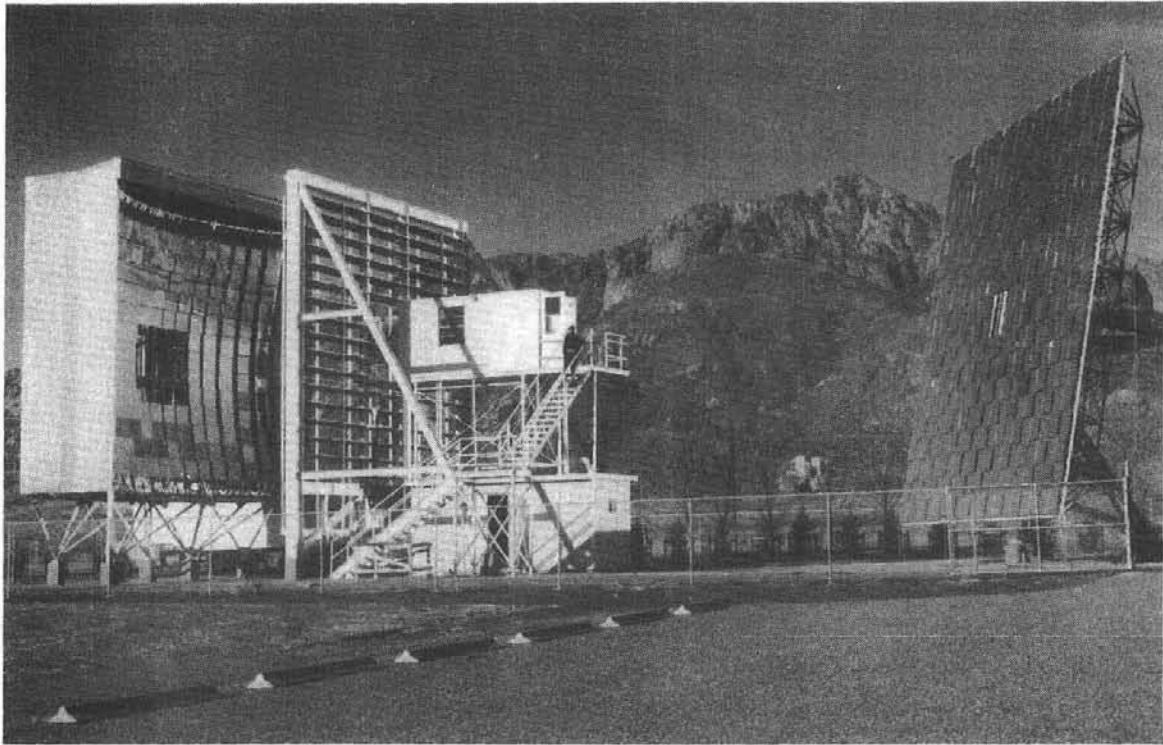
Figure 66. White Sands Solar Furnace
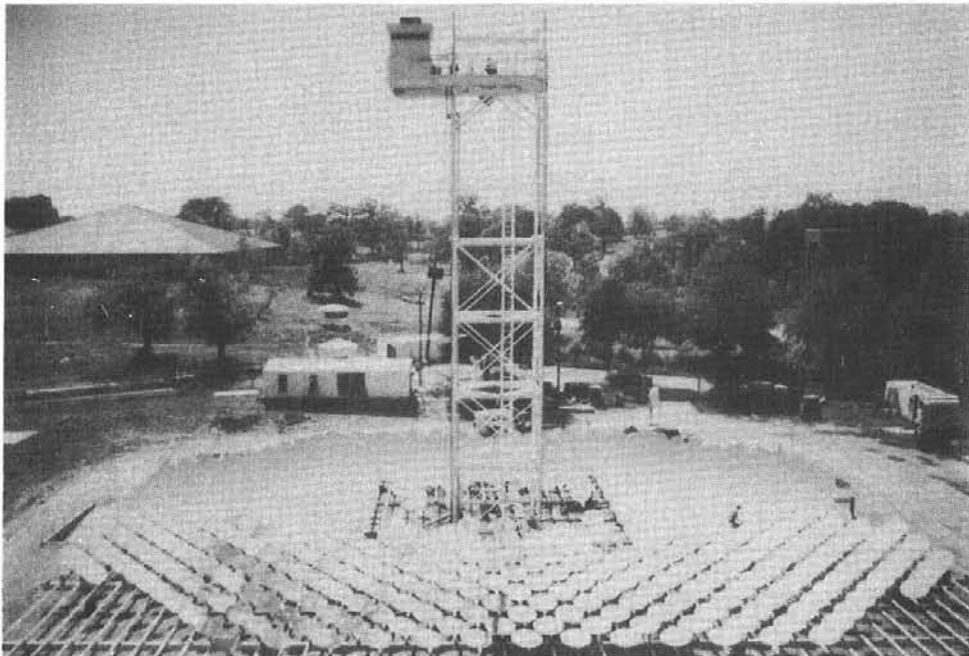
Figure 67. Georgia Tech Test Facility
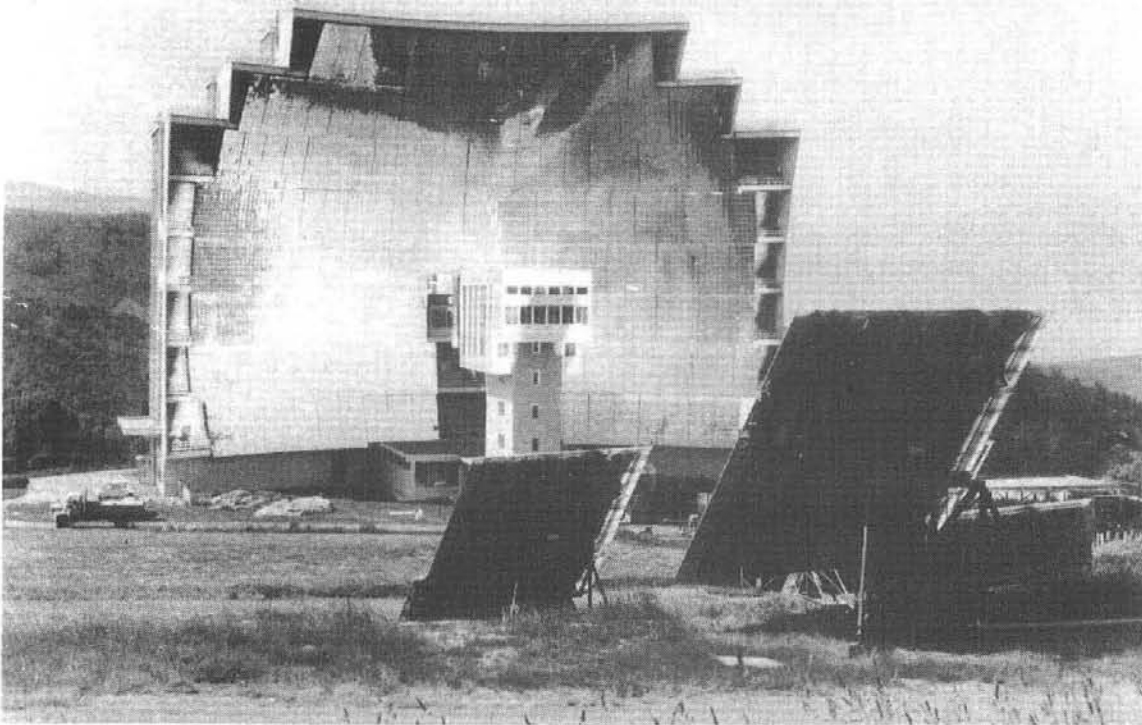
Figure 68. French CNRS Solar Furnace

The Sandia and Georgia Tech facilities both use large fields of heliostats to concentrate the sun's energy on test areas located on towers at the focal points of the heliostat fields. The White Sands and French solar furnaces are both double reflector systems consisting of flat mirrors which track the sun and reflect its energy to large fixed parabolic reflectors which in turn focus the energy onto the test area. A summary of the specifications of the four facilities is given in Table XXIX and a brief description of each facility follows. More information on these facilities is available from the Users Association* or from the facilities themselves.

Sandia 5-MW$_t$ Central Receiver Test Facility

The Sandia CRTF in Albquerque, NM, consists of a 200-ft tower and 222 heliostats in a north field capable of directing 5 MW of thermal energy to various locations on the tower. Each of the 400-sq ft (37 m^2) heliostats consists of 24 4 ft x 4 ft (1.2 m x 1.2 m)mirrors which are focused to

*Solar Thermal Test Facilities Users Association, Suite 1507, First National Bank Building East, Central and San Mateo, N.E., Albuquerque, NM 87108

135

TABLE XXIX

FACILITY CAPABILITIES

	CRTF Sandia	ACTF Georgia Tech	White Sands	Odeillo
Total Thermal Energy, KW	5000	400	30	1000
Number of Heliostats	222	550	356	63
Heliostat Size, m	6 x 6	1.10	0.6 x 0.6	6.0 x 7.5
Total Heliostat Area, m^2	8257	532	137	2835
Test Area Diameter,* m	2-3	0.5-1.0	0.08-0.15	0.25-1.0
Peak Flux, ** W/cm^2	250	200	400	1600
Maximum Calculated Equilibrium Temperature,** K	2600	2500	2900	4100

*The first number is area receiving approximately one-half of total energy; second number is area capturing 95% of total energy.
**Small area at center of beam.

produce a concentrated beam of solar radiation on a target test area. Peak thermal flux levels up to 250 W/cm^2 are available at the center portion of the beam. Approximately 1 MW_t is available within a 1-m diameter circle, 2.5 MW_t within a 2-m circle, and 5 MW_t within a 3-m circle.

Georgia Tech Advanced Components Test Facility

The Georgia Tech ACTF in Atlanta is modeled after the Italian facility designed by Giovanni Francia. It utilizes 550 round mirrors, each 111 cm in diameter, which are mechanically driven to track the sun and provide radiant heat fluxes up to about 200 W/cm^2 on a 0.5 to 1.0 m diameter test area centrally located about 20 m above the mirror field. Nominal concentration factors and equilibrium temperatures associated with these fluxes are about 2000X and 2200°C, respectively.

White Sands

The U. S. Army 30-kW White Sands Solar Furnace is operated by the U. S. Army and uses a double reflecting system. The primary reflector is a single heliostat consisting of 356 flat mirrors (each 62 x 62 cm) for a total of 137 m^2. These mirrors track the sun and reflect its energy to a parabolic

concentrator consisting of 180 62 x 62 cm spherical mirrors, which in turn reflect the energy to a target area, delivering about 30 kW_t with a maximum heat flux of about 400 W/cm^2 in a 5-cm diameter area at the center of the beam. The facility also incorporates a shutter system to provide thermal pulses of variable intensity and duration.

French CNRS Solar Furnace

The CNRS 1000-kW_t solar furnace, located in the Pyrenees at Odeillo Font-Romeu, in southern France, about 40 miles east of Andorra, consists of 63 heliostats (each 6 x 7 m) which follow the sun and reflect it's rays onto a parabolic reflector. The parabolic concentrator focuses 1 MW of thermal energy onto an area of about 40 cm diameter at the test area. At the center of the focal point, in an area 4 cm in diameter, the heat flux is 1600 W/cm^2 and stagnation temperatures approach 4100 K.

Users Association

The STTFUA was organized in 1977, under sponsorship fo the Department of Energy (DOE) and the Solar Energy Research Institute (SERI), to help expedite research and testing at solar thermal test facilities and to enable its members to keep better informed on advancements in high-temperature research, solar electric power generation and high-temperature solar testing facilities. The Users Association (UA) is managed by the University of Houston under a contract from SERI.

The purposes of the Association, as approved by the Department of Energy, are:

1. To act as the point of contact for Users of the STTFs and as primary access link between Users and STTFs.

2. To solicit and review proposals and make recommendations to DOE regarding utilization of the STTFs.

3. To disseminate STTF information on a regular basis.

4. To provide funding for STTF Users, subject to DOE program approval.

As noted above, the Association is authorized to receive and review proposals from persons seeking financial support for R&D or testing on the four solar facilities.

Dr. Alvin F. Hildebrandt, of the University of Houston, is President of the Association and Chairman of its Executive Committee. Mr. Frank Smith is Executive Director and heads the Association's office in Albuquerque. There are about 150 members and Association meetings are held once a year with workshops on specific subjects during the year as needed. A Newsletter is published approximately once per quarter.

APPENDIX A-- COMPUTER PROGRAMS

HELIOS

The code was developed to evaluate proposed designs for central receiver solar energy collector systems, to perform safety calculations on the threat to personnel and to the facility itself, to determine how various input parameters alter the power collected, to evaluate possible design trade-offs, and to judge heliostat compliance with some design criteria.

The code is designed with numerous subroutines for treating individual effects. This structure has facilitated additions that have been necessary as special requirements appeared or as improvements became necessary. The additions also resulted in non-optimum code design which will likely remain for some time as effort remains concentrated upon additional options.

The method for evaluating flux density is basically the cone-optics approach. Reflector surfaces are divided into small segments that are treated as infinitesimal mirrors that reflect a solar image onto the target surface. Surface uncertainties and other nondeterministic factors are accounted for by numerical convolution with the sunshape, using Fast Fourier transforms.

Input variables include atmospheric variables; sunshape parameters; coordinates for heliostat bases relative to the tower; heliostat design parameters, reflector shape information; data describing the uncertainty resulting from surface errors, suntracking errors, non-spectral reflection, and wind loading; focusing and alignment strategy; aim point coordinates; receiver design; calculation time; parameters indicating effects to be included; and the chosen output options.

Four output options are available. The first gives the flux density (W/cm^2) produced by all the heliostats at the grid of target points. The power intercepted by the mirrors and that incident upon the target are given. The facet area reduced by the angle of incidence effect and the area further reduced by shadowing and blocking effects are given. These data are given for each designated calculation time.

The second output option yeilds the above output variables for each heliostat in addition to the total. The loss factor caused by light propagation between facet and receiver is also given for each heliostat.

The third output option is still more complete. It is especially useful for detailed examination of results for checking prior to a large computer run. It includes facet and heliostat alignment information, sun orientation, target point alignment information, and detailed shadowing and blocking information including lists of the blocked (shadowed) and blocking (shadowing) heliostats.

All of the output options include (1) a table describing the built-in model of atmospheric mass as a function of apparent elevation angle of the sun, (2) a table describing the built-in model of atmospheric refraction as a function of solar elevation angle, (3) brief descriptions of the input data groups, (4) tabular distributions of the sunshape, the error cone, and the effective sunshape, (5) tower coordinates of each target point and the components of the unit vector normal to the target surface at each point in the grid, and (6) a listing of the main problem parameters. As a special output option, the three components of the energy flux density are available at each target point in the grid.

The fourth output option gives an abbreviated output similar to the first, but in a form convenient for typewriter or NOS output.

The present HELIOS limitations are:

$1 \leq$ number of heliostats ≤ 559

$1 \leq$ numbr of facets/heliostat ≤ 25

$1 \leq$ number of target points ≤ 121

$1 \leq$ number of prealignment points ≤ 20

$1 \leq$ number of aim points ≤ 20

The required running time is highly dependent upon input options. It is dominated by the flux density calculation except at very late or early times when shadowing and blocking may be extensive. On CDC-7600 with perfect-focus option, the flux density calculation requires 14.4 ms per facet for 121 target points. Zones A-B and A-C-D-E (222 heliostats) of the Solar Thermal Test Facility require 11 to 18 s for shadowing and blocking calculations as those effects reduce the effective mirror area by factors 0.99 to 0.81. Typical CDC-7600 run time for 222 heliostats with 25 facets/heliostat and 121 target points is 120 s including generation of the plot tape. These times should be multiplied by $\lesssim n^2$ if the facets are divided into a n x n mesh for more precise integration. Minor modifications would add a cell option to decrease run time for large heliostat fields.

HELIOS is operational on the Sandia Laboratories CDC-6600 computer operating under Scope 3.3. The code requires 104k octal storage locations. HELIOS is also operational on the Sandia Laboratories CDC-7600 under Scope 2.1.

140

Some auxiliary equipment is necessary.

Printer   - required

Microfiche output - useful

Punch   - necessary for some options

Auxiliary storage - necessary for recall of data temporarily on magnetic tape (disk).

The coding language is FORTRAN extended-version 4.

The following reports present information on HELIOS:

(1) C. N. Vittitoe, F. Biggs and R. E. Lighthill, HELIOS: A computer Program for Modeling the Solar Thermal Test Facility, A Users Guide, Sandia Laboratories Report SAND76-0346, March, 1977, Second edition, June, 1977, Third edition, October, 1978.

(2) F. Biggs and C. N. Vittitoe, The Helios Model for the Optical Behavior of Reflecting Solar Concentrators, Sandia Laboratories Report SAND76-0347, March, 1979.

DELSOL

DELSOL is a computer code for quantifying the performance, determining the field layouts, and optimizing the cost/performance of large central receiver systems. It is an easy to use, relatively fast and accurate engineering design tool based on a powerful new theoretical method for calculating the efficiency of heliostat fields. Special features of the code include: (1) the code's running time which is significantly sublinear with respect to the number of cases analyzed; (2) a detailed description of the various heliostat error sources; and (3) the range of problems that can be analyzed. The code and manual will be released in early 1979 and will probably be the first fully documented performance and optimization code available to the solar community. DELSOL is used at Sandia in the evaluation and selection of DOE contracts, as well as in fundamental studies of central receiver technology.

The performance calculations include the effects of time varying insolation, cosine, shadowing, blocking, atmospheric attenuation, spillage, reflectivity, and receiver losses. DELSOL is based, in part, on several significant extensions and modifications of the University of Houston's flux calculation technique involving a Hermite polynomial expansion. Unique features include: (1) the analytical dependence of the flux on tower height; (2) a more detailed and realistic model of heliostat errors; and (3) analytical formulae for analyzing focused or canted heliostats. As a result of the first capability,

DELSOL requires that only one annual performance calculation be made in order to analyze heliostat efficiency for any range of tower height and receiver size, receiver type, or aim point strategy. This contrasts with codes based on other calculational techniques that require a new annual performance calculation with each change in system design (e.g., tower height). This feature makes tractable the large number of performance calculations required in design tradeoff and optimization studies. Typically, the initial performance calculation requires 60-240 seconds on Sandia's CDC 6600 while additional performance calculations take only a few seconds each. The code includes a model of the cost of towers, receivers, land, wiring, etc., that allows the layout of cost effective fields and the optimization of the system design. An efficient optimization procedure is used to determine the optimum field layout, receiver type and size, and tower height as a function of design point power level. The code can handle a wide variety of systems including: rectangular or circular heliostats; flat, focused or canted heliostats; 2-d tracking, 2-d surface and 2-d reflection helisotat errors; external or cavity receivers; and single or multiple cavity apertures with rectangular or elliptical boundaries. DELSOL also has extensive plot output including: contours of the individual performance terms; layout of fields; and optimized energy cost, tower and receiver dimensions, land and mirror area efficiency and capital cost as a function of design power.

MIRVAL

MIRVAL[1] is a Monte Carlo program which simulates the heliostats and a portion of the receiver for solar energy central receiver power plants. Models for three receiver types and four kinds of heliostats are included in the code. The three receiver types modeled are an external cylinder, a cylindrical cavity with a downward-facing aperture, and a north-facing cavity. Three heliostats which track in elevation and azimuth are modeled, one of which is enclosed in a plastic dome. The fourth type consists of a rack of louvered reflective panels with the rack rotatable about a fixed horizontal axis.

Phenomena whose effects are simulated are shadowing, blocking, mirror tracking, random errors in tracking and in the conformation of the reflective surface, optical figure of the reflective surface, insolation, angular distribution of incoming sun rays to account for limb darkening and scattering, attenuation of light between the mirrors and the receiver, reflectivity of the mirror surface, and aiming strategy.

Ref 1: P. L. Leary, J. D. Hankins, "A User's Guide for MIRVAL--A Computer Code for Comparing Designs of Heliostat-Receiver Optics for Central Receiver Solar Power Plants," Sandia Laboratories, SAND77-8280, October 1978.

Power runs (pointing time) and energy runs (integration of power over time) execute in about the same length of time. Rays of light are selected from the vicinity of the sun and are traced until they either enter the receiver or are lost in a prior absorption process or are deflected enough to miss the receiver. For the cylindrical receivers, rays which enter the receiver are tracked to the heat transfer surface; while, for the north-facing cavity, tracking stops at the plane of the aperture.

For a power run, the output includes the thermal power entering the receiver, the power density on the terminal surface, the power shadowed by each of two processes (by mirrors, by tower or by either), the power blocked by mirrors, the power incident on the ground, the power that is reflected by and clears the mirrors but misses the receiver, and the power that clears the mirrors but which is absorbed or scattered between the mirrors and the receiver. For energy runs, the same set of alternatives are used, but the output refers to (time) averaged power. Output can be obtained for individual mirrors, groups of mirrors or for the total deployment.

MIRVAL accepts fields containing up to 30,000 heliostats which are arbitrarily positioned in space. The code can be modified for the evaluation of other mirrors or receivers by changing a small number of subroutines.

STEAEC

The Solar Thermal Electric Annual Energy Calculator (STEAEC) is a computer model developed at Sandia Laboratories as part of the 10 MW_e Solar Pilot Plant concept selection. The program was used to size subsystems and calculate annual energy production as input to the cost/performance analyses. STEAEC is used in conjunction with two other models developed at Sandia Laboratories. MIRVAL (1) provides field efficiencies as a function of sun position. The performance and subsystem sizes calculated by STEAEC are then used by the computer model BUCKS (2) to compute the plant levelized busbar energy cost. Figure 76 depicts the relation of these models.

A block diagram of the simulation model is presented in Figure 77. At each time step the power flows shown in this diagram are computed using a sun following thermal storage dispatch strategy. Auxiliary power requirements for each time step are computed on a subsystem basis. Simulation for a year yields a prediction of the annual net electrical output of the solar plant.

BUCKS is a computer model developed for economic analysis of solar thermal central receiver technology in utility networks and for comparative evaluation of alternate plant designs. The model described in this report calculates power production costs for a single solar thermal central receiver power plant. An extended version of BUCKS which is being developed will include the impact of solar electric plants on utility network economics.

The model calculates levelized busbar energy cost. This is the constant revenue per unit output required over the plant lifetime to compensate for its fixed and variable costs, pay interest to stockholders, and provide return to shareholders. It does not include transmission and distribution costs or other indirect utility costs.

BUCKS is used in conjunction with two other models developed at Sandia Laboratories as a part of the Central Receiver Solar Thermal Electric Program. MIRVAL provides heliostat field efficiencies as a function of sun position to the plant performance model, STEAEC. Plant performance and subsystem sizes are then calculated by STEAEC and used by BUCKS to compute the plant levelized busbar energy cost. BUCKS was designed to interface with these models, but can be used in conjunction with any plant annual performance model.

The basic inputs and components of the model are shown in Figure 78. The required input information to BUCKS includes cost estimates for the reference plant, and performance information for the subject plant. The reference plant is one for which detailed cost estimates are available. The subject plant represents a variation in size from the reference plant but maintains the basic design concept.

The model scales the reference plant estimates for both capital costs and operations and maintenance (O&M) costs to the subject plant size. The costs are then escalated to the time when they are required for payment on a plant expense. The escalated O&M costs are the total O&M costs accrued over the plant life. The escalated capital cost is added to the cost for use of money during the construction period to give the total capital investment at the year of commercial operation. This capital investment cost is added to additional fixed costs to give the total fixed costs over the plant life. Fixed costs are those which are independent of the plant annual generation level such as capital investment, depreciation income tax allowance, and insurance and property tax. Both the total fixed and O&M costs are then discounted and levelized to give the levelized annual required revenue. This estimate is normalized to the estimated annual generation to give the levelized busbar energy cost.

Insolation and Sun Location Model

This program gives an estimated insolation value, along with the solar position vector in local topocentric coordinates, for any input latitude, longitude, julian day, and hour from local noon. Several analytic insolation models are available. Inputs are required for site elevation, turbidity, percent percipitable water. Air mass is corrected for the spherical earth.

Collector Field Optimization Program

The RCELL program provides a cellwise method of optimization suitable for large solar central receiver systems. This program contains an adequate model for the central receiver system, and can output nearly complete performance data for an economically optimized collector field. The economic model evaluates the cost of thermal energy delivered at the base of the tower. The optimization is based on a figure of merit which is the total system cost divided by total annual thermal energy available at the base of the tower. The details of the heliostat and receiver design enter into RCELL through the receiver interception fractions, which are input data to RCELL. The heliostat size and shape play a role in the shading and blocking calculations, which basically determine the optimization of the collector field.

The RCELL program provides a neighborhood of heliostats surrounding the representative heliostat, which is located at the center of each cell in the collector field. There are four types of neighborhoods available: radial stagger, radial cornfield, north-south stagger, and north-south cornfield. Having selected the type of neighborhood, the RCELL program calculates the redirected energy from each representative heliostat for 7 days, 19 times per day and for each of 16 variations in the neighborhood geometry. This information allows the program to select optimized spacing coordinates for each cell, after which the arrays of spacing coordinates can be reduced to coefficients of a suitable polynomial fit. The optimization process balances losses and determines the extent of the collector field. It does not optimize the heliostat, receiver, or tower, but rather specifies the optimal heliostat field to deploy with a specified tower and receiver.

Central Receiver System Simulation with XY Arrays of Cells

This program consists of a complete set of source elements that simulate the optical behavior of large solar central receiver systems. The collector field is given an XY cell structure (i.e., squares with north-south orientation) and each cell contains a representative heliostat, located at the cell center

and surrounded by a specified array of neighbors. The number of cells across the field in the east-west and north-south direction are parametric inputs that determine the array size for all of the field related matrices and vectors. The base of the tower can be located at any cell center. An output subroutine prints the field related matrices with a border of averages and a contour print to the right of the matrix print. Input quantities are located in the input field along with expository comments.

The program can be operated in two modes:

1) If the program is used as a receiver study, no extra input data files are needed. The receiver study configuration includes the receiver model (i.e., CYLN2 for cylindrical receivers with a two- point aiming strategy, or CYLNF for flat panel receivers), and the image generator HCOEF or alternatives. Outputs are available for receiver flux density and receiver interception fractions. A receiver panel or receiver node data file is written to disk which contains the panel or node interception fraction for each representative heliostat at the input time.

2) If the program is used as an annual study, the panel or node data file obtained above must be input. The annual study configuration includes the integrating subroutines SUMIT and special output subroutines RELPOW and PANPOW. The output can include hourly values on seven representative days for the cosine, shading and blocking losses for each cell as well as the total redirected power from the field. A final summary combines this data with the interception data from the node file to produce a plot of daily and annual relative power from each cell as well as a tabulation of the power intercepted and the power delivered to the coolant for each receiver panel.

The shading and blocking subroutine SAB3 is always available but need not be used for initial interception calculations that must be performed before the collector field geometry is known. After the collector field is determined, another receiver run may be required to output actual receiver flux densities. Shading and blocking events are properly accounted for in this run.

Central Receiver System Simulation with Individual Heliostats

This program contains a complete set of source elements for simulating solar central receiver systems. Each heliostat is given an actual location and true time dependent orientation. Field related quantities such as X and Y coordinates of the heliostat, cosine, fraction of mirror reflecting, interception factor, etc. are output by a listing procedure which can be continued for arbitrary numbers of heliostats. This program is oriented toward small central receiver systems but should be able to handle 3000 heliostats (i.e., pilot scale systems).

APPENDIX B--INSOLATION DATA SOURCES

With the surge of interest in Solar Energy has come the need for solar radiation data and a knowledge of data sources. Consequently, a number of documents have been published on the subject. These reports vary (according to their purpose) from a comprehensive listing of observation stations in the United States to an exhaustive evaluation and presentation of data in one state e.g., California. Most of these documents attempt to reach a broad audience of architects, engineers, builders, homeowners and others. The purpose of this index is to list in a concise manner some of the primary sources of insolation data. A more extensive coverage and evaluation of sources is presented in the reference.

The major sources of insolation data are:

1. National Oceanic and Atmospheric Administration, Environmental Data Service, National Climatic Center (NCC), Asheville, North Carolina.

Entitled SOLMET for Solar and Meteorological data, this is the largest and most extensive source of data. This program contains hourly data form older National Weather Service stations with long records and from 37 newly established stations. Recording sites cover all regions of the United States and Puerto Rico. All data are stored on magnetic tape.

Data from old stations have been reworked to correct errors, fill gaps, and to calculate direct normal insolation. These tapes are known as Augmented SOLMET tapes.

The new stations are equipped with horizontal pyranometers to measure total horizontal insolation and normal incidence pyrheliometers to measure direct normal insolation. They also record other parameters such as air temperature. In addition, data from many governmental and private agencies are included in the tapes at NCC. For detailed information on SOLMET, see Reference 1. For more information on data tapes and models see Reference 2.

2. Southern California Edison, Research and Development, P. O. Box 800, Rosemead, California 91770

Southern California Edison manages a solar resources project for WEST Associates, a consortium of western utilities. They have instrumented sites in California, Nevada, Arizona, New Mexico, and Colorado; however, most sites are located in Southern California. All sites measure total horizontal insolation and air temperature, and most sites measure direct normal insolation as well. Recording is continuous and reported as 15 minute averages. Southern California

Edison publishes annual reports which contain statistical summaries of the data. In addition, they will provide detailed statistics (such as daily profiles) and data tapes on request. See Reference 3.

3. Energy and Environment Division, Lawrence Berkeley Laboratory, University of California, Berkeley, California 94720

a) Solar Manual

They have published a California Solar Data Manual dated January 1978 which presents solar radiation from 19 stations in California. This report contains a very comprehensive evaluation of the data, analyzing the errors, instrumentation and so forth. It also includes extensive climatic data. It is a very complete and reliable source of information. See Reference 4.

b) They are taking circumsolar measurements across the face of the sun at several sites in the U. S. These stations measure radiation from the center of the sun to a radius of about 3 degrees. See references 5 and 6.

4. Tennessee Valley Authority, Air Quality Branch River Oaks Building, Muscle Shoals, Alabama 35660

The Tennessee Valley Authority has a network of ten sites that measure solar radiation and surface meteorological parameters. Located in the southeast, some of these stations have been in operation for about ten years.

5. Solar Energy Laboratory, University of Wisconsin, Madison, Wisconsin.

The university has compiled a data tape with 8 years of solar radiation and surface meteorological data for Madison, Wisconsin.

6. Department of Energy Solar Energy Meteorological Research and Training Sites.

Eight sites have been set up to serve various regions of the United States. Their purpose is to provide research and training in their area. Since the responsibilities of these sites have not been fully defined as yet, it is not possible to state what type of measurements have been or will be taken at all sites. However, they should be aware of what data is available in their area. The stations are:

1. Southwest - University of California
   Department of Meteorology
   Davis, California

2. Northeast - State University of New York
   Atmospheric Sciences Research Center
   Albany, New York

3. Southeast - Georgia Institute of Technology
   School of Aerospace Engineering
   Atlanta, Ga.

4. South-Central - Trinity University
   Physics Department
   San Antonio, Texas

5. Northwest - Oregon State University
   Department of Atmospheric Sciences
   Corvallis, Oregon

6. North-Central - University of Michigan
   Department of Atmospheric Sciences
   Ann Arbor, Michigan

7. Arctic - University of Alaska
   Geophysical Institute
   Fairbanks, Alaska

8. Pacific - University of Hawaii - Manoa
   Meteorology Department
   Honolulu, Hawaii

7. Aerospace Corporation, Energy and Transportation Division, Los Angeles, California.

Aerospace Corporation has developed an hourly insolation data base for 34 locations across the United States. They used the 1962 and 1963 hourly data from the National Climatic Center in Asheville.

8. U. S. Army, Atmospheric Sciences Laboratory Meteorological Support Technical Area, White Sands Missile Range, New Mexico.

The meteorological team at the Yuma proving ground records total insolation and surface climatic data at Yuma, Arizona. The Atmospheric Sciences Laboratory at White Sands Missile Range, New Mexico, processes the data and publishes monthly reports of hourly averages. Several years of records are available. See Reference 7.

9. Canadian Meteorogical Service, Atmospheric Environment Service, Climatic Data Processing Division, 4905 Dufferin Street, Downsview, Ontario, Canada.

This is an organization similar to NOAA's Climatic Center. The National Climatic Center of NOAA at Asheville, N.C. should have data from Canada, particularly from areas near the border of the U. S. See Reference 8.

10. State Energy Office, Governors Office of any of the fifty states.

Most of the states have a state energy office which provides a clearinghouse of data. This is a good source of information on solar energy projects in that state. Contact can be made through the governor's office.

11. Sandia Laboratories, Albuquerque, New Mexico.

Sandia Laboratories have been measuring total horizontal and direct insolation at the CRTF in Albuquerque on an irregular basis since 1973. Usually the data are taken in support of tests. Several reports pertaining to solar insolation have been published e.g., Reference 2.

12. University of Alabama, Johnson Environmental and Energy Center, Huntsville, Alabama.

This center has compiled a very complete listing of solar observation stations, their equipment and record format. See Reference 9.

13. Solar Energy Research Institute, Golden, Colorado.

The Energy Resource Assessment Branch of SERI has the task of providing state-of-the-art data bases and physical models to ensure accurate design and analysis of solar energy devices. They have made preliminary research measurements of the thermal insolation on tilted surfaces in the Denver area. Meteorological and insolation research will be performed at the SERI site near Golden, Colorado. See reference 9.

In an appendix such as this, it is not practical to list every organization recording data. Many sources have been omitted. However, references have been included that do provide comprehensive coverage. Reference 7 has the most detailed list and promises to be updated each year. References 2 and 6, while not as extensive, provide good description of data sources.

REFERENCES

1. SOLMET, Hourly Solar Radiation-Surface Meteorological Observations, Volume 1 and 2 August 1978, Environmental Data Service, National Climatic Center, Asheville, NC.

2. E. Boes, Insolation Modeling Overview, SAND78-0963, Sandia Laboratories, Albuquerque, NM, December 1978.

3. Southern California Edison, The West Associates Solar Resource Evaluation Project, Southern California Edison Research and Development, Rosemead, California, June 1977.

4. P. Berdahl et al, California Solar Data Manual, LBL-5971; Energy and Environment Division, Lawrence Berkeley Laboratory, U.C. Berkeley, Berkeley, CA, January 1978.

5. A. J. Hunt, D. S. Grether, and M. Wahlig, "Circumsolar Radiation Data for Central Receiver Simulation," Proceedings of Solar Workshop on Methods for Optical Analysis of Central Receiver Systems, Houston, Texas, August 10 and 11, 1977. Also published as Lawrence Berkeley Laboratory Report 8371, August 11, 1977.

6. D. S. Grether, D. Evans, A. Hunt and M. Wahlig, "Application of Circum-
    solar Measurements to Concentrating Collectors," 1979 International
    Solar Energy Society, Atlanta, Ga., May 28-June 1, 1979, also published
    as Lawrence Berkeley Laboratory Report 9412, 1979.

7. --- Atmospheric Sciences Laboratory Meteorological Team Data, Yuma Proving
    Ground, AZ, Meteorological Support Technical Area, White Sands Missile
    Range, NM, July 1976.

8. --- U. of Alabama, Huntsville, Solar Radiation Data Sources, Applications
    and Network Design, (HCP/T5362-01) U. S. Department of Energy, Assistant
    Secretary for Energy Technology, Division of Solar Energy, Division of
    Solar Technology, Washington, DC, 20545.

9. E. A. Carter, et al, Solar Radiation Observation Stations, The University
    of Alabama, Johnson Environmental and Energy Center, Huntsville, Alabama,
    November 1978 (to be updated March 1979).

10. Watt Engineering Ltd., On the Nature and Distribution of Solar Radiation,
    (HCP/T2552-01) DOE, Assistant Secretary for Solar Technology, Division
    of Solar Technology, Environmental and Resource Assessments Branch,
    March 1978.

11. R. L. Hulstrom, Insolation Models, Data and Algorithms Annual Report
    FY78 (SERI/TR 36.110) Solar Energy Research Institute, Golden, Colorado,
    December 1978.

APPENDIX C--INTERIM STRUCTURAL DESIGN STANDARD

Foster Wheeler was authorized to develop an "Interim Structural Design Standard for Solar Energy Applications." This program is aimed at the development of a set of interim design rules and standards applicable to the Central Receiver Solar Thermal Power System (CRSTPS) components that generally fall under the scope of the ASME Boiler and Pressure Vessel Code. Test programs and additional development work required in order to upgrade the interim standard are also to be identified. This program has now been extended to perform creep-fatigue analysis of ANL tests and to evaluate these tests so that they may be used to update the Interim Design Standard.

The Interim Design Standard is specifically directed toward the first-generation solar power systems of the water/steam type. The Interim Standard was prepared by selecting rules from the Code and modifying these rules wherever necessary. In selecting the rules, the following criteria were considered to be important:

- Simplicity. The Interim Design Standard must be simple to use. An approach similar to that of Section I or Section VIII-Division 1 would be most appropriate from this point of view. This approach essentially involves Design-by-Rule. The thickness of the pressure boundary is set by limiting the primary stresses to conservative allowable stress values, thus preventing burst and gross distortion. The remaining failure modes are prevented by liberal safety factors and accepted design practices. This approach, however, may result in greater component weight.
- Design-by-Analysis Alternative. It is considered useful to give an option of Design-by-Analysis. Thus the user may decide whether to perform additional analyses that might justify a reduction in wall thickness. This approach is especially important in that modern computer methods of analysis are within reach of most engineers.
- Avoidance of Excessive Conservatism. One of the challenges in the development and commercialization of a viable solar power technology is the reduction in capital costs. A design standard which is unduly conservative will drive up the costs and price the technology out of the market.
- Appropriate Levels of Reliability. Although the prime consideration in the development of the Interim Design Standard is safety, effectiveness and reliability are also important.

The first part of the work, that is, the preparation of the Interim Design Standard and the identification of test and development needs, has been completed. The second part, analysis and evaluation of ANL tests, is continuing. Four tests have already been analyzed.

During Phase 1 of this program, CRSTPS system components were reviewed. To determine the range of loading conditions, the environment, and possible failure modes in CRSTPS components that fall under the scope of the ASME Boiler and Pressure Vessel Code. In this study, primary attention was given to the receiver and thermal storage subsystems, including the heat exchangers and piping. The electrical power generation subsystem, pumps, and valves were excluded. The various pertinent Sections of the Code were also reviewed to determine their applicability to solar power system components. A review of the available failure-rate data and other reliability information related to pressure components designed according to the Code was also done to establish the appropriate level of reliability for solar components.

In summary, the Interim Structural Design Standard is based on Section VIII-Division 1 of the Code. For subcreep temperatures, a design-by-analysis alternative of Section VIII-Division 2 is provided. The Interim Standard includes modified portions of other Sections of the Code in order to prevent failure modes that directly concern solar applications but not most Section VIII applications. In most cases the modifications were taken from Sections of the Code governing nuclear components. Thus the levels of reliability are much more stringent than needed for solar applications. An attempt was made in developing the Interim Design Standard to reach a reasonable compromise between the lack of adequate requirements of Section VIII and the overly conservative rules governing nuclear applications. The major changes relate to component applications at temperatures where creep is a factor.

154

BIBLIOGRAPHY

1. "Recommendations for the Conceptual Design of the Barstow, California, Solar Central Receiver Pilot Plant - Executive Summary," Sandia Laboratories Report SAND77-8035, October, 1977.

2. "Highlights Report - Solar Thermal Conversion Program - Central Power Projects," Sandia Laboratories Report SAND77-8011, March 1977.

3. "Highlights Report - Solar Thermal Conversion Program - Central Power Projects," Sandia Laboratories Report SAND77-8513, November, 1977.

4. "Semiannual Review of Solar Thermal Central Power Systems," Sandia Laboratories Report SAND78-8015, April, 1978.

5. Department of Energy Large Solar Central Power Systems Semiannual Review, Sandia Laboratories, November, 1978, SAND78-8511.

6. "Solar Central Receiver Systems," illustrated brochure published by Sandia Laboratories, Livermore, April, 1978.

7. Central Receiver Solar Thermal Power System, Phase I - McDonnell Douglas SAN-1108-8 M.

8. Central Receiver Solar Thermal Power System, Boeing SAN-1111-8.

9. Central Receiver Solar Thermal Power System, Martin Marietta Phase 1 Martin Marietta SAN-1110-77-2.

10. Central Receiver Solar Themal Power System, Phase 1 Honeywell, Inc SAN-1109.

11. "Technical and Economic Assessment of Solar Hybrid Repowering," Final Report, Public Service of New Mexico, SAN/1608-4.1, September 1978.

12. "Technical and Economic Assessment of Solar Hybrid Repowering, Appendix to Final Report" (Conceptual Design Drawings and Cost Estimates), Public Service of New Mexico, SAN/1608-4.2, September 1978.

13. Conceptual Design of Advanced Central Receiver Power Systems, General Electric Contract # EM-78-C-1725.

14. Conceptual Design of Advanced Central Receiver Power Systems, ESG Contract # EG-77-C-03-1483.

15. Conceptual Design of Advanced Central Receiver Power Systems, Boeing Contract # EG-77-C-03-1726.

16. Conceptual Design of Advanced Central Receiver Power Systems, Martin Marietta Contract # EG-77-C-03-1724.

17. Solar Thermal Conversion to Electricity Utilizing an Open Cycle Gas Turbine Design, Black and Veatch Report EPRI ER-387-SY, March, 1977.

18. "Integration of Solar Thermal Power Plants into Electric Utility Systems, Volumes I and II, Southern California Edison Company, No. 76-RD-63, September, 1976.

19. DELSOL: A Computer Code for Calculating the Optical Performance, Field Layout and Optical System Design for Solar Central Receiver Plants, T. A. Dellin, M. J. Fish, Sandia Laboratories, SAND79-8215.

20. "Users' Guide for MIRVAL - A Computer Code for Comparing Designs of Heliostat-Receiver Optics for Central Receiver Solar Power Plants," Sandia Laboratories Report SAND77-8280, February 1979.

21. "STEAEC - Solar Thermal Electric Annual Energy Calculator Documentation," J. Woodard, Sandia Laboratories Report SAND77-8278, January 1978.

22. "BUCKS - Economic Analysis Model for Solar Electric Power Plants," J. Brune, Sandia Laboratories Report SAND77-8279, January 1978.

23. "Technical and Economic Feasibility Study of Solar/Fossil Hybrid Power Systems," NASA Lewis Research Center, NASA-TM-73820.

24. "Solar Power Array for the Concentration of Energy (S.P.A.C.E.)," Sheldahl Incorporated, Report No. NSF/RA/N-74-090, July 1974.

25. "Status Report on The Direct Absorption Receiver," T. D. Brumleve, Sandia Laboratories Report SAND78-8702, June, 1978.

26. Turner, R. H., "Economic Optimization of the Energy Transport Component of a Large Distributed Collector Solar Power Plant," presented at the 11th IECEC, State Line, Nevada, Sept 12-17, 1976.

27. Doane, J. W., et al, "The Cost of Energy from Utility-Owned Solar Electric Systems, a Required Revenue Methodology for ERDA/EPRI Evaluations," Internal Report 5040-29, ERDA/JPL-1012-7613, Jet Propulsion Laboratory, Pasadena, CA, June 1976.

28. MDAC/Rocketdyne Solar Receiver Design Review (by Combustion Engineering) November, 1978, SAND78-8188.

29. "Technical and Economic Feasibility of Solar Augmentation for Boiler Feedwater Heating in Steam-Electric Power Plants," Franklin Institute Research Laboratories, Report COO-2864, November 1976.

30. Performance Analysis for the MDAC Rocketdyne Pilot and Commercial Receivers, General Electric, SAND78-8183.

31. "Survey of High Temperature Thermal Energy Storage" by T. T. Bramlette, 8313; R. M. Green, 8111; J. J. Bartel and D. K. Otteson, 8313; C. T. Schafer and T. D. Brumleve, 8184, March 1976 (SAND75-8063).

32. "Analysis of the Thermal Fatigue Induced by DNB Oscillations in the MDAC Rocketdyne Pilot and Commercial Plant Solar Receiver Designs," by J. F. Jones and D. L. Siebers, Sandia Laboratories, SAND77-8283, December 1977.

33. "Analysis of Thermally Degraded Sensible Heat Storage Hydrocarbons," by V. P. Burolla, Sandia Laboratories, SAND77-8265, December 1977.

34. "The Effectiveness of Spectrally Selective Surfaces for Exposed, High-Temperature Solar Absorbers," M. Abrams, Sandia Laboratories, SAND77-8300, February 1978.

35. "Summary of Energy Storage Activities Within ERDA's Division of Solar Energy Central Receiver Program," T. D. Brumleve, Sandia Laboratories, SAND78-8500, March 1978.

36. "Penetration Analyses and Margin Requirements Associated with Large-Scale Utilization of Solar Power Plants," prepared by the Aerospace Corporation for EPRI, August 1976, EPRI Contract No. ER-198.

37. "Requirements Definition and Impact Analysis of Solar Thermal Power Plants," prepared by the Westinghouse Electric Corporation for EPRI, December 1978, EPRI Contract No. RP648.

38. "Systems and Applications Analysis Studies - Advanced Central Power Projects," Mid term Report, Aerospace Corporation, September 1977.

39. Solar Repowering of Utility Electric Plants, Aerospace Report ATR-79(7773-01)-4. DOE Semi-Annual Review Paper, Washington D.C., March 21, 1979.

40. "Line Focus Central Power System Cost and Performance Objectives," Aerospace Report ATR-78(7773-03)-1, 2, 3, February 1979.

41. "High Temperature Industrial Process Technical Assessment and Rationale," Aerospace Report ATR-78(7691-03)-2, March 1978.

42. "Technical and Economic Assessment of Phase Change and Thermochemical Advanced Thermal Energy Storage (TES) Systems," Electric Power Research Insititue Report EPRI EM-256, Vol. 1-4, December 1976.

43. "Thermal Energy Storage for Advanced Solar Central Receiver Power Systems," L. G. Radosevich, Sandia Laboratories, SAND78-8221, August 1978.

44. "Final Report (Phases 1 and 2) An Interim Structural Design Standard for Solar Energy Applications," Sandia Laboratories, SAND79-8183, April 1979.

45. E. D. Eason, "The Cost and Value of Washing Heliostats," Sandia Laboratories, Livermore, SAND78-8813, June 1979.

UC-62 (268)

Claudio A. Arano
Centro Estudios Energia
Agustin De Foxa 29
Madrid, Spain

John W. Arlidge
Nevada Power Company
P.O. Box 230
Las Vegas, NV 89151

Dr. A. F. Baker
Beethovenalle 79 - CORNER
Vikloria STR.
53 Bonn 2
West Germany

James A. Barnes
Department of Chemistry
Austing College
Sherman, TX 75090

M. A. Bergougnou
The University of Western Ontario
Faculty of Engineering Science
London, Canada N6A 5B9

W. B. Bienert
Dynatherm Corp.
One Industry Lane
Cockeysville, MA 21030

John Bigger
Electric Power Research Inst.
P.O. Box 10412
Palo Alto, CA 93403

Floyd A. Blake
Solar Consultant
7102 S. Franklin
Littleton, CO 80122

Steve Blutton
JPL 506-316
4800 Oak Grove Dr.
Pasadena, CA

C. R. Bozzuto
Combustion Engineering, Inc.
1000 Prospect Hill Road
Windsor, CT 06095

G. W. Braun, Asst. Director
Thermal Power Systems
Division of Central Solar Technology
Department of Energy
Washington, DC 20545

John Britt
Transportation Systems Div.
General Motors Technical Center
Warren, MI 48090

J. E. Brown, Program Manager
El Paso Electric Company
P.O. Box 982
El Paso, TX 79960

Paul Brown
Martin Marietta Aerospace
P.O. Box 179
Denver, CO 80201

Thomas B. Brown
Babcock and Wilcox
P.O. Box 835
Alliance, OH 44601

Joe Buggy
Westinghouse Electric Corp
P.O. Box 10864
Pittsburgh, PA 15236

Barry Butler
Solar Energy Res. Institute
1536 Cole Blvd
Golden, CO 80401

J. Calogeras
NASA Lewis Research Center
2100 Brook Park Road
Cleveland, OH 44135

Leon Chen, Ph.D.
Mechanical Engineering Department
Manhatten College
Riverdale, NY 10471

A. M. Clausing
University of Illinois
266 Mech. Eng. Bldg.
Urbana, IL 61801

160

Dr. Roy L. Cox
Engineering Project Manager
Vought Corporation
P.O. Box 225907
Dallas, TX 75265

James W. Doane
Solar Energy Res. Institute
1536 Cole Blvd.
Golden, CO 80401

Dr. rer. nat. Wolfgang Dönitz
7990 Friedrichshafen 1
Germany

Kirk Drumheller
Battelle Pacific Northwest Labs
P.O. Box 999
Richland, WA 99352

Richard F. Durning
Salt River Project
P.O. Box 1980
Phoenix, AZ 85001

Ernie Eason
The Failure Analysis Associates
1750 Welch Road
Suite 116
Palo Alto, CA 94304

C. R. Easton, Program Manager   (A)
McDonnell Douglas Astronautics Company
5301 Bolsa Avenue
Huntington Beach, CA 92647

S. D. Elliott
Solar Energy Division
DOE/SAN Office
133 Broadway
Oakland, CA 94612

James A. Elsner
Gen Elec Blvd 6 Rm 325
1 River Rd
Schenectady, NY 12345

Hal E. Felix
Solaramics
1301 East El Segundo Blvd.
El Segundo, CA 90245

J. M. Friefeld
Rocketdyne Division
Rockwell International
6633 Canoga Ave.
Canoga Park, CA 91304

J. Garate
Energy Systems Program Department
General Electric Co.
1 River Road
Schenectady, NY 12345

Fred D. Gardner
Badger America, Inc.
One Broadway
Cambridge, MA 02142

Richard Gentilman
Research Division
Raytheon Company
Waltham, MA 02154

William O. Gentry, Manager
Technological Planning
Globe-Union Inc
5757 N. Green Bay Ave.
Milwaukee, WI 53201

R. Gillette
Boeing Engr. and Const. Co.
P.O. Box 3707
Seattle, WA 98124

J. R. Gintz
Boeing Engr. and Const. Co.
P.O. Box 3707
Seattle, WA 98124

L. W. Glover, Program Manager (B)
McDonnell Douglas Astronautics Company
5301 Bolsa Avenue
Huntington Beach, CA 92647

David N. Gorman, Program Manager
Martin Marietta Aerospace
P.O. Box 179
Denver, CO 80201

Wilfried D. Grasse
DFVLR
Cologne, Germany

Mr. J. C. Grosskreutz
Solar Energy Res. Institute
1536 Cole Blvd.
Golden, CO   80401

M. U. Gutstein
Division of Solar Technology
Department of Energy
Washington, DC   20545

Ray Hallet
McDonnell Douglas Astronautic
5301 Bolsa Avenue
Huntington Beach, CA   92647

Keith W. Halvorson, Program Manager
Boeing Engineering & Construction
P.O. Box 3707
Seattle, WA   98214

T. R. Heaton
Martin Marietta Aerospace
P.O. Box 179
Denver, CO   80201

R. L. Henry, Program Manager
Northrup, Incorporated
302 Nichols Drive
Hutchins, TX   75141

Dr. - Phil. H. Hertlein
DFVLR
5 KOLN 90, Linder Hohe
POSTFACH 90 60 58
Cologne, Germany

Stan Hightower
Bureau of Reclamation
Code 1500 E
P.O. Box 25007
Denver Federal Center
Denver, CO   80225

Alvin F. Hildebrandt
Univ. of Houston
Solar Energy Laboratory
Houston, TX   77004

Takayuki Hirano
Japan Trade Center New York
44th Floor McGraw-Hill Bldg.
1221 Avenue of the Americas
New York, NY   10020

Dennis H. Horgan
Solar Energy Res. Institute
1536 Cole Blvd
Golden, CO 80401

Richard H. Horton
General Electric
1 River Road No. 6-325
Schenectady, NY 12345

Travis L. O. Horton
Systems Engineer
United Technologies
Research Center
MS. 79
Silver Lane
East Hartford, CO 06108

R. W. Hughey
Deputy Division Director
Solar Energy Division
Department of Energy/SAN
1333 Broadway
Oakland, CA 94612

Bill Irving
California State Energy Commission
Suite 329
1111 Howe Ave.
Sacramento, CA 95825

Philip O. Jarvinen M/S I-213
MIT Lincoln Laboratory
P.O. Box 73
Lexington, MA 02173

George M. Kaplan
Large Solar Thermal Power Systems
Division of Central Solar Technology
Department of Energy
Washington, DC 20545

Elliott L. Katz, Director
Solar Thermal Projects
Energy Systems Group
The Aerospace Corporation
P.O. Box 92957
Los Angeles, CA 90009

Luk Yun Kim
Professor
Inha University
Ichon, Korea

John Kintigh
Black and Veatch
P.O. Box 8405
Kansas City, MO   64114

Joseph H. Kitchen
Bureau of Reclamation
P.O. Box 427
Boulder City, NV   89005

Ernest Lam
Bechtel International, Inc.
P.O. Box 3965
San Francisco, CA   94119

W. R. Lang
Stearns - Roger
P.O. Box 5888
Denver, CO   80217

Werner Luft
Solar Energy Res. Institute
1536 Cole Blvd
Golden, CO   80401

Prem N. Mathur
The Aerospace Corp
El Segundo, CA

Louis Melamed
Large Solar Thermal Power Systems
Division of Central Solar Technology
Department of Energy
Washington, DC   20545

Lee Neinstein
McDonnell Douglas Astronautics Co.
5301 Bolsa Ave
Huntington Beach, CA   92647

James W. Overby III
JAYCOR
205 South Whiting Street
Alexandria, VI   22304

Edward S. Pierson
Engineering Division
Argonne National Laboratory
9700 South Cass Avenue
Argonne, IL   60439

J. Pietch
Northrop, Inc.
302 Nichols Dr.
Hutchins, TX 75141

Armand Poirier
Sanders Associates
95 Canal St.
Nashua, NH 03060

John W. Rauscher
Union Camp Corp
Reseach and Development Division
P.O. Box 412
Princeton, NJ 08540

Joseph N. Reeves
Southern Calif Edison
2244 Walnut Grove
Rosemead, CA 91770

A. S. Robertson, Program Manager
Foster Wheeler Development Corporation
12 Peach Tree Hill Road
Livingston, NJ 07039

Claude Royere
CNRS
Lab. DE L; Energie Solaire
B. P. 5 Odeillo
66120 - Font Romeu, France

Tzvi Rozenman, Program Manager
PFR Engineering Systems, Inc.
4676 Admiralty Way, Sutie 832
Marina Del Rey, CA 90291

Robert Salemme
General Electric
1 River Rd
Schenectady, NY 12345

R. N. Schweinberg
DOE/STMPO
9550 Flair Park Drive
Suite 210
El Monte, CA 91731

Dr. Thomas C. Schweizer
E- Systems
Center for Advanced Planning and Analysis
7900 West Park Drive, Suite 700
McLean, VI 22101

Arthur Slemmons
Stanford Research Institute
333 Ravenswood Avenue
Menlo Park, CA 94025

Frank Smith
Solar Users Assoc Suite 1204
First Natl Bank E
Albuquerque, NM 87108

Tom Springer
Rockwell International ESG
8900 DE Soto Ave
Canoga Park, CA 91304

V. Thiagarajan
Reynolds Aluminum
P.O. Box 1200
Sheffield, Al 35660

U. S. Department of Energy
Albuquerque Operations Office
P.O. Box 5400
Albuquerque, NM 87185
Attn: D. K. Nowlin

U. S. Department of Energy
Washington, DC 20545
Attn: S. Hansen
       R. A. Miller

Mr. Eric R. Weber
Research Programs
Arizona Public Service Co.
P.O. Box 21666
Phoenix, AZ 85036

J. Weisiger
Small Power Systems Branch
Division of Central Power
   Systems
Department of Energy
Washington, DC 20545

Bernard Yudow
Institute of Gas Technology
3424 South State Street
IIT Center
Chicago, IL 60616

Joel P. Zingeser
Division of Solar Technology
Department of Energy
Washington, DC 20545

R. J. Zoschak
Foster Wheeler Dev. Corp.
12 Peach Tree Hill Road
Livingston, NJ   07039

A. Narath, 4000
B. W. Marshall, 4713
V. L. Dugan, 4720
J. Otts, 4721
G. E. Brandvold, 4710
J. A. Leonard, 4725
W. Marshall; 4713
R. S. Claassen, 5800
R. G. Kepler, 5810
M. J. Davis, 5830
H. J. Saxton, 5840
F. P. Gerstle, Jr., 5844
T. B. Cook, 8000
W. J. Spencer, 8100
W. E. Alzheimer, 8120
A. N. Blackwell, 8200
P. W. Dean, 8265
B. F. Murphey, 8300
D. M. Schuster, 8310
T. S. Gold, 8320
P. J. Eicker, 8326 (3)
L. Gutierrez, 8400
C. S. Selvage, 8420
J. F. Genoni, 8450
R. C. Wayne, 8450
D. N. Tanner, 8450A
W. G. Wilson, 8451
A. C. Skinrood, 8452 (50)
J. D. Gilson, 8453
All Personnel, 8451, 8452, 8453 (26)
J. L. Mortley, 1521
F. J. Cupps, 8265/Technical Library Processes Division, 3141
Technical Library Processes Division, 3141 (2)
Library and Security Classification Division, 8266-2 (3)